

https://dspace.org/

# Effect of monthly rainfall uncertainty on streamflow simulation

**Chetty, Prinavan Carl**

**2022**
https://hdl.handle.net/10539/34941

Downloaded from a DSpace repository. https://dspace.org/




**UNIVERSITY OF THE WITWATERSRAND, JOHANNESBURG**

**SCHOOL OF CIVIL AND ENVIRONMENTAL ENGINEERING**

**CIVN 7019A – RESEARCH PROJECT**

# Effect of Monthly Rainfall Uncertainty on Streamflow Simulation

**Student Name:** Prinavan C. Chetty

**Student No.:** 345712

**Supervisor:** Prof. John G. Ndiritu

**Date:** February 2022

**UNIVERSITY OF THE WITWATERSRAND**
**SCHOOL OF CIVIL AND ENVIRONMENTAL ENGINEERING**

# CIVN7019A: Research Project
**MSc(Eng) Research Report**

## STUDENT DECLARATION

I, Prinavan Carl Chetty; Student Number: 345712
am a student registered for the course CIVN7019A in the academic year 2020. I hereby declare the following:

- I am aware that plagiarism (the use of someone else's work without their permission and/or without acknowledging the original source) is against University Policy.
- I confirm that the work submitted for assessment for the above course is my own unaided work except where I have explicitly stated otherwise.
- I have followed the required conventions in referencing the thoughts, ideas, and visual materials of others.

**I understand that the University of the Witwatersrand may take disciplinary action against me if there is a belief that this is not my own unaided work, or that I have failed to acknowledge the source of the ideas or words in my writing.**

Signature:  Date: 05 February 2022

# Abstract

The estimation of areal rainfall from point measurements by rain gauges are key inputs into various water resource modelling applications including streamflow simulation. A major uncertainty in these estimates arises from the inadequacy of rain gauges in capturing the variation of rainfall between rain gauges.

This study aimed to quantify monthly areal rainfall uncertainty and assess the impacts of this uncertainty on streamflow simulation. This was achieved by: i) quantifying areal rainfall uncertainty and generating monthly stochastic areal rainfalls incorporating this uncertainty; ii) using the stochastically generated areal rainfalls to generate stream flows, and iii) comparing variability and quality of these stream flows with those obtained using historical rainfall.

A stochastic areal rainfall generator that has been used in previous studies was selected to quantify areal rainfall uncertainty on seven catchments in South Africa; while the assessment of streamflow simulation was carried for two of the catchments using the Pitman model. A manual-automatic calibration approach using the SCE-UA optimizer was applied.

The assessment of areal rainfall uncertainty with alternate omission of 4 rainfall stations obtained an average monthly areal rainfall difference equal to 18.3% of the average monthly rainfalls. The generated stochastic rainfalls were unbiased with the average mean, standard deviation and skewness matching the respective historic values closely.

The streamflow simulation revealed that incorporating areal rainfall uncertainty by using stochastic areal rainfalls lead to a significant increase in the range of simulated stream flows without significant loss of simulation performance in calibration and validation runs. The areal rainfall uncertainty quantification applied is therefore considered realistic.

# Acknowledgements

I would like to express my sincere gratitude to my supervisor, Professor John Ndiritu, for the assistance and guidance provided me throughout this research.

I would also like to thank those close to me for all the patience, support and encouragement provided during this period.

# Contents

1. Introduction ..... 1
1.1 Background Statement ..... 1
1.2 Research Objectives ..... 1
1.4 Structure of the Research Report ..... 2
2. Literature Review ..... 3
2.1 Precipitation ..... 3
2.1.1 Mechanisms of Precipitation ..... 3
2.1.2 Forms of Precipitation ..... 5
2.2 Areal Rainfall and Uncertainty ..... 5
2.2.1 Estimation of Areal Rainfall from Point Rainfall ..... 5
2.2.2 Uncertainty and Uncertainty Quantification in Simulation Models ..... 5
2.2.3 Areal Rainfall Uncertainty ..... 6
2.3 Catchment Modelling for Water Resources Assessment in South Africa ..... 8
2.3.1 Hydrological Models ..... 8
2.3.2 Parameter Uncertainty in Pitman Model Applications ..... 10
2.4 Summary ..... 11
2.4.1 Rainfall Uncertainty Modelling Approach ..... 11
2.4.2 Catchment Modelling Method ..... 11
3. Investigative Approach and data acquisition ..... 13
3.1 Overview ..... 13
3.2 Methodology ..... 13
3.2.1 Generation of Stochastic Areal Rainfall ..... 13
3.2.2 Streamflow simulation ..... 16
3.2.3 Comparison of Calibration Performance ..... 17
3.3 Data and Study Catchments ..... 18
3.3.1 Rainfall Data ..... 18
3.3.2 Selection of Study Catchments and Rain Gauge Groups ..... 19
3.3.3 Naturalised Streamflow Data ..... 19

3.3.4 Study Catchments ..... 20
4. Results, Analysis, and Discussion of Stochastic Rainfall Generation ..... 33
4.1 Overview ..... 33
4.2 Average Differences of Areal Rainfalls and their significance ..... 33
4.2.1 Overview ..... 33
4.2.2 Areal rainfall differences for the Study Catchments ..... 33
4.3 Cumulative Density Plots and Determination of Scaling Factors ..... 35
4.3.1 Overview ..... 35
4.4 Analysis of Stochastically Generated Areal Rainfall ..... 40
4.5 Analysis of Stochastic Areal Rainfalls for Individual Catchments ..... 40
4.5.1 Overview ..... 40
4.5.2 Bella Vista ..... 42
4.5.3 Bonjanala ..... 42
4.5.4 Ficksburg ..... 43
4.5.5 Howick ..... 44
4.5.6 Potchefstroom ..... 44
4.5.7 Sabie ..... 45
4.5.8 Vanderkloof ..... 46
5. Results, Analysis, and Discussion of Streamflow Simulation ..... 47
5.1 Overview ..... 47
5.2 Comparison of Pitman Model Parameters ..... 47
5.2.1 Overview ..... 47
5.2.2 Bella Vista ..... 47
5.2.3 Bonjanala ..... 49
5.3 Comparison of Calibration Performance ..... 50
5.3.1 Bella Vista ..... 50
5.3.2 Bonjanala ..... 51
5.4 Comparison of Simulated Stream Flows ..... 52
5.4.1 Overview ..... 52

5.4.2 Bella Vista ..... 52
5.4.3 Bonjanala ..... 56
5.5 Discussion ..... 60
6. Conclusion and Recommendations ..... 63
7. References ..... 65

# List of Figures

Figure 2-1: Precipitation Mechanisms (Robinson & Ward, 2017) ..... 3
Figure 2-2: Formation of Cyclonic Precipitation (Robinson & Ward, 2017) ..... 3
Figure 2-3: Formation of Convective Precipitation (Robinson & Ward, 2017) ..... 4
Figure 2-4: Formation of Orographic Precipitation (Robinson & Ward, 2017) ..... 4
Figure 2-5: Structure of the Pitman Model (Mwelwa, 2004) ..... 10
Figure 3-1: A representative Catchment with 8 rain gauge stations ..... 13
Figure 3-2: The creation of rainfall groups of different rain gauge densities ..... 14
Figure 3-3: Monthly areal rainfall difference CDF plots and matching ..... 16
Figure 3-4: Rain Gauges available in theWR2012 database (Bailey and Pitman, 2016) ..... 19
Figure 3-5: Study Catchments ..... 21
Figure 3-6: Bella Vista Catchment ..... 22
Figure 3-7: Rainfall groupings for Bella Vista Catchment ..... 22
Figure 3-8: Bonjanala Catchment ..... 23
Figure 3-9: Rainfall groupings for Bonjanala ..... 24
Figure 3-10: Ficksburg Catchment ..... 25
Figure 3-11: Rainfall groupings for Ficksburg ..... 25
Figure 3-12: Howick Catchment ..... 26
Figure 3-13: Rainfall groupings for Howick ..... 27
Figure 3-14: Potchefstroom Catchment ..... 28
Figure 3-15: Rainfall groupings for Potchefstroom ..... 28
Figure 3-16: Sabie Catchment ..... 29
Figure 3-17: Rainfall groupings for Sabie ..... 30
Figure 3-18: Vanderkloof Catchment ..... 31
Figure 3-19: Rainfall groupings for Vanderkloof ..... 32
Figure 4-1: Monthly areal rainfall difference CDF plots and matching for Bella Vista ..... 36

Figure 4-2: Monthly areal rainfall difference CDF plots and matching for Bonjanala ..... 37
Figure 4-3: Monthly areal rainfall difference CDF plots and matching for Ficksburg ..... 37
Figure 4-4: Monthly areal rainfall difference CDF plots and matching for Howick ..... 38
Figure 4-5: Monthly areal rainfall difference CDF plots and matching for Potchefstroom ..... 38
Figure 4-6: Monthly areal rainfall difference CDF plots and matching for Sabie ..... 39
Figure 4-7: Monthly areal rainfall difference CDF plots and matching for Vanderkloof ..... 39
Figure 4-8: Absolute Mean Deviation for Stochastically Generated Rainfall ..... 41
Figure 4-9: Coefficient of Variation for Stochastically Generated Rainfall ..... 41
Figure 4-10: Box plots of representative stochastic rainfalls for Bella Vista ..... 42
Figure 4-11: Box plots of representative stochastic rainfalls for Bonjanala ..... 43
Figure 4-12: Box plots of representative stochastic rainfalls for Ficksburg ..... 43
Figure 4-13: Box plots of representative stochastic rainfalls for Howick ..... 44
Figure 4-14: Box plots of representative stochastic rainfalls for Potchefstroom ..... 45
Figure 4-15: Box plots of representative stochastic rainfalls for Sabie ..... 45
Figure 4-16: Box plots of representative stochastic rainfalls for Vanderkloof ..... 46
Figure 5-1: Boxplots of scaled parameters for the 100 initialised calibration-validation runs for Bella Vista ..... 49
Figure 5-2: Boxplots of scaled parameters for the 100 initialised calibration-validation runs for Bonjanala ..... 50
Figure 5-3: Box plots of Pitman model simulation performance for Bella Vista (H: Historic Observed Rainfall; S: Monthly Stochastic Rainfalls) ..... 51
Figure 5-4: Box plots of Pitman Model calibration simulation performance for Bonjanala (H: Historic Observed Rainfall; S: Monthly Stochastic Rainfalls) ..... 52
Figure 5-5: Box plots of representative calibration stream flows for Bella Vista (H: Historic Observed Rainfall; S: Monthly Stochastic Rainfalls) ..... 53
Figure 5-6: Box plots of representative validation stream flows for Bella Vista (H: Historic Observed Rainfall; S: Monthly Stochastic Rainfalls) ..... 54
Figure 5-7: Bias and Coefficients of Variation for Bella Vista (H: Historic Observed Rainfall; S: Monthly Stochastic Rainfalls) ..... 54
Figure 5-8: Range of simulated stream flows from 100 calibration runs for Bella Vista ..... 55
Figure 5-9: Range of simulated stream flows from 100 validation runs for Bella Vista ..... 56
Figure 5-10: Box plots of representative calibration stream flows for Bonjanala (H: Historic Observed Rainfall; S: Monthly Stochastic Rainfalls) ..... 57
Figure 5-11: Box plots of representative validation stream flows for Bonjanala (H: Historic Observed Rainfall; S: Monthly Stochastic Rainfalls) ..... 58

Figure 5-12: Bias and Coefficients of Variation for Bonjanala (H: Historic Observed Rainfall; S: Monthly Stochastic Rainfalls) ..... 58
Figure 5-13: Range of simulated stream flows from 100 calibration runs for Bonjanala ..... 59
Figure 5-14: Range of simulated stream flows from 100 verification runs for Bonjanala ..... 60

# List of Tables

Table 3-1: Parameters of the Pitman Model (Hughes, 2013) ..... 17
Table 3-2: Summary of Study Catchments ..... 20
Table 3-3: Bella Vista Catchment Rain Gauge Data ..... 21
Table 3-4: Bonjanala Catchment Rain Gauge Data ..... 23
Table 3-5: Ficksburg Catchment Rain Gauge Data ..... 24
Table 3-6: Howick Catchment Rain Gauge Data ..... 26
Table 3-7: Potchefstroom Catchment Rain Gauge Data ..... 27
Table 3-8: Sabie Catchment Rain Gauge Data ..... 29
Table 3-9: Vanderkloof Catchment Rain Gauge Data ..... 30
Table 4-1: Average differences of areal rainfalls at various rain gauge densities for Bella Vista catchment ..... 33
Table 4-2: Average differences of areal rainfalls at various rain gauge densities for Bonjanala catchment ..... 34
Table 4-3: Average differences of areal rainfalls at various rain gauge densities for Ficksburg catchment ..... 34
Table 4-4: Average differences of areal rainfalls at various rain gauge densities for Howick catchment ..... 34
Table 4-5: Average differences of areal rainfalls at various rain gauge densities for Potchefstroom catchment ..... 34
Table 4-6: Average differences of areal rainfalls at various rain gauge densities for Sabie catchment ..... 35
Table 4-7: Average differences of areal rainfalls at various rain gauge densities for Vanderkloof catchment ..... 35
Table 4-8: Computed Scaling Factors [higher scaling factor] ..... 36
Table 4-9: Summary of the Bias of Stochastically Generated Rainfall ..... 40
Table 5-1: Statistics of Pitman model parameters for Bella Vista obtained from 100 randomly-initialised runs (H: simulation using single historic rainfall series; S: simulation using 100 stochastic rainfall series) ..... 48

Table 5-2: Statistics of Pitman model parameters for Bonjanala obtained from 100 randomly-initialised runs (H: simulation using single historic rainfall series; S: simulation using 100 stochastic rainfall series) ..... 49

# List of Abbreviations

| | |
|---|---|
| ACRU | Agricultural Catchments Research Unit |
| CC | Correlation Coefficient |
| CDF | Cumulative Density Function |
| CE | Coefficient of Efficiency |
| IDW | Inverse Distance Weight |
| MAP | Mean Annual Precipitation |
| MAR | Mean Areal Rainfall |
| RMCC | Residual Mass Curve Coefficient |
| SCDEV | The Coefficient of Mean Absolute Deviation |
| SCE-UA | Shuffled Complex Evolution Method |
| UQ | Uncertainty Quantification |
| WMA | Water Management Area |

# List of Symbols

| **Symbol** | **Units** | **Description** |
|---|---|---|
| AI | **None** | Ratio of impervious to total area |
| FT | **mm/month** | Runoff from moisture storage at full capacity |
| GL | **Months** | Lag for groundwater runoff |
| GW | **mm/month** | Maximum ground water runoff |
| $H_t$ | **mm** | Monthly areal rainfall |
| $L^1_t$ and $L^2_t$ | **mm** | Areal rainfalls obtained from lower rain gauge densities by alternately omitting half of the rain gauges |
| PI | **mm** | Interception storage |
| POW | **None** | Power of moisture storage-runoff equation |
| R | **None** | Evaporation-moisture storage relationship parameter |
| $R_A$ | **mm** | Areal rainfalls obtained using all 8 rain gauges |
| SL | **mm** | Moisture storage capacity below which no runoff occurs |
| ST | **mm** | Maximum moisture storage capacity |

| | | |
|---|---|---|
| TL | **Months** | Lag for surface and soil moisture |
| u | **None** | Uncertainty Factor |
| ZMax | **mm/month** | Maximum catchment absorption rate |
| ZMin | **mm/month** | Minimum catchment absorption rate |

# 1. Introduction

## 1.1 Background Statement

Water shortage problems are recurrent in South Africa, impacting on the livelihoods of people, therefore making adequate planning and sustainable management of the country's freshwater resources crucial for its socio-economic growth (Hughes, et al., 2008). Water resource models play an important role in supporting water resource management decision making and the design of reservoirs and abstraction systems in Southern Africa (Hughes, et al., 2008). The quality of rainfall-runoff modelling, which is a significant part of water resource modelling, can be evaluated from various aspects such as model selection, model parameter estimation and the quality of the input data (Yoo, et al., 2012).

The quality of hydrological input data is influenced by hydrological processes which could have high variability in space and time. In this regard, the lack of satisfactory information about spatial distribution of rainfall has always been one of the most important errors in runoff estimation (Cristiano, et al., 2017).

The estimation of areal rainfall from point measurements by rain gauges are key inputs into various water resource modelling applications (Ndiritu, 2013). There is a degree of uncertainty in these estimates that arises from the variation of rainfall between rain gauges due to various spatial, temporal and climatic factors (Ndiritu & Mkhize, 2017); and quantifying the uncertainty in these estimates would increase the value and credibility of predictions. The incorporation of uncertainty estimation in models should help to quantify the level of confidence in the results, inform and improve decision and policy-making processes, leading to better risk assessment (Hughes, et al., 2008).

Approaches have been developed and applied to deal with areal rainfall uncertainty and to assess its effect on catchment modelling/water resources assessment. Ndiritu & Mkhize (2017) assessed monthly areal rainfall uncertainty and its effect on monthly streamflow simulation on two South African catchments by adopting a non-parametric stochastic areal rainfall generator developed by Ndiritu (2013).

## 1.2 Research Objectives

The objectives of this research are:

- To assess the performance of an approach of quantifying rainfall uncertainty that is applicable for water resource assessment, and
- To assess the impacts of the rainfall uncertainty obtained from this approach on streamflow simulation using a suitable hydrological model.

## 1.3 Research Approach

Water resources assessment in Southern Africa is typically conducted at a monthly time step therefore areal rainfall uncertainty quantification and streamflow modelling at the monthly time step were most appropriate for this study. A stochastic areal rainfall generator that has been used in previous studies (Ndiritu, 2013, Ndiritu & Mkhize, 2017) was selected for the areal rainfall uncertainty quantification and the Pitman model (Pitman, 1973) which is widely used for water resources assessment in southern Africa (Bailey, 2015, Bailey and Pitman, 2016) was selected for streamflow modelling. The approach to the study entailed the following main steps:

- The selection of catchments with rainfall and streamflow data that could enable the study objectives to be achieved with reasonable confidence.
- The application of the stochastic areal rainfall generator and the assessment of its performance.
- Streamflow modelling using a calibration-validation approach in a manner that could differentiate the uncertainty in streamflow modelling resulting from areal rainfall uncertainty from the uncertainty relating to other aspects such as parameter uncertainty.
- Assessing the effect of areal rainfall uncertainty on streamflow generation.

## 1.4 Structure of the Research Report

The literature review is presented under Chapter 2 and explores mechanisms of precipitation, estimation of areal rainfall from point rainfall measurements, uncertainty in simulation modelling, uncertainty in estimating areal rainfall, and catchment modelling techniques for water resources assessment in South Africa. The assessment of parameter uncertainty of a widely applied model in South Africa is also reviewed.

Chapter 3 presents the investigative approach which sets out the methodology that is based on the data-based stochastic areal rainfall generator developed by Ndiritu (2013) and streamflow modelling using the Pitman model as implemented by Ndiritu & Mkhize (2017). The study catchments selected for the study are also presented in this Chapter.

In Chapter 4, the analysis and discussion of the assessment of the stochastic areal rainfall generation is presented, while Chapter 5 presents the streamflow simulation including the assessment of the effect of areal rainfall uncertainty on the simulation. Chapter 6 then presents the conclusions and recommendations of the study.

# 2. Literature Review

## 2.1 Precipitation

### 2.1.1 Mechanisms of Precipitation

#### *2.1.1.1 Overview*

Precipitation occurs when a body of moist air is cooled sufficiently for it to become saturated; condensation nuclei are present; and conditions are suitable for the formation of water droplets or ice crystals (Ward & Robinson, 2000). Precipitation mechanisms provide a source of inflow of moisture to clouds, resulting in precipitation (Robinson & Ward, 2017). These mechanisms, shown in Figure 2-1, are classified based on the factors which lead to the lifting up of air masses (Robinson & Ward, 2017).

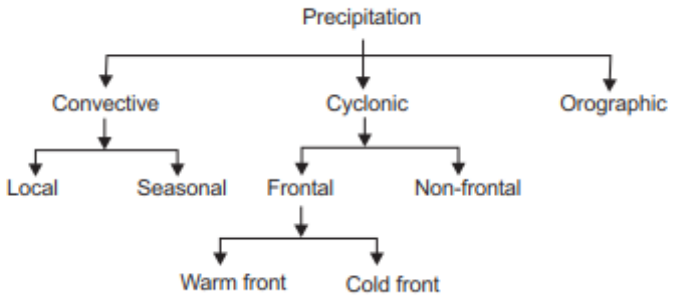



***Figure 2-1: Precipitation Mechanisms (Robinson & Ward, 2017)***

#### *2.1.1.2 Cyclonic Precipitation*

Cyclonic precipitation results from the convergence of air masses, of different characteristics, moving in opposite directions as shown in Figure 2-2 (Selase, et al., 2015). Most precipitation outside of tropical regions are a result of cyclonic systems, which are characterised by relatively weak vertical air motions and typically produce moderate rain intensities of fairly long duration (Robinson & Ward, 2017).

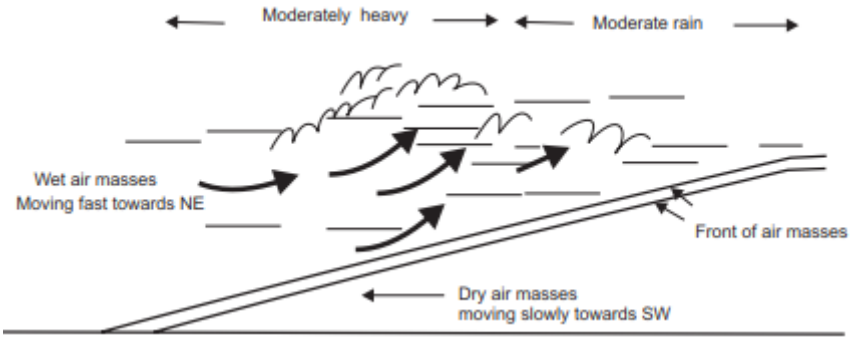
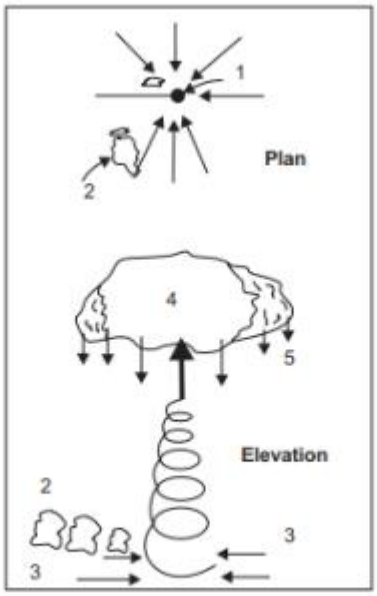



***Figure 2-2: Formation of Cyclonic Precipitation (Robinson & Ward, 2017)***

### *2.1.1.3 Convective Precipitation*

Convective precipitation occurs from the convective lifting of air masses due to local differences in heating close to the ground surface, leading to short-term, locally intense precipitation (Robinson & Ward, 2017). Figure 2-3 illustrates the formation of convective precipitation.




Formation of convective precipitation: (1) Centre of low pressure (2) Wet air masses (3) Air moving towards low pressure (4) Rising air mass (5) Precipitation

***Figure 2-3: Formation of Convective Precipitation (Robinson & Ward, 2017)***

### *2.1.1.4 Orographic Precipitation*

Orographic precipitation occurs due to the mechanical lifting of moist air over barriers (such as mountain ranges, islands etc.) as shown in Figure 2-4 (Robinson & Ward, 2017).

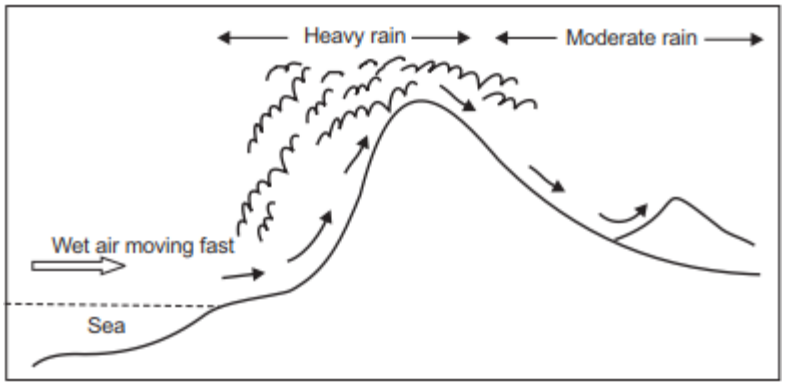



***Figure 2-4: Formation of Orographic Precipitation (Robinson & Ward, 2017)***

### 2.1.2 Forms of Precipitation

The various forms of precipitation are a result of the extent to which and mechanisms by which vapour laden air cools before falling (Robinson & Ward, 2017). These forms include mist, rain, snow, hail, sleet and dew.

## 2.2 Areal Rainfall and Uncertainty

### 2.2.1 Estimation of Areal Rainfall from Point Rainfall

Rain gauges provide rainfall measurements that are only indicative of a limited spatial extent (Robinson & Ward, 2017). There are various techniques that exist to estimate areal rainfall from point rainfall measurements, ranging from simple linear combination to geostatic techniques (Barbalho, et al., 2014). The techniques that are commonly used in several studies/applications include the Thiessen Polygon Method, the Reciprocal Distance Squared Method, the Kriging Method and the Multiquadric Equations Method (Barbalho, et al., 2014).

Since rainfall is highly variable in space and time (Leonhardt, et al., 2014), areal rainfall estimation accuracy is expected to increase with a denser gauging network (Robinson & Ward, 2017). Other influential factors include climate characteristics and topography (Robinson & Ward, 2017).

### 2.2.2 Uncertainty and Uncertainty Quantification in Simulation Models

Mathematical models, usually implemented through computer simulations, are useful tools for studying complex real-word phenomena. However, mathematical modelling is bound to involve some degree of uncertainty when used to make inferences about real-world behavior (Ghanem, et al., 2017).

Miller, et al. (2014) defines uncertainty quantification in simulation models as the process of quantifying uncertainties associated with model calculations of true, physical quantities of interest, with the goals of accounting for all relevant sources of uncertainty and quantifying the contributions of specific sources to the overall uncertainty. Common sources of uncertainty associated with simulation models include uncertainties in the model parameters (including model initial and boundary conditions), uncertainties in the mathematical form of the models, as well as uncertainties in the experimental data used to calibrate the models (Miller, et al., 2014).

Barth (2005) defines the sources of uncertainty in most numerical simulations as geometric uncertainty, initial geometric and boundary uncertainty, structural uncertainty and parametric uncertainty.

Volodina & Challenor (2021) categorises uncertainty in simulation models as either aleatory or epistemic. Aleatoric uncertainty is associated with the internal variability in the system, and therefore cannot be reduced by conducting more experiments or collecting more data. A probabilistic framework would ideally be employed to model this type of uncertainty. Epistemic uncertainty arises from the deficiency in the model, caused by limited knowledge about the phenomena and therefore this type of uncertainty may be reduced by improving knowledge about the system (Volodina & Challenor, 2021).

Volodina & Challenor (2021) inform that uncertainty quantification in computer models is important as the analysis of physical processes based on computer models is usually accompanied by uncertainty, which needs to be addressed to perform credible model-based inference. Reporting uncertainties encountered in modelling is crucial in maintaining credibility in the modelling results and associated decisions.

### 2.2.3 Areal Rainfall Uncertainty

The quality of rainfall-runoff modelling, which is often a significant part of water resource modelling, can be assessed from various aspects such as model selection, model parameter estimation and the quality of the input data (Yoo, et al., 2012). The quality of rainfall input data is influenced by hydrological processes which have high variability in space and time; and the lack of satisfactory information about spatial distribution of rainfall has been one of the most impactful errors in runoff estimation (Cristiano, et al., 2017).

Yoo, et al. (2012) quantitatively evaluted the effect of estimation error of the areal average rainfall on runoff simulation for the Chungju Dam Basin located in the upstream part of the Han River, Korea. First the Monte Carlo simulation technique was used to generate several sets of areal average rainfall data including the estimation error (Yoo, et al., 2012). 'Reference' data sets were prepared by estimating the areal average rainfall using the Thiessen polygon method (Yoo, et al., 2012). The generated and reference data was then used as inputs to the runoff simulation. A relationship between the rainfall error and runoff error was derived using the results of the the simulation (Yoo, et al., 2012). The estimation error of areal average rainfall (rainfall error) was found roughly proportional to the areal average rainfall itself. Also, both the rainfall and runoff errors were found to have no obvious biases. However, the variances of runoff error were found to be significantly higher than that of rainfall error.

Merker, et al. (2019) presented a method to estimate spatially and temporally variable uncertainty for a combined area precipitation product by using data assimilation to merge precipitation measurements from different sources and an ensemble nowcasting method to evolve the uncertainty estimate over time. The method was evaluated in a proof of concept

study focusing on weather radar data of preciptation events. The study demonstrated that the dynamic areal uncertainty estimate outperforms a constant benchmark uncertainty value in all cases for one of the evaluated scores, and in half the number of cases for the other score (Merker, et al., 2019). The flow dependency introduced by the coupling of data assimilation and nowcasting enables a more accurate spatial and temporal distribution of uncertainty.

Moulin, et al. (2008) investigated the influence of mean area rainfall estimation errors on the use of lumped conceptual rainfall-runoff models to simulate flood hydrographs for small to medium-sized catchments which were densely covered by an operational network of stream and rain gauges. Moulin, et al. (2008) developed an error model for rainfall estimation, consistent with data to produce realistic streamflow simulation uncertainty ranges, which combined geostatistical tools based on kriging and an autoregressive model to account for temporal dependence of errors. The study revealed that a siginificant part of the rainfall ruoff modelling errors arise from uncertainties on rainfall estimates.

Hughes, et al. (2008) classified the sources of uncertainity in water resource modelling as those related to input data and those related to the structure and parameter uncertainties. A common source of input data uncertainty in South Africa is the inadequate hydrometerological gauging network which brings about difficulty in representing the spatial variations in the major model inputs of rainfall (Hughes, et al., 2008). Sawunyama & Hughes (2007) identified that the use of different combinations of rain gauges can have substantial impacts on spatially averaged rainfall and therefore on simulated runoff.

Steiner (1996) employed highly time-resolved data sets collected by rain gauge networks to determine how much uncertainty, on average, was introduced to monthly areal rainfall estimates as a function of decreasing temporal representation. Using data from Darwin and Florida in Australia , Steiner (1996) sampled rainfall rates at various time intervals to investigate the uncertainty of the estimated mean rainfall introduced by decreasing sampling time resolution. A key result of this analysis was that the sampling uncertainty scales with rainfall depth and spatial scale. For a given frequency of observations and domain size the sampling uncertainty is small for months with a large areal rainfall accumulation, while large uncertainties occur for months with moderate or small areal rainfall totals. The average uncertainty of a monthly areal rainfall estimate, introduced by a finite sampling frequency, therefore appears to be constrained by the rainfall depth, the sampling time interval, and the domain size of interest.

Ndiritu (2013) formulated a method of generating stochastic daily areal rainfall from point rainfalls using any areal rainfall estimation method, whilst incorporating uncertainties (Ndiritu,

2013). The basic approach was to stochastically generate groups of plausible uncertainty-impacted areal rainfalls, instead of the common approach of computing a single areal rainfall value that is assumed to be error free (Ndiritu, 2013). Ndiritu (2013) stated that uncertainty in areal rainfall can be reasonably estimated from the differences in areal rainfall when half (or about half) the rainfall stations are alternately omitted while maintaining uniform catchment coverage to the extent possible. Ndiritu (2013) analysed these differences and found them to depend on i) the rain gauge density ii) the area rainfall magnitude. This method is presented in detail as part of the methodolgy under Section 3.2. Ndiritu (2013) tested the model, at a daily time step, on two South African catchments with different characteristics and found that it exhitbited expected behaviour and realistic quantification of uncertainties.

Ndiritu & Mkhize (2017) assessed monthly areal rainfall uncertainty and its effect on monthly streamflow simulation on two South African catchments by adopting the non-parametric stochastic areal rainfall generator, developed by Ndiritu (2013), and applying it at a daily time step. Monthly streamflow simulation then was carried out on one of the catchments using the Pitman model which is a widely applied catchment model in Southern Africa.

Ndiritu & Mkhize (2017) found that the differences in areal rainfall averaged to 20% of the mean monthly rainfall which meant that monthly areal rainfall uncertainty was significant. The monthly stochastic areal rainfall generation replicated the historic rainfalls reasonably well and an alternative in which stochastic areal rainfalls were generated at a daily time step and then aggregated to monthly values also obtained unbiased stochastic rainfalls. The aggregated stochastic rainfalls were found to have lower variability than those obtained by direct monthly time step generation.

## 2.3 Catchment Modelling for Water Resources Assessment in South Africa

### 2.3.1 Hydrological Models

A hydrological model may be defined as a set of mathematical relations describing the various components of the hydrological cycle, with the aim of simulating runoff and other fluxes of the land phase of the hydrological cycle. In the hydrological cycle, the transformation of input (rainfall) into output (runoff) involves a number of interrelated processes. In hydrological models, attempts are made to replicate this transformation of rainfall into runoff (Pitman, 1973), albeit with varying degrees of simplification and generality.

According to Pitman (1973), a practical hydrologic model should meet the following requirements:

- Represent to an acceptable degree of accuracy, the hydrologic regimes of a wide variety of catchments;
- It should be easily applied with existing hydrologic data to different catchments; and
- The model should be physically relevant so that, in addition to streamflow, estimates of other useful components such as actual evaporation or soil moisture state can be made.

The hydrological models widely used in South Africa are the Pitman model, a conceptual, semi-distributed monthly time-step model; and the ACRU (Agricultural Catchments Research Unit), a conceptual, physically-based daily time-step agro-hydrological modelling system (Sawunyama, 2008).

The ACRU model has its origins in a catchment evapotranspiration-based study carried out in Natal in the early 1970s (Schulze, 1989). ACRU is a multipurpose model that integrates water budgeting and runoff components of the terrestrial hydrological system with risk analysis, and can be applied in crop yield modelling, design hydrology, reservoir yield simulation and irrigation water demand/supply, regional water resources assessment, planning optimum water resource allocation and utilisation, climate change, land use and management impacts, and resolving conflicting demands on water resources (Schulze & Tarboton, 1991). The ACRU model uses daily multilayer soil water budgeting and was developed essentially into a versatile total evaporation model. It has, therefore, been structured to be highly sensitive to climate and to land cover/use changes on the soil water and runoff regimes, and its water budget is responsive to supplementary watering by irrigation, to changes in tillage practices, or to the onset and degree of plant stress (Schulze & Tarboton, 1991).

The Pitman model, also referred to as the WRSM2000/Pitman model, was initially developed in 1973 (Pitman, 1973) and is widely used in Southern Africa to generate catchment-based rainfall runoff from rainfall stations (or rain gauges). Figure 2-5 presents the main components of the basic Pitman model (Mwelwa, 2004). Further versions of the model have been developed which has introduced hydrological modelling of surface water-ground water interactions, afforestation, alien vegetation, dryland crops, off channel wetlands and mine and irrigation water including quality aspects (Ndiritu, 2009).

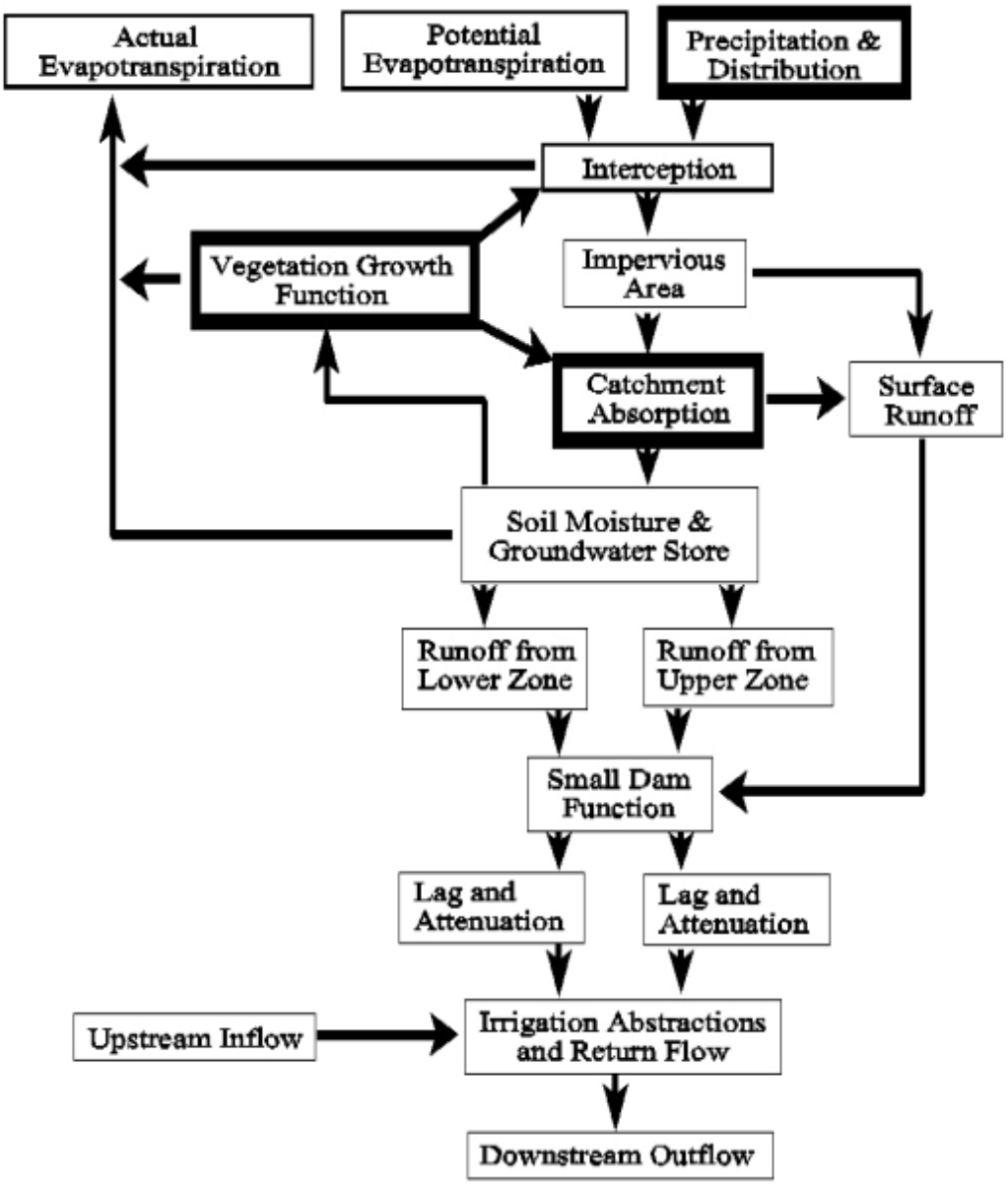



***Figure 2-5: Structure of the Pitman Model (Mwelwa, 2004)***

### 2.3.2 Parameter Uncertainty in Pitman Model Applications

Hughes, et al. (2008) adopted an approach based on a priori estimation of parameters of the Pitman model using estimates of physical basin properties on a test basin (Upper Vaal River subasin C12D with an area of 898km²). The quanitification of uncertainty in the parameter sets during this study was based on a subjective approach of defining the uncertainty in the interpretation of the available information on physical basin property data. Hughes, et al. (2008) generated three parameter sets; a 'best' estimate using recommendations of Kapangaziwiri & Hughes (2008) and two additional sets that would result in generally more (upper) or less (lower) runoff. No calibration was applied to during this process. The approach used by Sawunyama & Hughes (2007) to quantify input uncertainties associated with rainfall

and evaporation data in the Pitman model for South African basins was applied in this study and three rainfall input time series were generated for the test catchment. Hughes, et al. (2008) generated 18 possible natural flow scenarios with the combination of parameter, rainfall and evaporation uncertainty. Hughes, et al. (2008) found that the dominant source of uncertainty in this study in the simulation of naturalised stream flow was the quantification of model parameters. This was due to the low topography of the study catchment which affects model parameter estimations and contributes to relatively small variations in monthly rainfall totals.

Ndiritu & Mkhize (2017) applied stochastic areal rainfalls (generated using the stochastic areal rainfall generator first development by Ndiritu (2013)) in the Pitman model on two study catchments in South Africa (i.e. Tzaneen (B81D) and George (K50A, K50B,K60E, K60F, and K60G). During the streamflow modelling, Ndiritu & Mkhize (2017) applied a hybrid manual-automatic calibration approach where the parameter ranges within which to search for optimal parameters were specified manually and iteratively and the actual searches within those ranges were carried out automatically using SCE-UA method. An objective function that maximizes the Nash coefficient of efficiency (CE) of flows and log of flows (maximize [0.5CE(flows) + 0.5CE(log10flows)]) was applied in to assign value to the simulation of both high and low flows in optimization. To assess the effect of areal rainfall uncertainty while allowing for parameter uncertainty, Ndiritu & Mkhize (2017) carried out 100 randomly-initialised calibration-validation runs using the single observed monthly rainfalls and compared these with 100 randomly-initialised runs using 100 stochastic rainfall sequences. Ndiritu & Mkhize (2017) found significant parameter interactions between ST and POW, ST and ZMAX, FT and POW, and PI and ZMAX. These were strongest when observed rainfalls were used and weakest for the calibrations using stochastic monthly rainfalls. Ndiritu & Mkhize (2017) concluded that applying the areal rainfall generation method would add confidence in streamflow simulation results and analyses and decisions based on them.

## 2.4 Summary

### 2.4.1 Rainfall Uncertainty Modelling Approach

To promote the quantification of uncertainty in areal rainfall estimates based on point rainfall measurements in South Africa, a simple and practical model is required (Ndiritu & Mkhize, 2017). The stochastic rainfall generator by Ndiritu (2013) - is considered to embody the main characteristics of typical non-parametric methods as it is simple and manageable, easy to apply and robust.

### 2.4.2 Catchment Modelling Method

The Pitman model is a widely applied catchment modelling method for regional scale water resources planning in South Africa. The ACRU modelling system has been shown to simulate

observed streamflow; however studies on large catchments and data are limited. The application of the Pitman model is also simpler and better suited to this study. It is therefore proposed that the Pitman model be used for this study.

# 3. Investigative Approach and data acquisition

## 3.1 Overview

This research used the stochastic areal rainfall generator, developed by Ndiritu (2013) and later applied by Ndiritu and Mkhize (2017), to first quantfy the uncertainty in the areal rainfall and then to generate monthly stochastic areal rainfall from point rainfall data. The effect of these uncertainties on streamflow simulation was assessed using the Pitman Model. For this study, the selection of catchment with adequately long and reliable rainfall and streamflow data was required.

## 3.2 Methodology

### 3.2.1 Generation of Stochastic Areal Rainfall

The stochastic areal rainfall generator (Ndiritu,2013; Ndiritu and Mkhize, 2017) is described below. To enable clarity of description, a representative catchment is presented (Figure 3-1) with 8 rainfall stations.

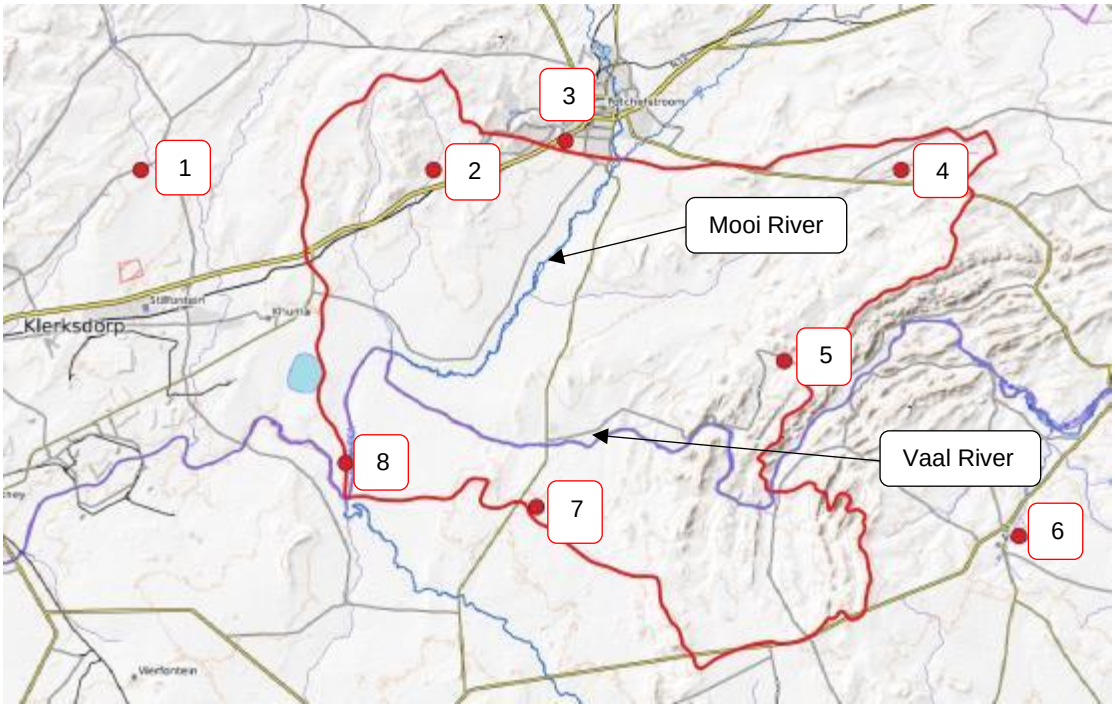



***Figure 3-1: A representative Catchment with 8 rain gauge stations***

Let $H_t$ be the monthly areal rainfall for month t obtained using all the rain gauges available using an appropriate method of determining areal rainfall such as inverse distance weighting. If areal rainfall uncertainty were ignored, $H_t$ would be the single time series that would be applied for streamflow generation or other water resourcing assessment modelling for the catchment. However, this time series would be certain as it is based on rainfall measurements at only 8 locations within and around the catchment.

By alternately omitting half of the rain gauges whilst maintaining as uniform a spread of rain gauges over the catchment as possible, a lower rain gauge density is achieved and areal rainfalls $L^1_t$ and $L^2_t$ are obtained. Figure 3-2 shows how this could be done for the catchment. The second column shows two groups of 4 rain gauges each that obtain the areal rainfall time series' $L^1_t$ and $L^2_t$.

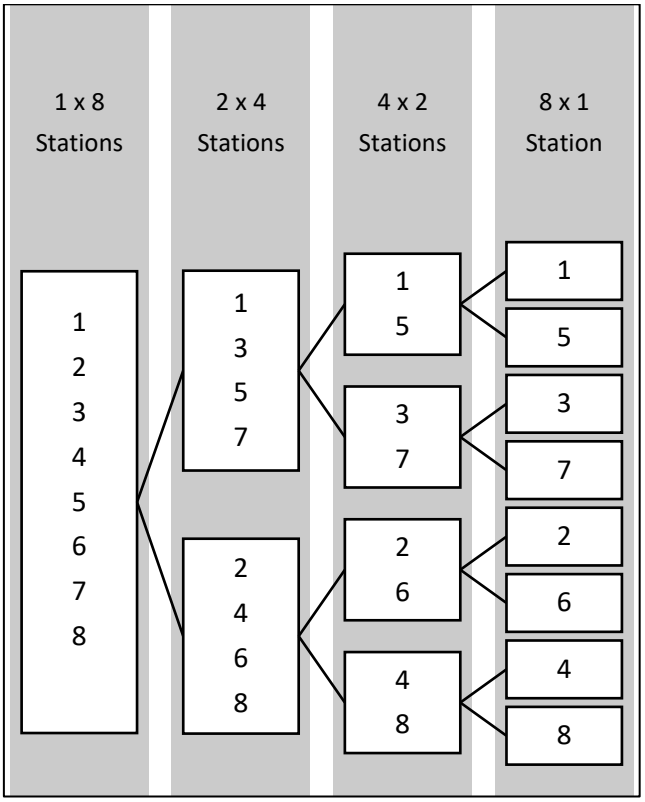



***Figure 3-2: The creation of rainfall groups of different rain gauge densities***

The differences ($P^1_t$ and $P^2_t$) in the areal rainfalls estimates for each time t can then be obtained for period t as:

$$P_t^1 = L_t^1 - L_t^2 \tag{3-1}$$

and

$$P_t^2 = L_t^2 - L_t^1 \tag{3-2}$$

The differences $P^1_t$ and $P^2_t$ indicate that areal rainfall is different from $H_t$ would have been obtained had the 8 rainfall stations been located at locations other than those on Figure 3-1. These differences, that are deemed to be smaller than $P^1_t$ and $P^2_t$, are considered as indicators and quantifiers of the uncertainty. These differences cannot be obtained using the data from 8 gauging stations, but their statistical properties could be estimated from those of $P^1_t$ and $P^2_t$. This requires the determination of the variation of the statistical characteristics of the

differences in areal rainfall with rain gauge density and the extrapolation of this variation from a rain gauge density of 4 stations to that of 8 stations. This first requires the determination of the differences for appropriate rain gauge densities using the available data. The 3rd and 4th columns of Figure 3-2 show how rainfall groups of rain gauge densities of 2 stations and 1 station could be obtained. Ndiritu (2013) found that the cumulative density plots of the differences for different rain gauge densities could be scaled by single factors to equal each other as illustrated on Figure 3-3. For a rain gauge density of 2 and 1 stations where there are more than 1 group, the cumulative density (CDF) plots from the different groups are averaged to obtain the single plots shown on Figure 3-3. The scaling factors of 0.69 and 0.65 (Figure 3-3) in shifting from a lower density to a higher density CDF plot could assumed to be applicable for the scaling from a rain gauge density of 4 stations (which is available) to that of 8 stations which could then be applied to perturb $H_t$ to obtain stochastic areal rainfalls. A conservative approach could use the higher of the two values (0.69) to obtain the CDF plot applicable to 8 stations. Ndiritu (2013) and Ndiritu and Mkhize (2017) termed this factor as the uncertainty factor (***u***) and this name and notation are retained in this study. Randomly generated perturbations from the resulting CDF plot are applied on Ht to obtain an ensemble of stochastic areal rainfalls. Constraints to ensure that negative rainfalls are not generated are imposed. The stochastic rainfalls are then considered as incorporating rainfall uncertainties and can therefore be used instead of the single areal rainfall time series ($H_t$). Ndiritu (2013) and Ndiritu and Mkhize (2017) provide more detailed descriptions of the generator.

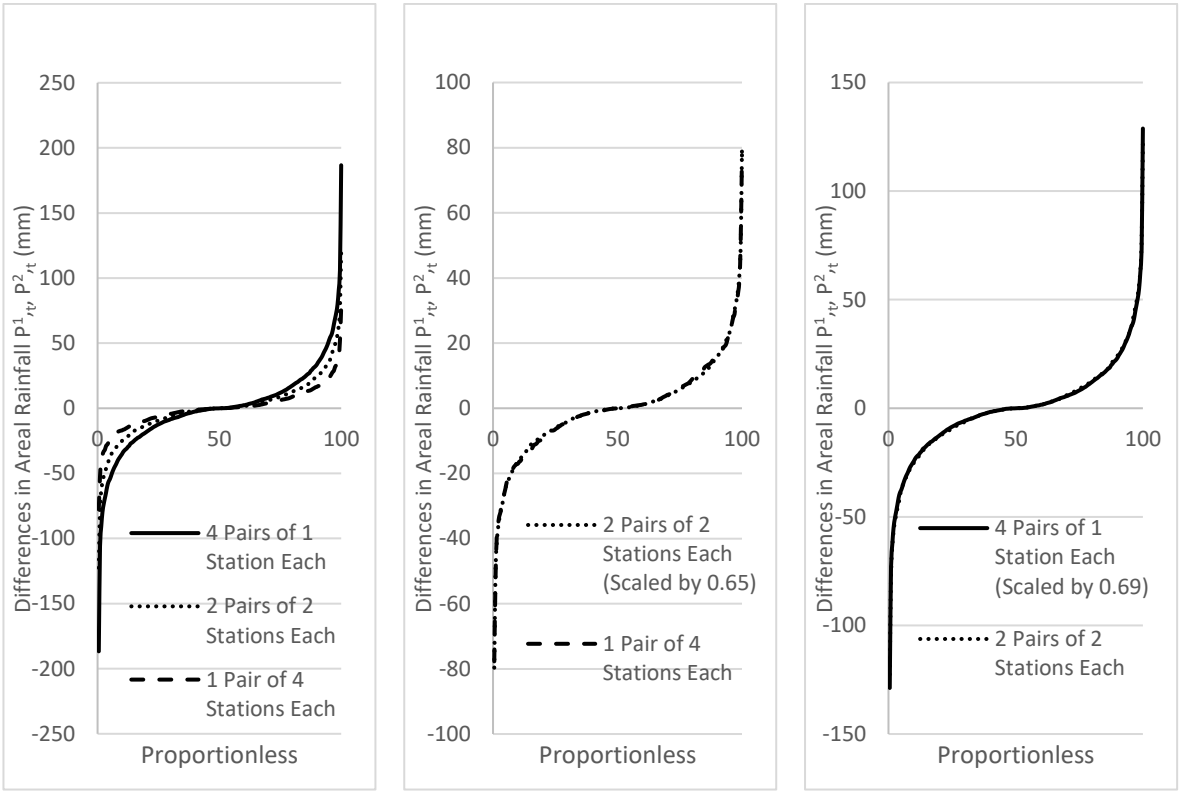



***Figure 3-3: Monthly areal rainfall difference CDF plots and matching***

### 3.2.2 Streamflow simulation

The streamflow modelling was carried out using the GW version of the Pitman model (Hughes, 2004) which consists of 18 parameters, shown in Table 3-1. A hybrid manual-automatic calibration approach that had been previously applied to calibrate the Pitman model (Ndiritu, 2009; Ndiritu & Mkhize, 2017) was applied. The shuffled complex evolution (SCE-UA) optimisation method (Duan et. al., 1992), was setup to automatically search through manually specified parameter ranges for optimal parameter values based on recommedations in the Pitman Model user manual. An objective function that sought to maximize the coefficient of efficiency of the flows (equation 3-3) and the log10 of flows was applied in the calibration. This function enabled a calibration that seeks to match both low and high streamflows to naturalised streamflows. To provide realistic values for the parameters, the parameter ranges was sourced from the WR2012 study (Bailey and Pitman, 2016). The SCE-UA optimizer applied the optimization parameters recommended by Duan et. al. (1994) and calibration was terminated if the proportionate change of the objective function in consecutive epochs of search reduced to less that 0.5 (Ndiritu, 2009). The typical convergence parameter is usually range from 0.05 to 0.1 and the high value (0.5) used here was assigned to reduce the computation intensity due to time constraints.

$$Minimize\ 1 - 0.5\left(C_{eff} + C_{effL}\right) \quad \text{3-3}$$

Where $C_{eff}$ and $C_{effL}$ are the coefficient of efficiency of the flows and the coefficient of efficiency of the log of flows respectively.

***Table 3-1: Parameters of the Pitman Model (Hughes, 2013)***

| Parameter | Units | Description |
|---|---|---|
| PI | mm | Interception storage |
| AI | None | Ratio of impervious to total area |
| Z1 | mm/month | Minimum catchment absorption rate |
| Z3 | mm/month | Maximum catchment absorption rate |
| ST | mm | Maximum moisture storage capacity |
| SL1 | mm | Moisture storage capacity below which no runoff occurs |
| SL2 | mm | |
| FT | mm/month | Runoff from moisture storage at full capacity |
| GW | mm/month | Maximum ground water runoff |
| R | None | Evaporation-moisture storage relationship parameter |
| POW | None | Power of moisture storage-runoff equation |
| GPOW | None | Parameter of the storage-recharge relationship |
| TL | Months | Lag for surface and soil moisture |
| GL | Months | Lag for groundwater runoff |
| Prop of Catchment with Lower Side GW Table | None | Proportion of Catchment with Lower Side GW Table |
| Riparian Strip | m | Riparian strip factor |
| Transmissivity | None | |
| RWL | m | Rest Water Level |
| Porosity | None | |
| Initial Lower GW Slope | m | Initial regional lower ground water slope |
| Initial Upper GW Slope | m | Initial regional upper groundwater slop |

To assess the effect of areal rainfall uncertainty while allowing for parameter uncertainty, 100 randomly initialised calibration-validation runs using the single observed monthly rainfalls were compared with 100 randomly initalised runs using 100 stochastic rainfall sequences. The stochastic rainfalls were derived by direct application of the stochastic rainfall generator described in Section 3.2.1.

### 3.2.3 Comparison of Calibration Performance

The quality of the modelling is a reflection of factors such as the model structure, the effectiveness of calibration and the quality of data (Ndiritu, 2009). Ndiritu (2009) and Ndiritu & Mkhize (2017) used the coefficient of efficiency of the flows (CE) and of the logs of flows (CEL10), the correlation coefficient (CC), the bias, the coefficient of mean absolute deviation

(SCDEV) and the residual mass curve coefficient (RMCC) to evaluate the quality of the stream flow modelling. The same approach was adopted in this study. The CE, CEL10, CC and bias are commonly used parameters used to evaluated modelling quality (Ndiritu, 2009). The SCDEV, defined by Ndiritu (2009) in equation 5-1, is a more informative bias measure in which absolute differences between the observed and simulated flows are applied (Ndiritu & Mkhize, 2017).

The RMCC, as defined by Ndiritu (2009) in presented in equations 3-4 to 3-9 and is designed to quantify the extent of systemic errors in the simulated time series. It takes a maximum value of 1 with lower values indicating greater systematic errors (Ndiritu & Mkhize, 2017).

$$SCDEV = \frac{\sum_{i=1}^{n}\left|q_i^{sim} - q_i^0\right|}{\sum_i^n q_i^0} \tag{3-4}$$

$$RMCC = 1 - \frac{\sum_{j=1}^{n}\left|q_j^{sim^{res}} - q_j^{0^{res}}\right|}{\sum_j^n q_j^{0^{res}}} \tag{3-5}$$

$$q_j^{0^{res}} = \sum_{i=1}^{j}\left(q_i^0 - \overline{q^0}\right) \tag{3-6}$$

$$q_j^{sim^{res}} = \sum_{i=1}^{j}\left(q_i^{sim} - \overline{q^{sim}}\right) \tag{3-7}$$

$$\overline{q^0} = \frac{1}{n}\sum_{i=1}^{n} q_i^0 \tag{3-8}$$

$$\overline{q^{sim}} = \frac{1}{n}\sum_{i=1}^{n} q_i^{sim} \tag{3-9}$$

Where: $q_i^{sim}$ and $q_i^0$ is the simulated and observed monthly flows; n is the number of months of analysis

## 3.3 Data and Study Catchments

### 3.3.1 Rainfall Data

The WR2012 study (Bailey and Pitman, 2016) is the latest revision of a series of water resource appraisals in South African commissioned by the Water Resources Commission

(WRC) (Bailey & Pitman, 2016). The rainfall data for this study was sourced from the WR2012 study and is freely available on the WR2012 website. The rain gauges available in the WR2012 database are shown on Figure 3-4 which shows wide coverage across South Africa.

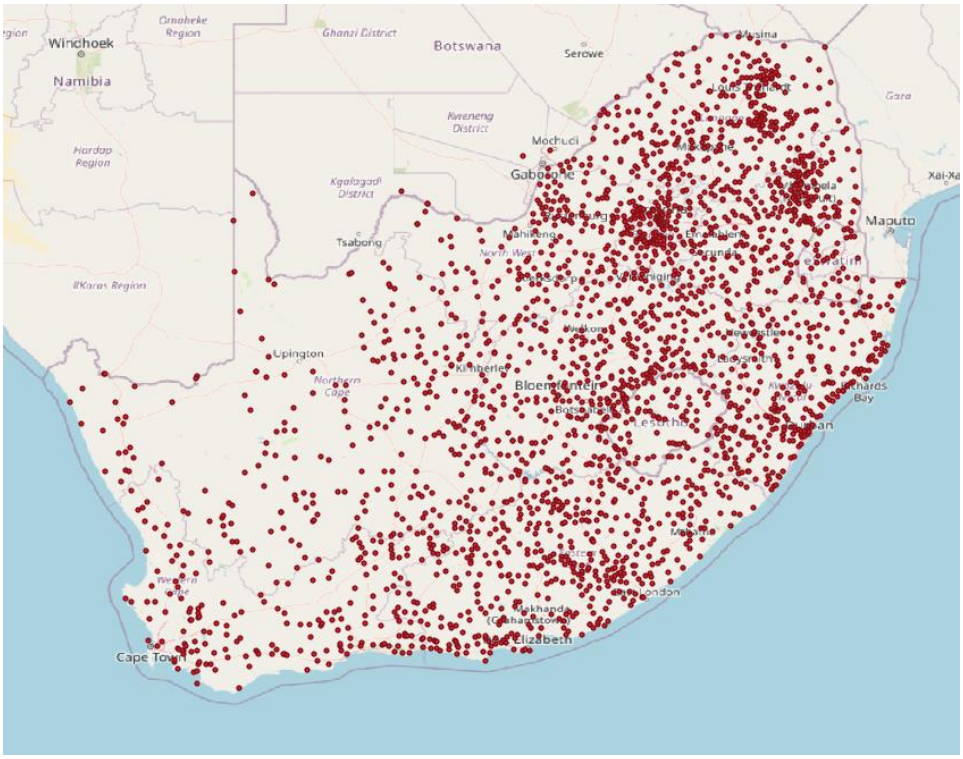



***Figure 3-4: Rain Gauges available in theWR2012 database (Bailey and Pitman, 2016)***

### 3.3.2 Selection of Study Catchments and Rain Gauge Groups

The study catchments were selected from locations in South Africa that do not receive significant amounts of snowfall. Rain gauge groups were then selected from each of the proposed study catchments, such that reasonably uniform catchment coverage could be achieved, as required for the stochastic areal rainfall generation (Ndiritu ,2013; Ndiritu & Mkhize, 2017).

The use of measured rainfall data with minimal patching leads to more dependable analysis with less patching errors and biases and catchments with such rain gauge records were therefore sought.

### 3.3.3 Naturalised Streamflow Data

The WR2012 study uses quaternary level catchments for the modelling of water resources in South Africa (Bailey & Pitman, 2016). Naturalised monthly stream flows for these quaternary catchments are readily available on the WR2012 website (www.waterresourceswr2012.co.za) and were used in this study as sufficient data for catchments with insignificant human impacts (i.e., impacts from dams, agricultural activities etc.) could not be found. These were

incremental contributions of the from the WR2012 data. Although it would be preferable to use observed natural stream flows, there is generally significant land use and/or water resource infrastructure in gauged catchments.

### 3.3.4 Study Catchments

#### *3.3.4.1 Overview*

Seven quaternary catchments across South Africa were selected for this study based on the following criteria:

- Availability of at least 8 rain gauges, with a minimum period of 10 years' worth of rainfall data, inside or in proximity to the catchment;
- Naturalised streamflow data available for the stream(s) at the catchment outlet.

Table 3-2 provides basic information on these catchments while Figure 3-2 shows their locations within South Africa. Additional details for each catchment are provided in the following sections including the locations of the rain gauging stations and the rainfall grouping applied for stochastic rainfall generation. The grouping aimed to obtain coverage that is representative of the catchment area to the best extent possible which is revealed in the adopted groupings. This grouping is not applicable for the lowest rain gauge density of 1 rain gauge although having a single station in (or in the vicinity of) a catchment is a reality of practical water resources assessment in many regions of the world.

***Table 3-2: Summary of Study Catchments***

| WR2012 Catch. No. | Catchment Name | Water Management Area | Province | Size (km²) | Start Year | End Year |
|---|---|---|---|---|---|---|
| D31E | Vanderkloof | Upper Orange | Northern Cape | 910 | 1930 | 1977 |
| A21J | Bonjanala | Crocodile (West) and Marico | North West | 1030 | 1963 | 2000 |
| X31B | Sabie | Inkomati | Mpumalanga | 170 | 1972 | 1993 |
| C23L | Potchefstroom | Upper Vaal | North West | 1100 | 1929 | 1981 |
| U20E | Howick | Mvoti to Umzimkulu | Kwa Zulu Natal | 360 | 1974 | 1988 |
| H10C | Bella Vista | Breede | Western Cape | 250 | 1969 | 2004 |
| D22B | Ficksburg | Upper Orange | Free State | 420 | 1940 | 1989 |

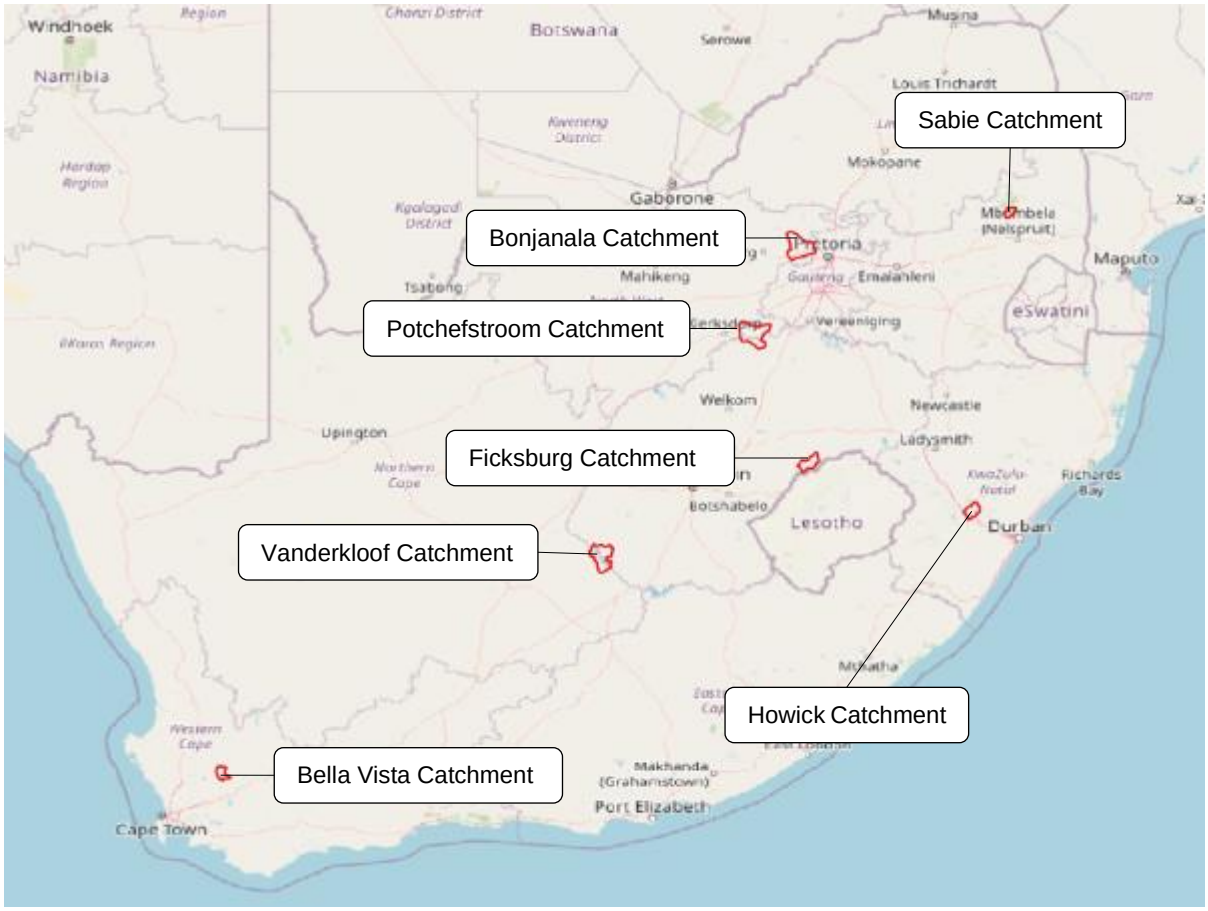



***Figure 3-5: Study Catchments***

### *3.3.4.2 Bella Vista Catchment (WR2012 Catchment No. H10C)*

The Bella Vista Catchment (shown in Figure 3-6), which is approximately 250km² in size, is located in the Western Cape province of South Africa and falls within the Breede WMA. The catchment contains the Ceres Koekedouw Dam reservoir and is traversed by the Koekedou and Dwars River.

***Table 3-3: Bella Vista Catchment Rain Gauge Data***

| ID | Gauge Number | Location | | MAP (mm) | Period (years) | |
|---|---|---|---|---|---|---|
| | | Lat | Long | | Start | End |
| 1 | 0042355 W | 33.42 | 19.20 | 595 | 1989 | 2004 |
| 2 | 0042227 W | 33.28 | 19.15 | 479 | 1989 | 2004 |
| 3 | 0042281 W | 33.20 | 19.17 | 984 | 1989 | 2004 |
| 4 | 0042669 W | 33.15 | 19.38 | 379 | 1989 | 2004 |
| 5 | 0042582 W | 33.20 | 19.33 | 687 | 1989 | 2004 |
| 6 | 0042588 W | 33.30 | 19.33 | 544 | 1989 | 2004 |
| 7 | 0042621 W | 33.35 | 19.35 | 572 | 1989 | 2004 |
| 8 | 0042532 W | 33.37 | 19.32 | 1049 | 1989 | 2004 |

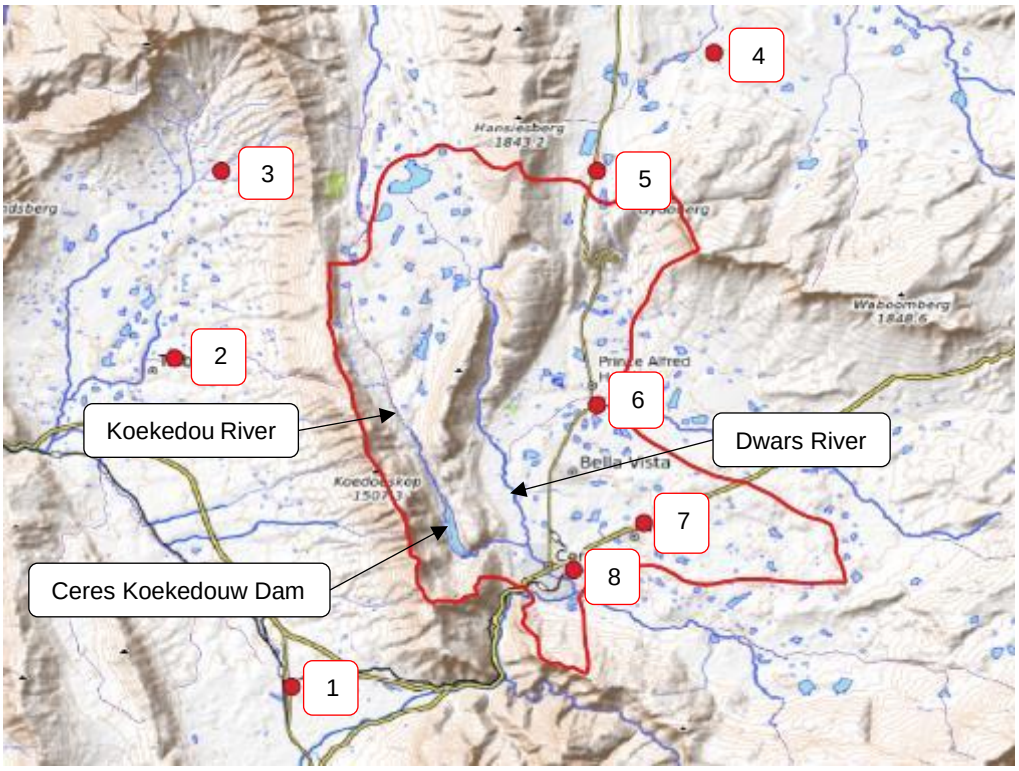



***Figure 3-6: Bella Vista Catchment***

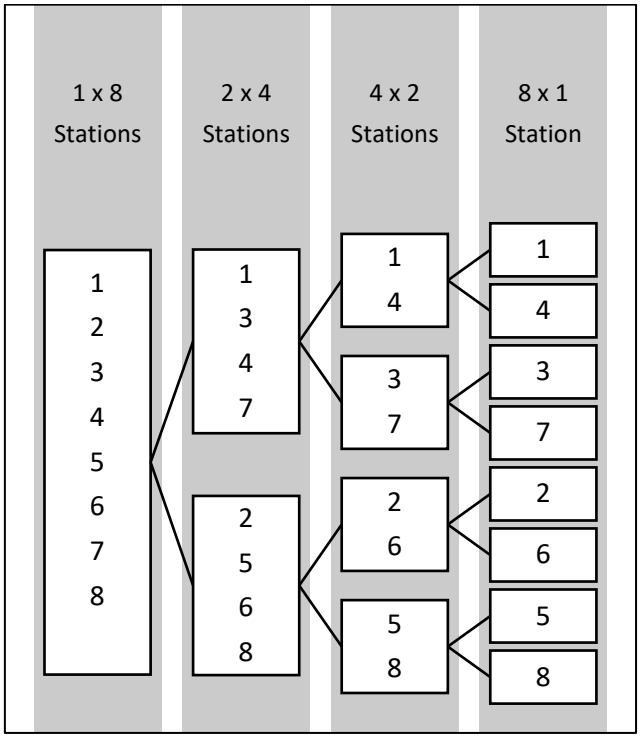



***Figure 3-7: Rainfall groupings for Bella Vista Catchment***

### *3.3.4.3 Bojanala Catchment (WR2012 Catchment No. A21J)*

The Bonjanala Catchment (shown in Figure 3-8), which is approximately 1030km² in size, is located in the North West province of South Africa and falls within the Crocodile (West) and Marico WMA. The catchment is immediately downstream of the Hartbeespoort Dam reservoir from which the crocodile river emerges and traverses through the catchment.

***Table 3-4: Bonjanala Catchment Rain Gauge Data***

| ID | Gauge Number | Location | | MAP (mm) | Period (years) | |
|---|---|---|---|---|---|---|
| | | Lat | Long | | Start | End |
| 1 | 0549354 W | 25.40 | 27.65 | 506 | 1963 | 2000 |
| 2 | 0512451 W | 25.52 | 27.78 | 579 | 1963 | 2000 |
| 3 | 0512757 W | 25.63 | 27.95 | 620 | 1963 | 2000 |
| 4 | 0512613 W | 25.72 | 27.85 | 672 | 1963 | 2000 |
| 5 | 0512280 W | 25.67 | 27.67 | 645 | 1963 | 2000 |
| 6 | 0512580 W | 25.65 | 27.83 | 620 | 1963 | 2000 |
| 7 | 0512552 W | 25.70 | 27.80 | 643 | 1963 | 2000 |
| 8 | 0512246 W | 25.60 | 27.65 | 602 | 1963 | 2000 |

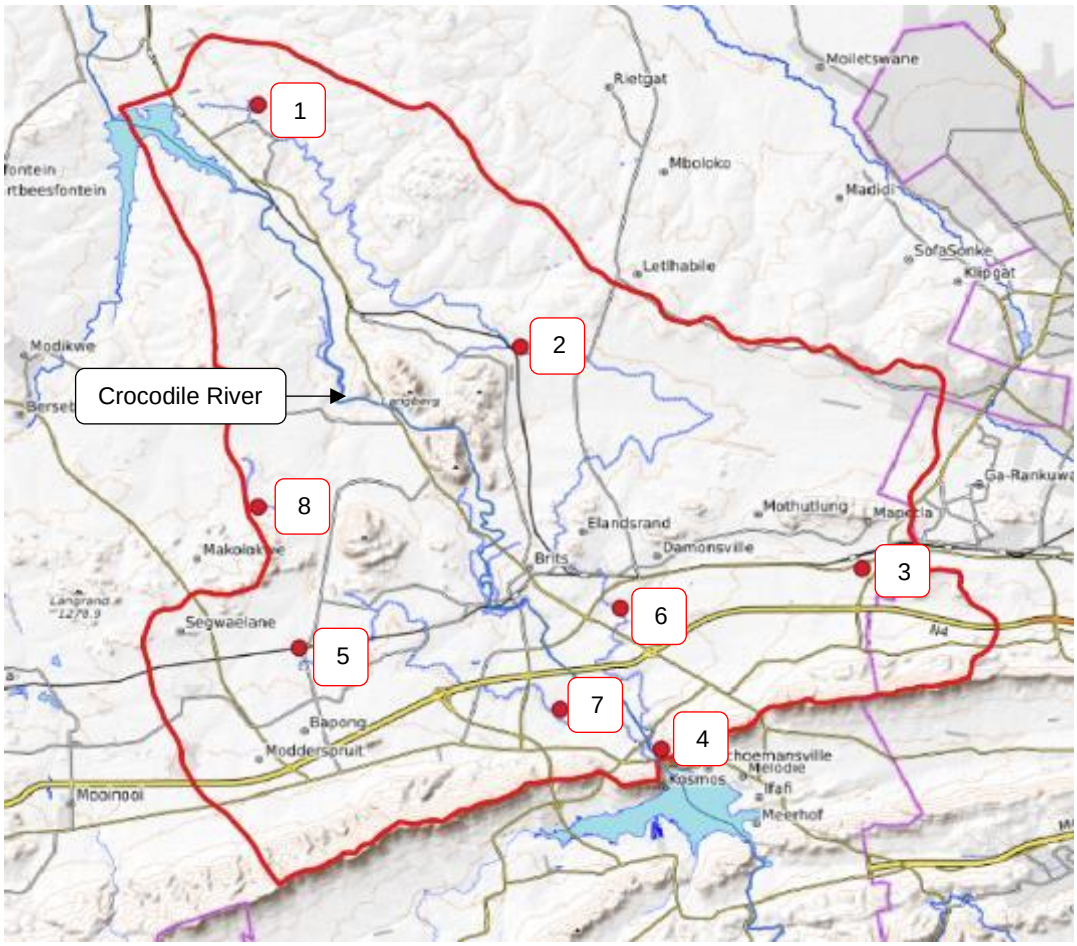



***Figure 3-8: Bonjanala Catchment***

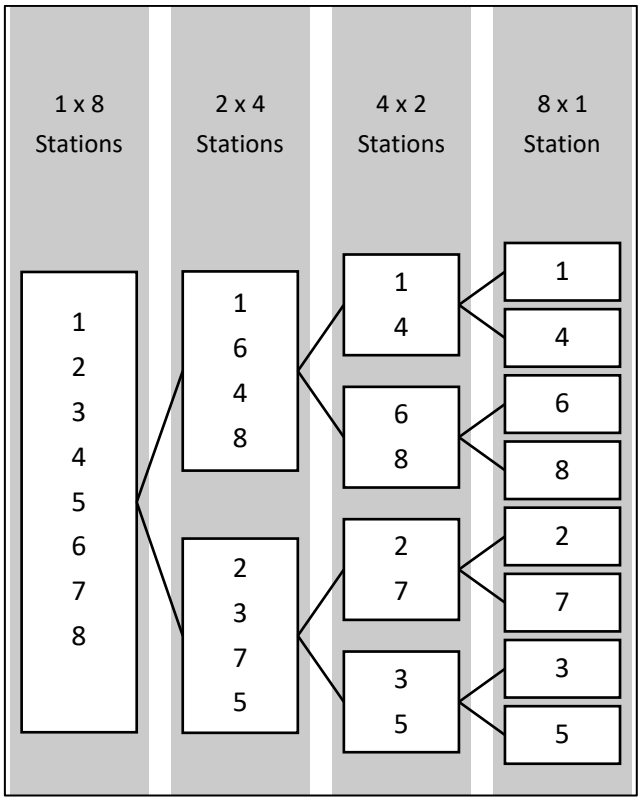



***Figure 3-9: Rainfall groupings for Bonjanala***

### *3.3.4.4 Ficksburg Catchment (WR2012 Catchment No. D22B)*

The Ficksburg Catchment (shown in Figure 3-10), which is approximately 420km² in size, is located in the Free State province of South Africa and falls within the Upper Orange WMA. The catchment is traversed by the Meulspruit River.

***Table 3-5: Ficksburg Catchment Rain Gauge Data***

| ID | Gauge Number | Location | | MAP (mm) | Period (years) | |
|---|---|---|---|---|---|---|
| | | Lat | Long | | Start | End |
| 1 | 0296583 W | 28.83 | 27.72 | 694 | 1940 | 1989 |
| 2 | 0296731 W | 28.73 | 27.85 | 684 | 1940 | 1989 |
| 3 | 0297092 W | 28.87 | 27.88 | 735 | 1940 | 1989 |
| 4 | 0296886 W | 28.70 | 27.92 | 687 | 1940 | 1989 |
| 5 | 0296825 W | 28.78 | 27.93 | 776 | 1940 | 1989 |
| 6 | 0296767 W | 28.75 | 27.97 | 729 | 1940 | 1989 |
| 7 | 0296682 W | 28.78 | 28.00 | 722 | 1940 | 1989 |
| 8 | 0296379 W | 28.53 | 28.08 | 775 | 1940 | 1989 |

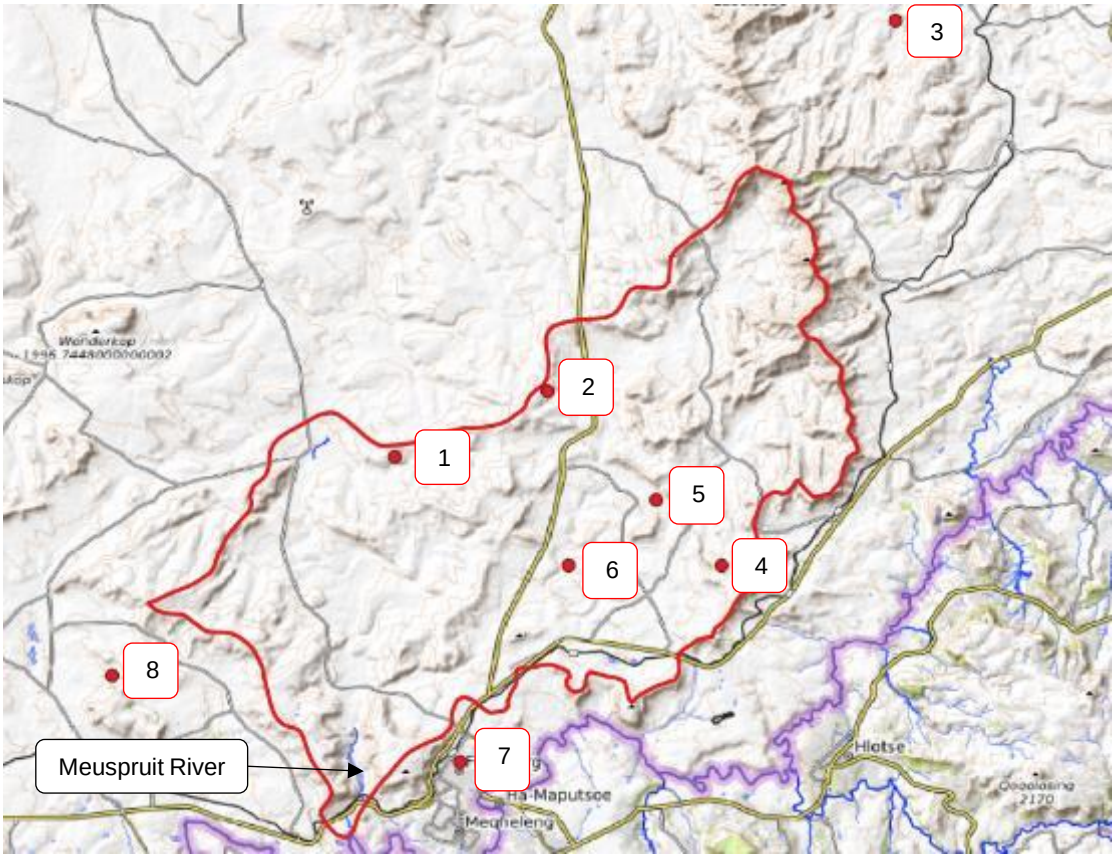



***Figure 3-10: Ficksburg Catchment***

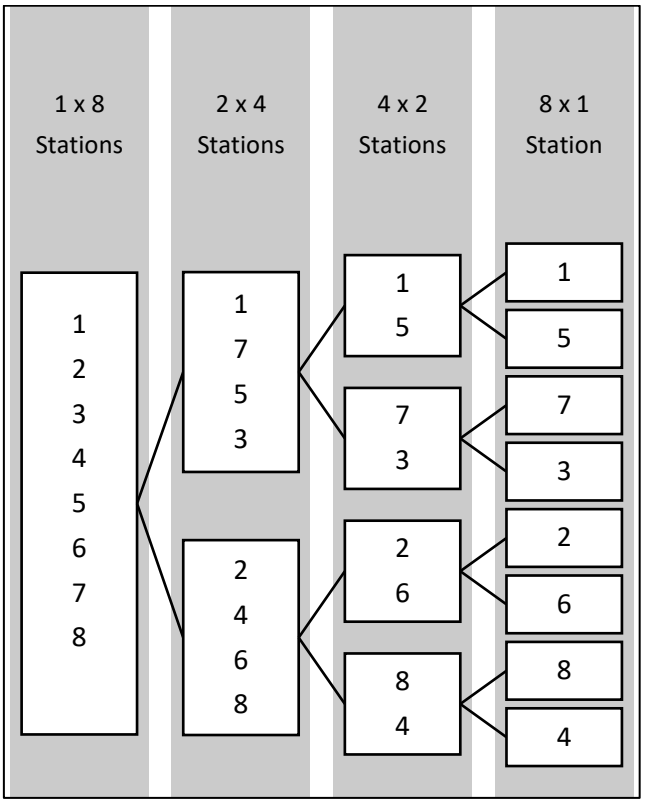



***Figure 3-11: Rainfall groupings for Ficksburg***

### *3.3.4.5 Howick Catchment (WR2012 Catchment No. U20E)*

The Howick Catchment (shown in Figure 3-12), which is approximately 360km² in size, is located in the Kwa Zulu Natal province of South Africa and falls within the Mvoti to Umzimkulu WMA. The catchment is immediately upstream of the Midmar Dam reservoir, contains the Albert Falls Dam reservoir; and is traversed by the uMngeni and Karkloof Rivers.

***Table 3-6: Howick Catchment Rain Gauge Data***

| ID | Gauge Number | Location | | MAP (mm) | Period (years) | |
|---|---|---|---|---|---|---|
| | | Lat | Long | | Start | End |
| 1 | 0269532 A | 29.37 | 30.30 | 1196 | 1974 | 1988 |
| 2 | 0269647 W | 29.28 | 30.37 | 1696 | 1974 | 1988 |
| 3 | 0269712 W | 29.37 | 30.42 | 1078 | 1974 | 1988 |
| 4 | 0269775 W | 29.42 | 30.43 | 787 | 1974 | 1988 |
| 5 | 0269744 S | 29.40 | 30.42 | 1231 | 1974 | 1988 |
| 6 | 0239482 W | 29.53 | 30.28 | 853 | 1974 | 1988 |
| 7 | 0239604 W | 29.58 | 30.35 | 999 | 1974 | 1988 |
| 8 | 0269883 U | 29.50 | 30.20 | 878 | 1974 | 1988 |

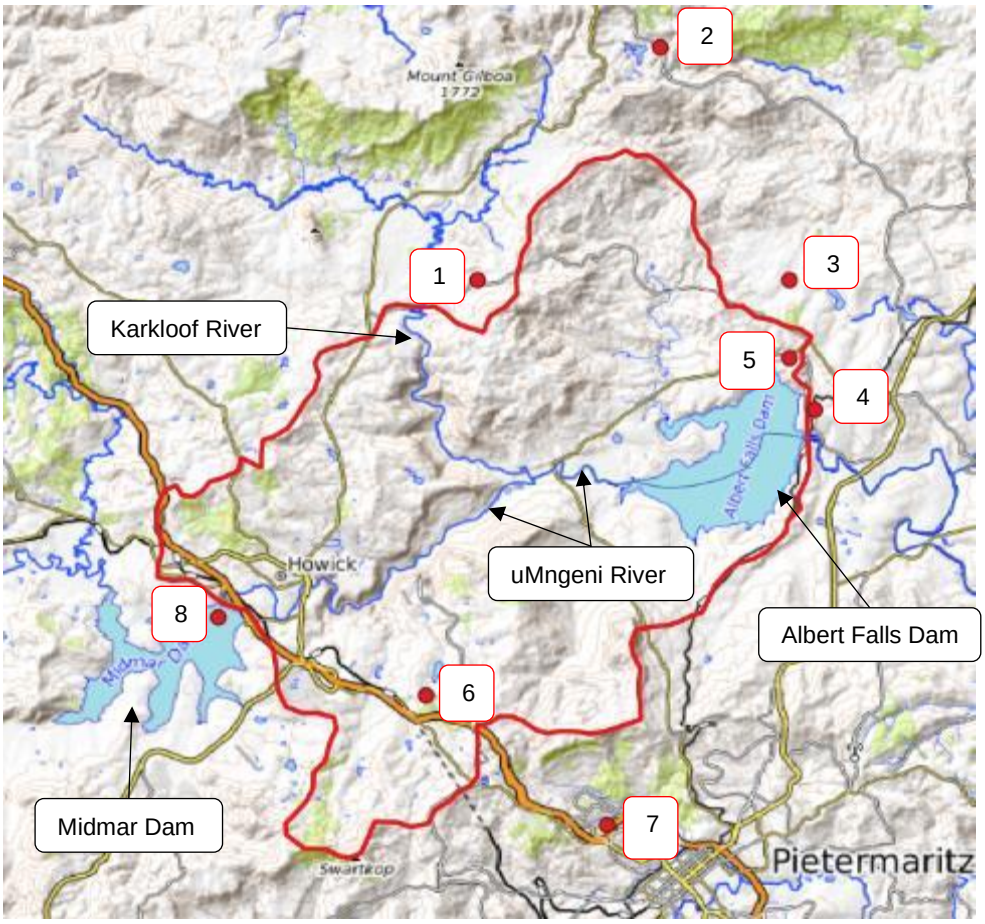



***Figure 3-12: Howick Catchment***

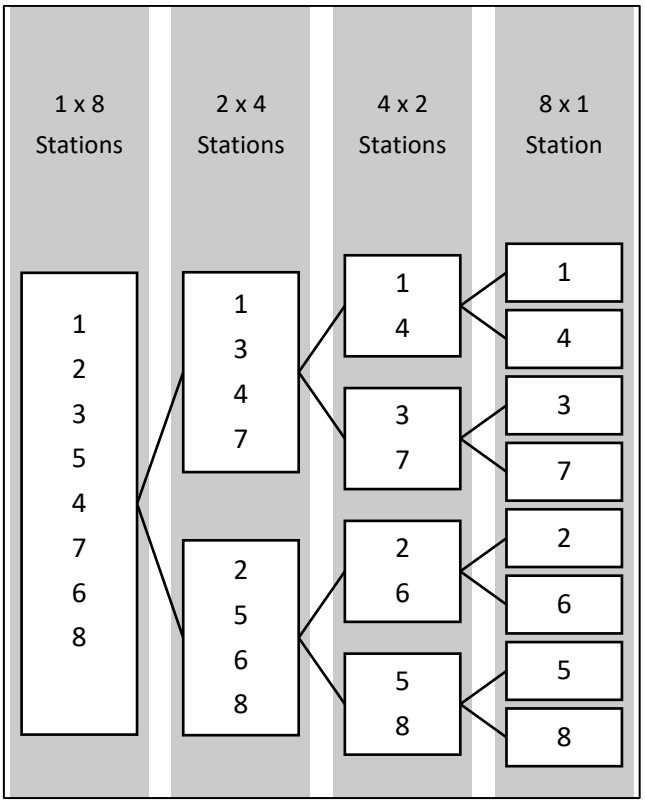



***Figure 3-13: Rainfall groupings for Howick***

### *3.3.4.6 Potchefstroom Catchment (WR2012 Catchment No. C23L)*

The Potchefstroom Catchment (shown in Figure 3-14), which is approximately 1100km² in size, is located in the North West province of South Africa and falls within the Upper Vaal WMA. The catchment is traversed by the Mooi River and Vaal River.

***Table 3-7: Potchefstroom Catchment Rain Gauge Data***

| ID | Gauge Number | Location | | MAP (mm) | Period (years) | |
|---|---|---|---|---|---|---|
| | | Lat | Long | | Start | End |
| 1 | 0436495 W | 26.75 | 26.78 | 598 | 1929 | 1981 |
| 2 | 0436855 A | 26.75 | 26.98 | 628 | 1929 | 1981 |
| 3 | 0437104 W | 26.73 | 27.07 | 619 | 1929 | 1981 |
| 4 | 0437555 W | 26.75 | 27.30 | 605 | 1929 | 1981 |
| 5 | 0437383 W | 26.88 | 27.22 | 643 | 1929 | 1981 |
| 6 | 0437660 W | 27.00 | 27.38 | 669 | 1929 | 1981 |
| 7 | 0436577CP | 26.98 | 27.05 | 684 | 1929 | 1981 |
| 8 | 0436747 W | 26.95 | 26.92 | 601 | 1929 | 1981 |

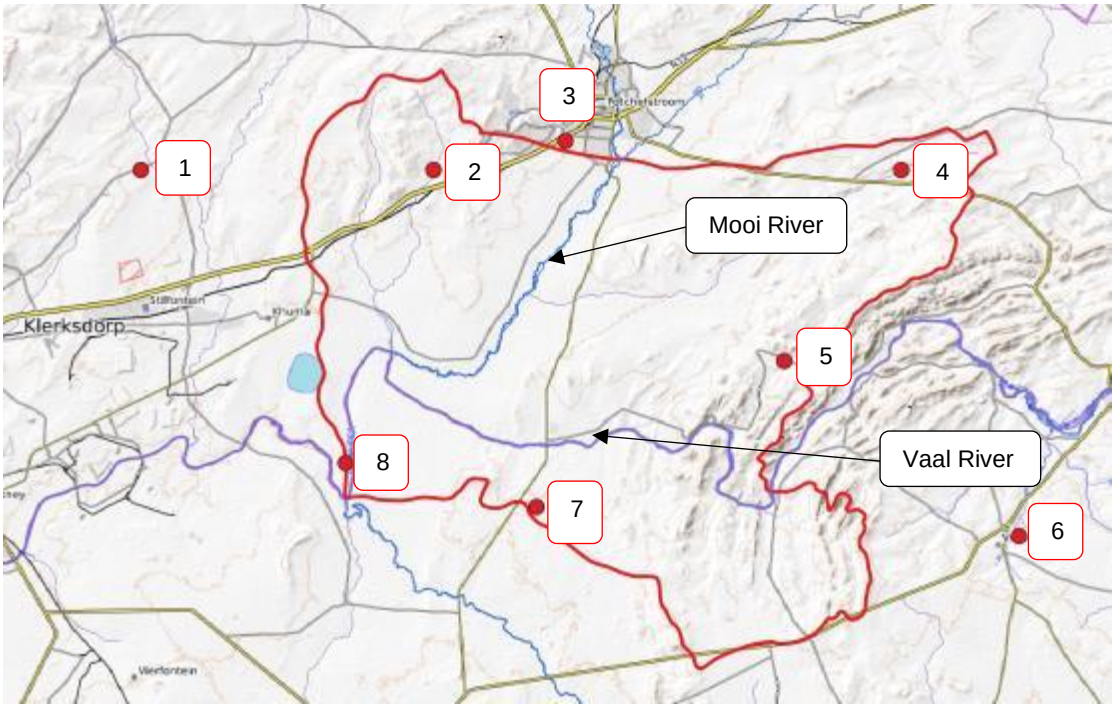



***Figure 3-14: Potchefstroom Catchment***

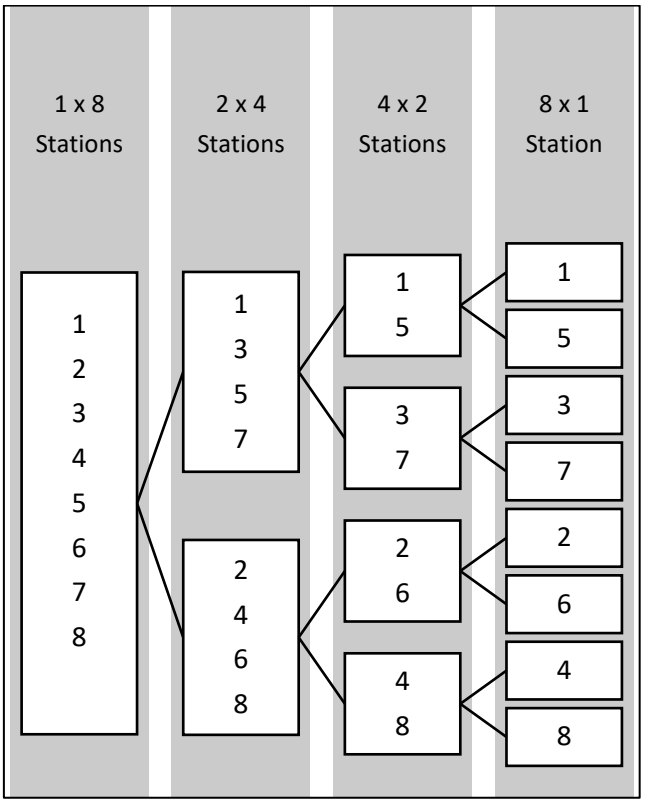



***Figure 3-15: Rainfall groupings for Potchefstroom***

### *3.3.4.7 Sabie Catchment (WR2012 Catchment No. X31B)*

The Sabie Catchment (shown in Figure 3-16), which is approximately 170km² in size, is located in the Mpumalanga province of South Africa and falls within the Inkomati WMA. The catchment is traversed by the Sabie River.

***Table 3-8: Sabie Catchment Rain Gauge Data***

| ID | Gauge Number | Location | | MAP (mm) | Period (years) | |
|---|---|---|---|---|---|---|
| | | Lat | Long | | Start | End |
| 1 | 0555455 W | 25.10 | 30.75 | 1213 | 1972 | 1993 |
| 2 | 0555483 W | 25.05 | 30.78 | 1233 | 1972 | 1993 |
| 3 | 0555486 W | 25.10 | 30.78 | 1111 | 1972 | 1993 |
| 4 | 0555573 W | 25.05 | 30.83 | 1620 | 1972 | 1993 |
| 5 | 0555631 W | 25.02 | 30.87 | 1673 | 1972 | 1993 |
| 6 | 0555662 W | 25.03 | 30.88 | 1450 | 1972 | 1993 |
| 7 | 0555664 W | 25.07 | 30.88 | 1242 | 1972 | 1993 |
| 8 | 0555579 W | 25.15 | 30.83 | 1220 | 1972 | 1993 |

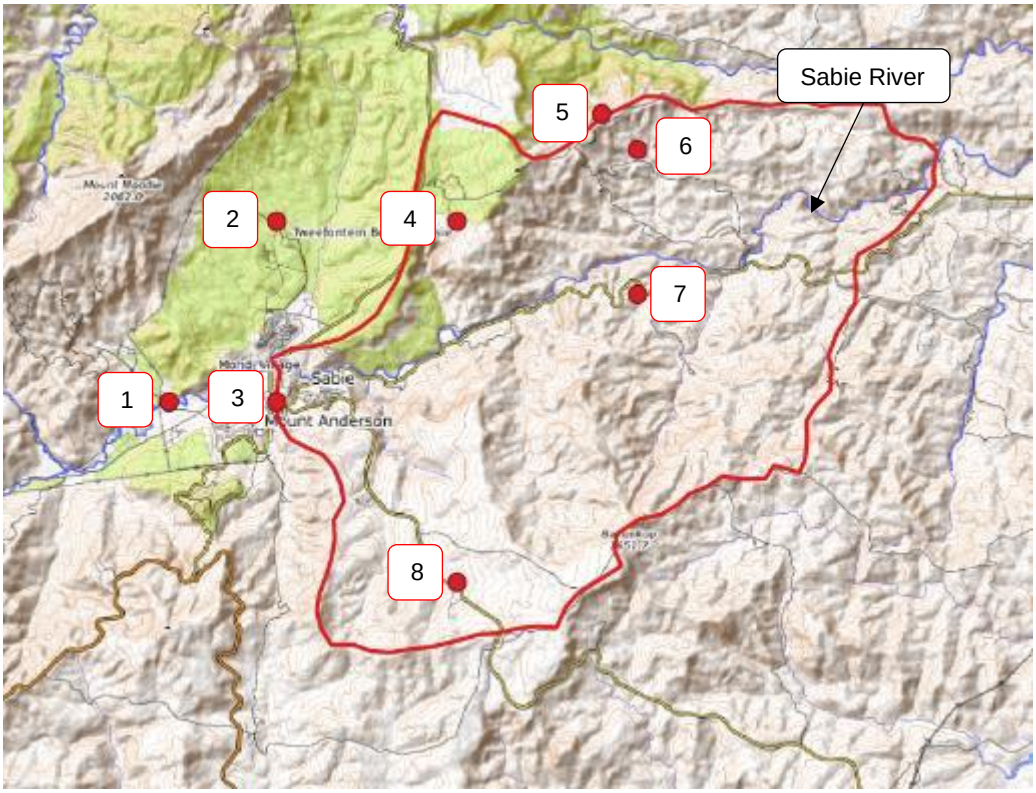



***Figure 3-16: Sabie Catchment***

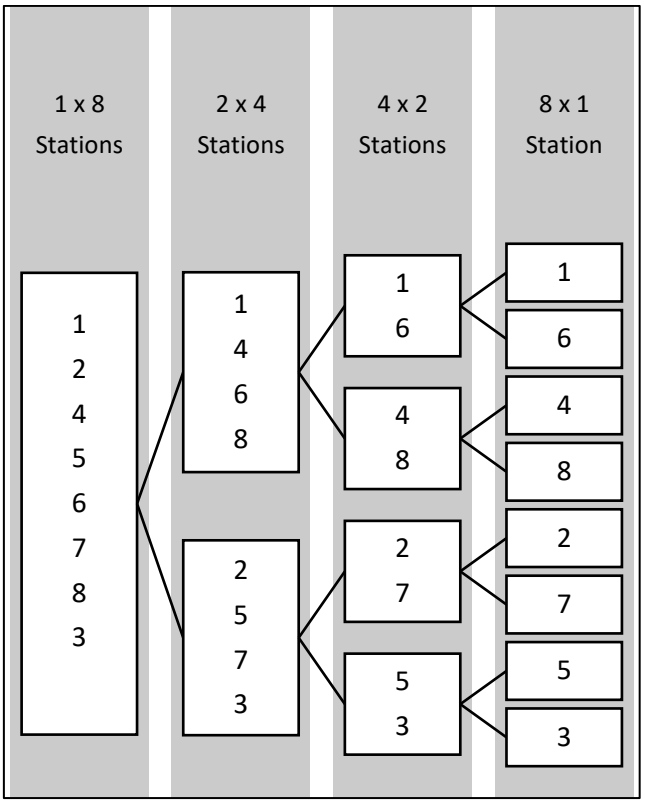



***Figure 3-17: Rainfall groupings for Sabie***

### *3.3.4.8 Vanderkloof Catchment (WR2012 Catchment No. D31E)*

The Vanderkloof catchment (shown in Figure 3-18), which is approximately 910km² in size, is located in the along the Northern Cape / Free State border in South Africa and falls within the Upper Orange Water Management Area (WMA). The Vanderkloof Dam reservoir, which is formed on the Orange River, falls within the catchment.

***Table 3-9: Vanderkloof Catchment Rain Gauge Data***

| ID | Gauge Number | Location | | MAP (mm) | Period (years) | |
|---|---|---|---|---|---|---|
| | | Lat | Long | | Start | End |
| 1 | 0199275 W | 30.08 | 24.67 | 350 | 1930 | 1977 |
| 2 | 0228170 W | 29.85 | 24.60 | 345 | 1930 | 1977 |
| 3 | 0228567 W | 29.97 | 24.83 | 390 | 1930 | 1977 |
| 4 | 0229089 W | 29.98 | 25.07 | 414 | 1930 | 1977 |
| 5 | 0200166 W | 30.25 | 25.10 | 395 | 1930 | 1977 |
| 6 | 0200058 W | 30.47 | 25.02 | 339 | 1930 | 1977 |
| 7 | 0171546 W | 30.60 | 24.83 | 396 | 1930 | 1977 |
| 8 | 0199435 W | 30.27 | 24.75 | 361 | 1930 | 1977 |

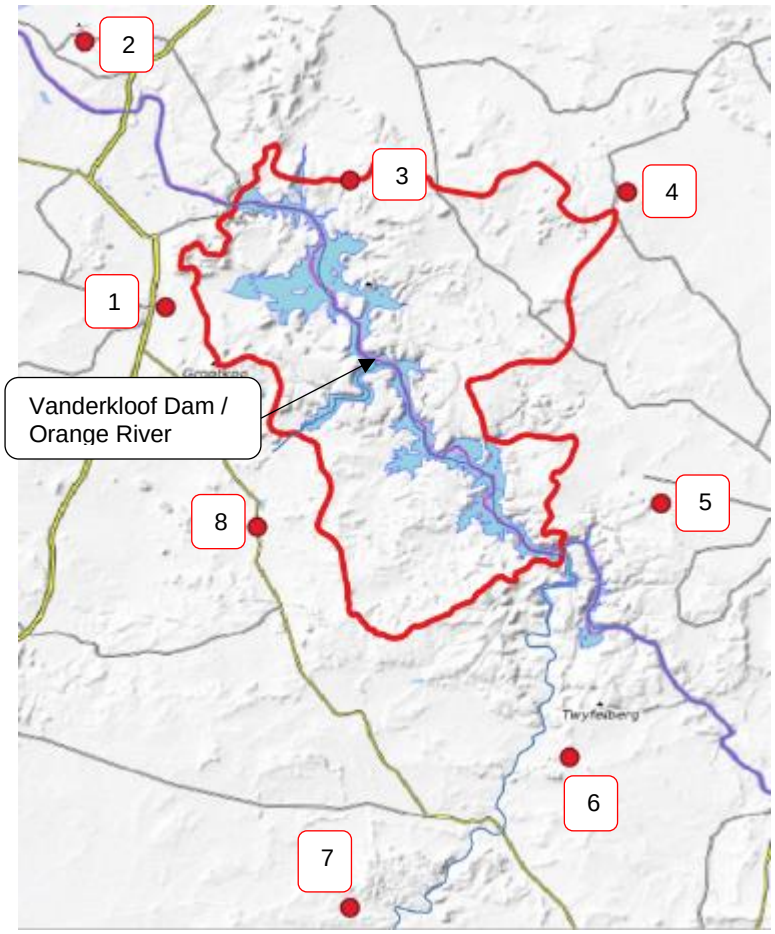



***Figure 3-18: Vanderkloof Catchment***

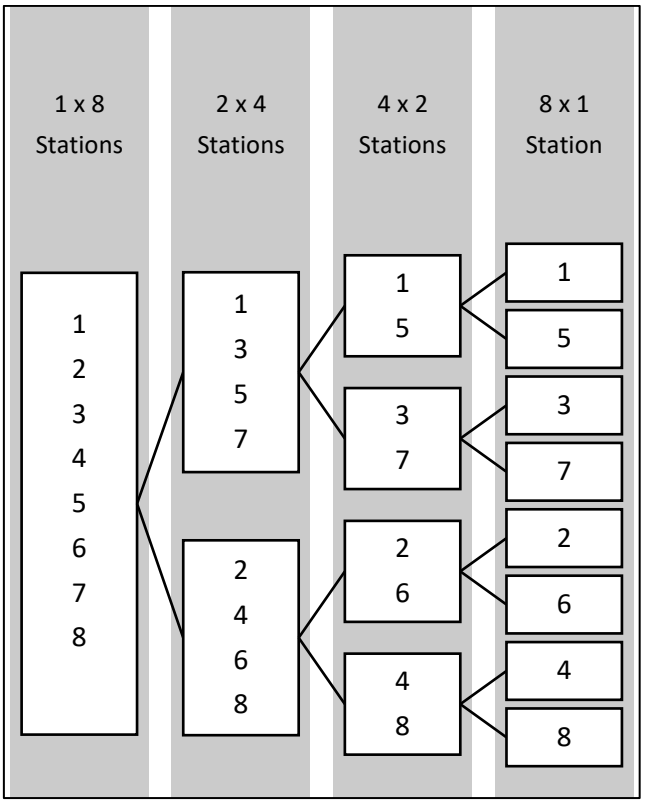



***Figure 3-19: Rainfall groupings for Vanderkloof***

# 4. Results, Analysis, and Discussion of Stochastic Rainfall Generation

## 4.1 Overview

The average differences of areal rainfalls obtained, cumulative density plots, scaling factors and analysis of the stochastically generated rainfalls are discussed in this section. Inverse distance weighting using an index of 2 was applied to determine areal rainfall.

## 4.2 Average Differences of Areal Rainfalls and their significance

### 4.2.1 Overview

The values of the computed differences in areal rainfall ($P_t^1$ and $P_t^2$ ; equation 3-1 and 3-2) in relation to the areal rainfall indicate the magnitude of the areal rainfall uncertainty (Ndiritu & Mkhize, 2017). These differences are expected to reduce as rain gauge density increases and would ideally converge to zero once the rain gauge density exceeds that required to perfectly measure all rain falling in the catchment (Ndiritu & Mkhize, 2017). This section presents the average differences in areal rainfall obtained for the various rain gauge densities for the study catchments; and also expresses these averages as percentages of the average monthly rainfall ($R_A$) to assess their significance.

### 4.2.2 Areal rainfall differences for the Study Catchments

The average differences of areal rainfalls for the seven study catchments are shown in Table 4-1 to Table 4-7. The average differences increase as the rain gauge density reduces. This indicates an increase in the significance of rainfall uncertainty with decreasing rain gauge density. The average differences at the rain gauge density of 4 stations ranges from 13% to 21% of the monthly average rainfall for the seven catchments and averages 18.3% which is close to the average of 20.4% obtained for the two catchments studied by Ndiritu & Mkhize (2017).

***Table 4-1: Average differences of areal rainfalls at various rain gauge densities for Bella Vista catchment***

| No of rain gauges | Group 1 | Group 2 | Average difference ($\overline{P_t^1}$) | $\frac{\overline{P_t^1}}{R_A}$ |
|---|---|---|---|---|
| 4 | 1, 3, 4, 7 | 2, 5, 6, 8 | 11.9 | 20% |
| 2 | 1, 4 | 3, 7 | 16.8 | 29% |
| | 2, 6 | 5, 8 | 21.6 | 37% |
| 1 | 1 | 4 | 54.0 | 93% |
| | 3 | 7 | 14.7 | 25% |
| | 2 | 6 | 39.4 | 67% |
| | 5 | 8 | 27.0 | 46% |

***Table 4-2: Average differences of areal rainfalls at various rain gauge densities for Bonjanala catchment***

| No of rain gauges | Group 1 | Group 2 | Average difference ($\overline{P_t^1}$) | $\frac{\overline{P_t^1}}{R_A}$ |
|---|---|---|---|---|
| 4 | 1, 6, 4, 8 | 2, 3, 7, 5 | 10.3 | 21% |
| 2 | 1, 4 | 6, 8 | 15.9 | 32% |
| | 2, 7 | 3, 5 | 15.3 | 30% |
| 1 | 1 | 4 | 21.4 | 42% |
| | 6 | 8 | 27.6 | 55% |
| | 2 | 7 | 26.7 | 53% |
| | 3 | 5 | 21.8 | 43% |

***Table 4-3: Average differences of areal rainfalls at various rain gauge densities for Ficksburg catchment***

| No of rain gauges | Group 1 | Group 2 | Average difference ($\overline{P_t^1}$) | $\frac{\overline{P_t^1}}{R_A}$ |
|---|---|---|---|---|
| 4 | 1, 7, 5, 3 | 2, 4, 6, 8 | 7.8 | 13% |
| 2 | 1, 5 | 7, 3 | 8.4 | 14% |
| | 2, 6 | 8, 4 | 12.1 | 20% |
| 1 | 1 | 5 | 14.4 | 24% |
| | 7 | 3 | 13.2 | 22% |
| | 2 | 6 | 21.4 | 35% |
| | 8 | 4 | 21.4 | 35% |

***Table 4-4: Average differences of areal rainfalls at various rain gauge densities for Howick catchment***

| No of rain gauges | Group 1 | Group 2 | Average difference ($\overline{P_t^1}$) | $\frac{\overline{P_t^1}}{R_A}$ |
|---|---|---|---|---|
| 4 | 1, 3, 4, 7 | 2, 5, 6, 8 | 15.6 | 17% |
| 2 | 1, 4 | 3, 7 | 27.9 | 31% |
| | 2, 6 | 5, 8 | 17.7 | 19% |
| 1 | 1 | 4 | 78.1 | 86% |
| | 3 | 7 | 41.0 | 45% |
| | 2 | 6 | 24.6 | 27% |
| | 5 | 8 | 29.7 | 33% |

***Table 4-5: Average differences of areal rainfalls at various rain gauge densities for Potchefstroom catchment***

| No of rain gauges | Group 1 | Group 2 | Average difference ($\overline{P_t^1}$) | $\frac{\overline{P_t^1}}{R_A}$ |
|---|---|---|---|---|
| 4 | 1, 3, 5, 7 | 2, 4, 6, 8 | 9.7 | 18% |
| 2 | 1, 5 | 3, 7 | 14.6 | 28% |
| | 2, 6 | 4, 8 | 14.3 | 27% |
| 1 | 1 | 5 | 18.7 | 36% |
| | 3 | 7 | 21.7 | 41% |
| | 2 | 6 | 16.9 | 32% |
| | 4 | 8 | 23.7 | 45% |

***Table 4-6: Average differences of areal rainfalls at various rain gauge densities for Sabie catchment***

| No of rain gauges | Group 1 | Group 2 | Average difference ($\overline{P_t^1}$) | $\frac{\overline{P_t^1}}{R_A}$ |
|---|---|---|---|---|
| 4 | 1, 4, 6, 8 | 2, 5, 7, 3 | 19.8 | 18% |
| 2 | 1, 6 | 4, 8 | 19.7 | 18% |
| | 2, 7 | 5, 3 | 25.4 | 24% |
| 1 | 1 | 6 | 46.8 | 44% |
| | 4 | 8 | 34.7 | 32% |
| | 2 | 7 | 29.9 | 28% |
| | 5 | 3 | 32.5 | 30% |

***Table 4-7: Average differences of areal rainfalls at various rain gauge densities for Vanderkloof catchment***

| No of rain gauges | Group 1 | Group 2 | Average difference ($\overline{P_t^1}$) | $\frac{\overline{P_t^1}}{R_A}$ |
|---|---|---|---|---|
| 4 | 1, 3, 5, 7 | 2, 4, 6, 8 | 6.5 | 21% |
| 2 | 1, 5 | 3, 7 | 9.6 | 31% |
| | 2, 6 | 4, 8 | 10.6 | 34% |
| 1 | 1 | 5 | 15.3 | 49% |
| | 3 | 7 | 12.4 | 40% |
| | 2 | 6 | 12.3 | 40% |
| | 4 | 8 | 15.0 | 49% |

## 4.3 Cumulative Density Plots and Determination of Scaling Factors

### 4.3.1 Overview

The development of the cumulative density plots is discussed in Section 3.2.1. Data for two cumulative probability plots were obtained from the 2 pairs of 2 stations each and data for four cumulative probability plots were obtained from the 4 pairs of 1 station each. To compute the scaling factors between the sets of rain gauge groups, the individual cumulative probability densities for a given rain gauge density were then averaged to obtain a single probability density plot. The monthly area rainfall difference cumulative density plots for the study catchments and their matching are shown in Figure 4-1 to Figure 4-7.

The scaling factors subjectively selected for the study catchments are shown in Table 4-8 and are considered to be realistic estimates of the uncertainty factor ***u***. Therefore, ***u*** was set to equal the scaling factor obtained between the average cumulative probability plots between the 2 pairs of 2 rainfall stations each and the 1 pair of 4 rainfall stations each listed in Table 4-8. The stochastic areal rainfall generator was then used to generate 100 stochastic areal rainfall sequences for each catchment.

The cumulative density function (CDF) plots for all the study catchments, shown in Figure 4-1 to Figure 4-7, indicated that at a rain gauge density of 8 stations, the CDF would be similar to that of a density of 4 stations scaled by a factor as noted by Ndiritu, (2013) and Ndiritu &

Mkhize (2017). The method that was adopted was to use the highest scaling factor obtained in matching the CDFs at the lower densities (Ndiritu, 2013).

***Table 4-8: Computed Scaling Factors [higher scaling factor]***

| Catchment | Scaling Factor for 2 Pairs of 2 Stations Each | Scaling Factor for 4 Pairs of 1 Station Each | Applied uncertainty factor (*u*) |
|---|---|---|---|
| Bella Vista | 0.60 | 0.58 | 0.60 |
| Bonjanala | 0.65 | 0.62 | 0.65 |
| Ficksburg | 0.75 | 0.59 | 0.75 |
| Howick | 0.75 | 0.45 | 0.75 |
| Potchefstroom | 0.65 | 0.69 | 0.69 |
| Sabie | 0.80 | 0.58 | 0.80 |
| Vanderkloof | 0.65 | 0.69 | 0.65 |

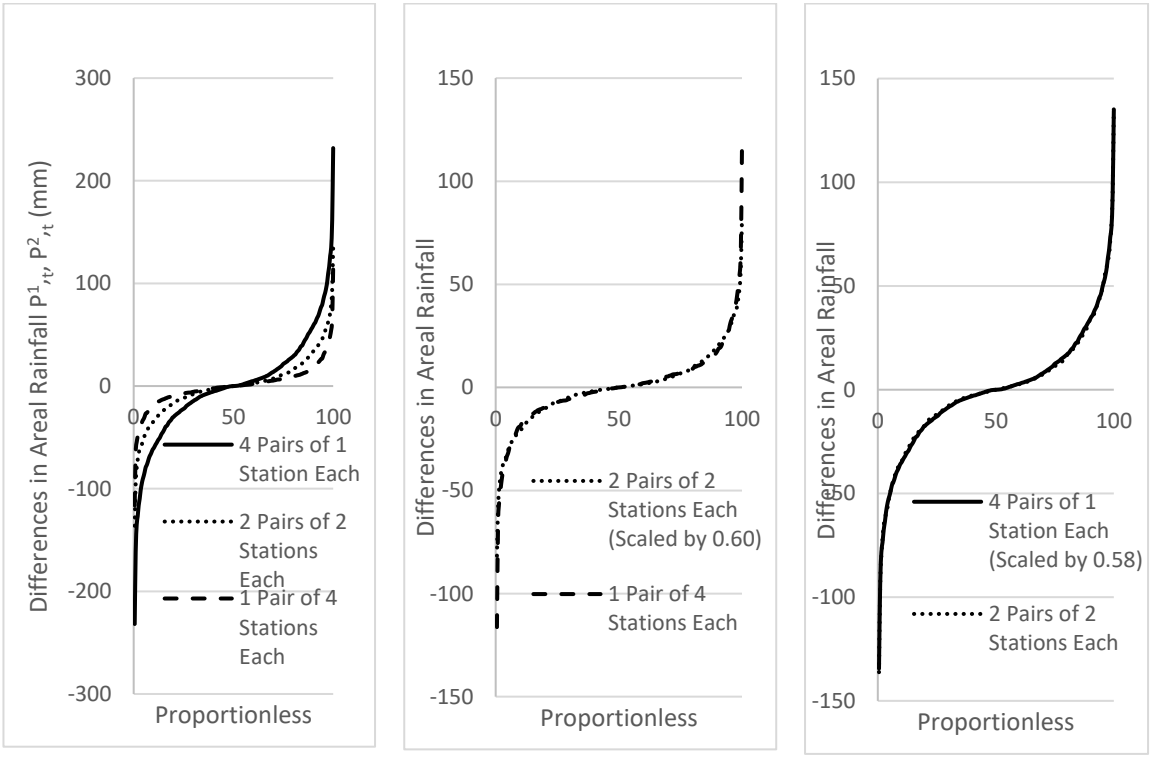



***Figure 4-1: Monthly areal rainfall difference CDF plots and matching for Bella Vista***

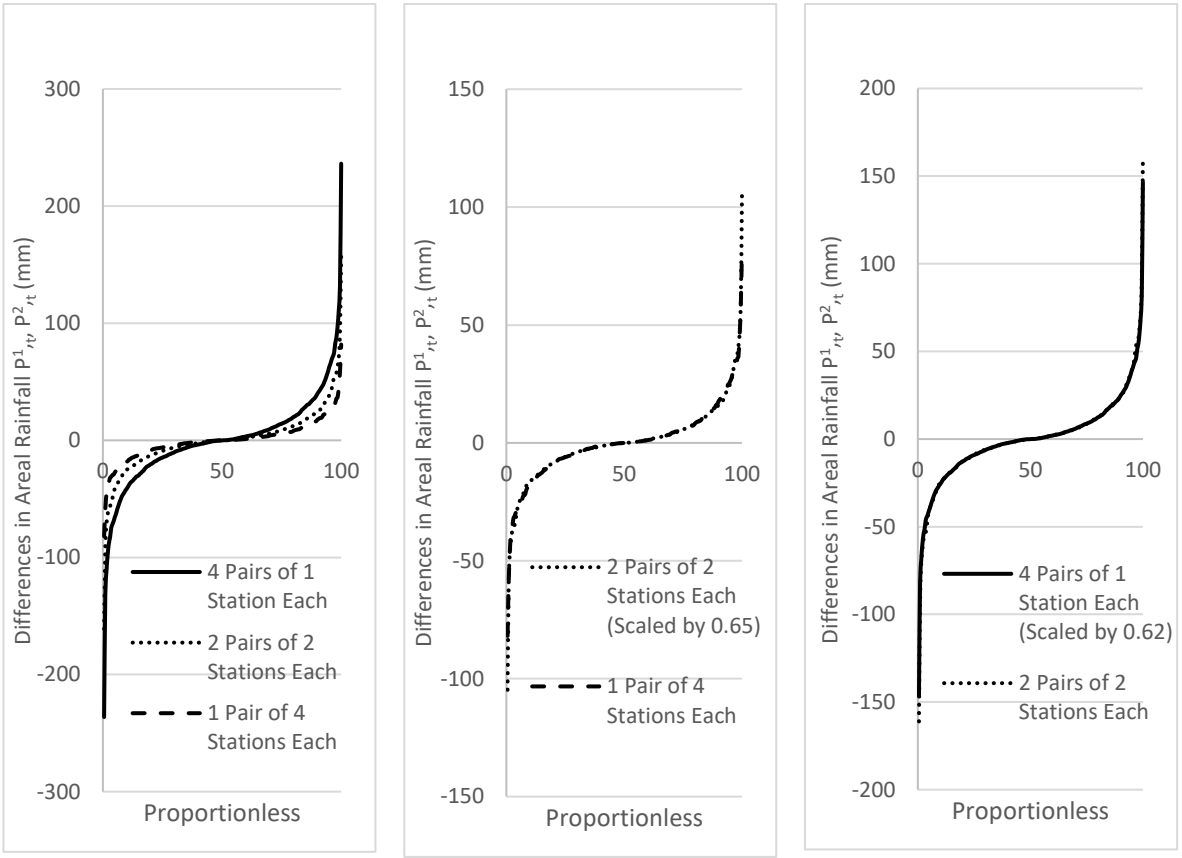



***Figure 4-2: Monthly areal rainfall difference CDF plots and matching for Bonjanala***

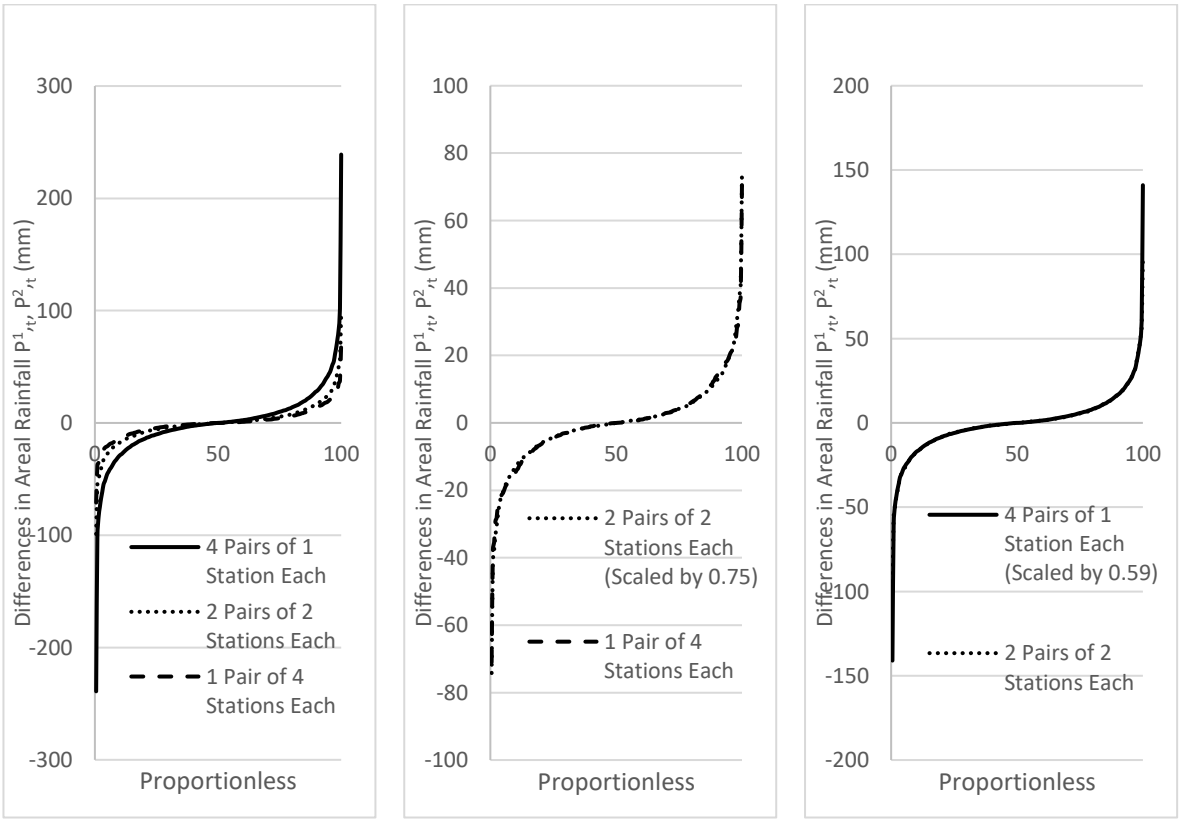



***Figure 4-3: Monthly areal rainfall difference CDF plots and matching for Ficksburg***

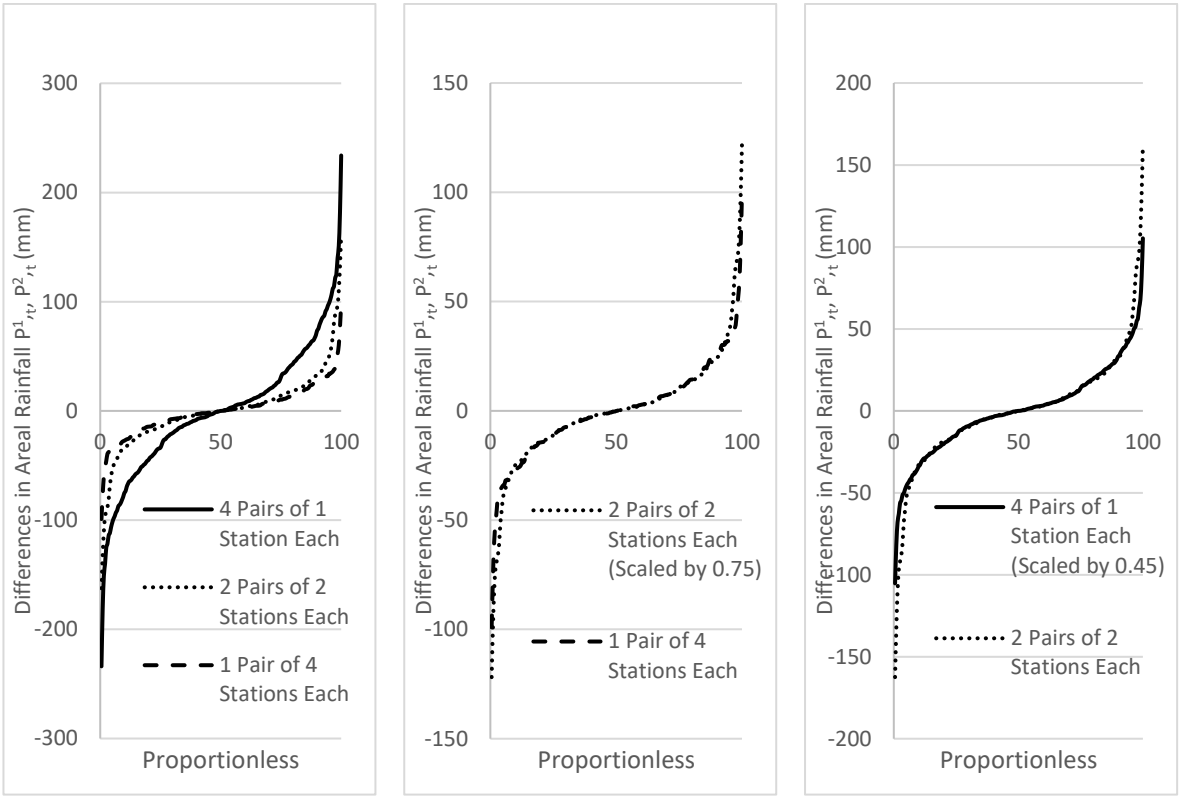



***Figure 4-4: Monthly areal rainfall difference CDF plots and matching for Howick***

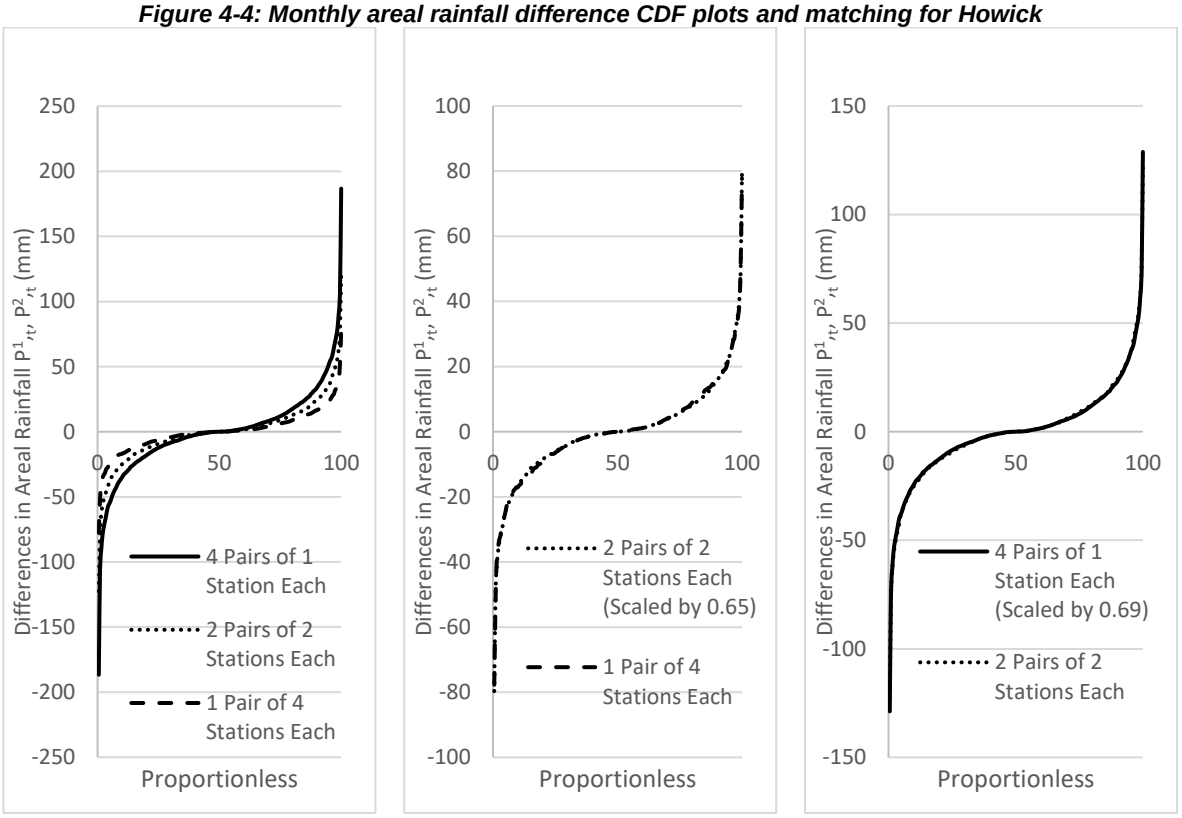



***Figure 4-5: Monthly areal rainfall difference CDF plots and matching for Potchefstroom***

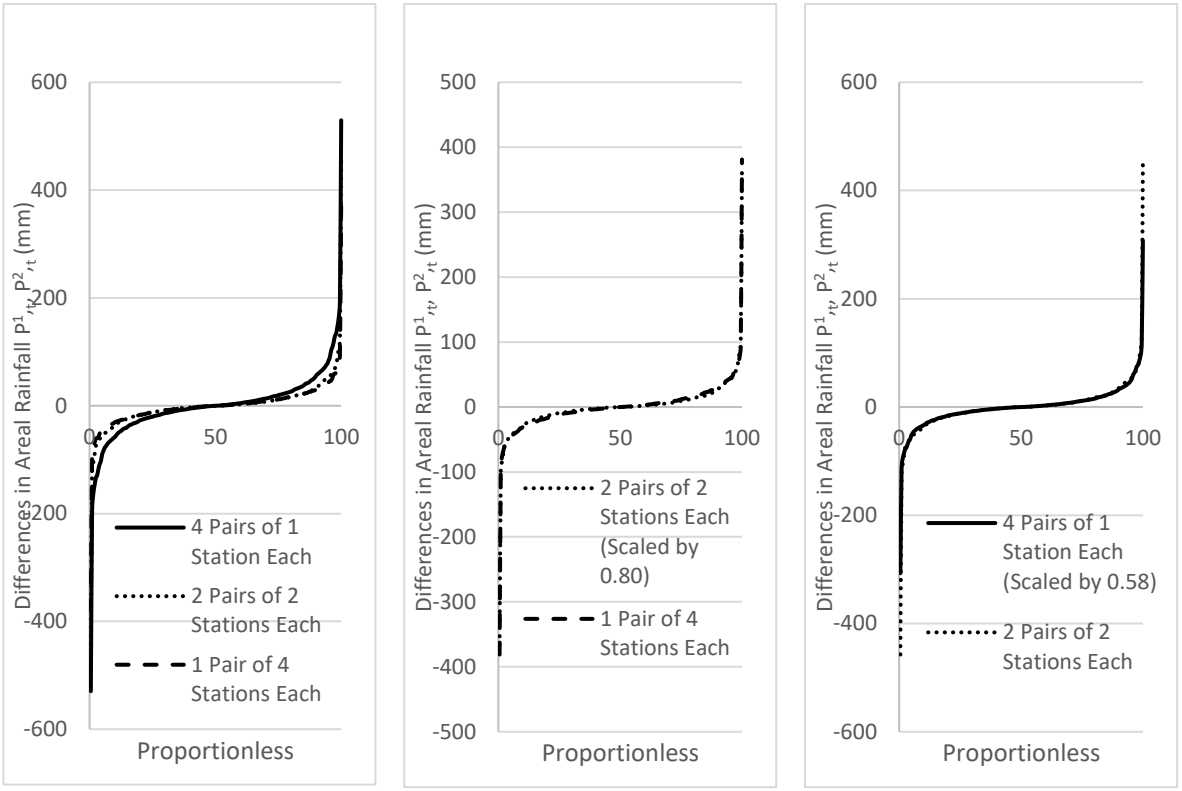



***Figure 4-6: Monthly areal rainfall difference CDF plots and matching for Sabie***

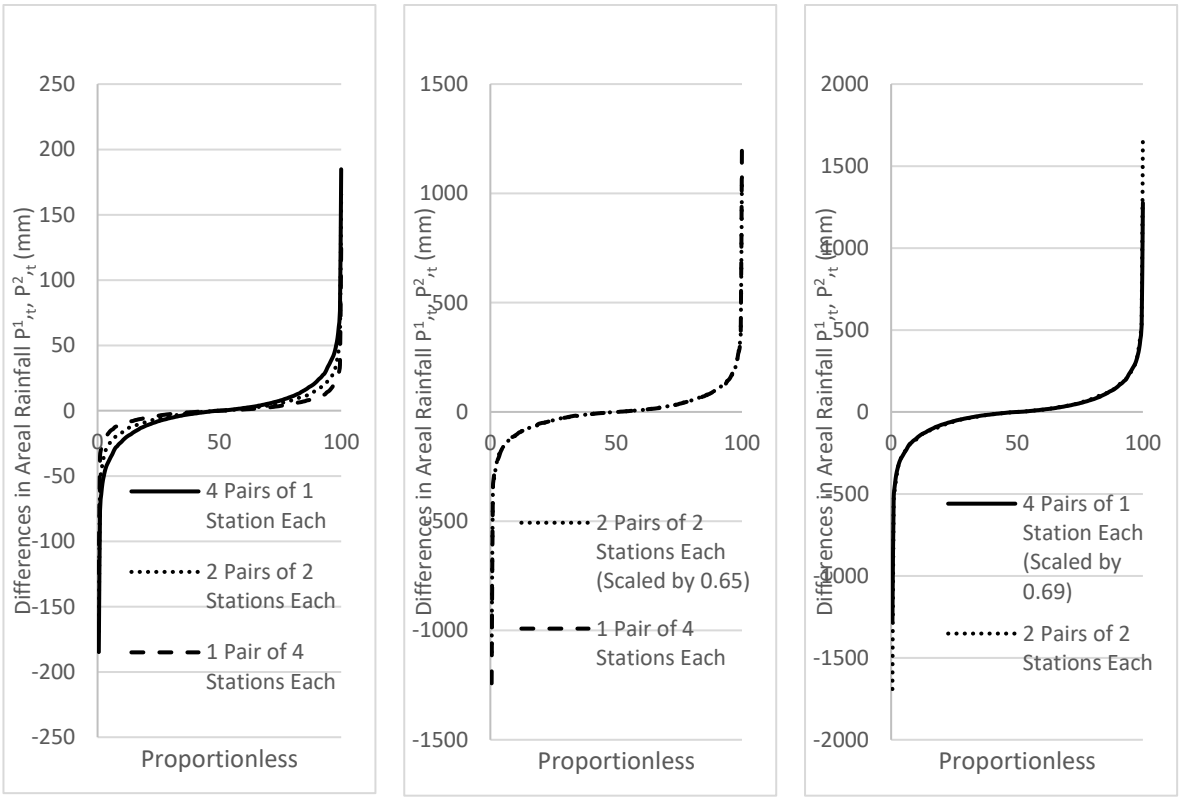



***Figure 4-7: Monthly areal rainfall difference CDF plots and matching for Vanderkloof***

## 4.4 Analysis of Stochastically Generated Areal Rainfall

The bias for the stochastically generated areal rainfall was calculated to assess the reliability of the data-based stochastic rainfall generator. The degree of bias for the mean of the 100 stochastically generated areal rainfalls are negligible as they average to 0.14% and are below 0.5% for all the study catchments. The standard deviations and skewness values are however slightly higher than the respective historic values as observed by Ndiritu (2013). For the purpose of quantifying areal rainfall uncertainty, these biases average to 1.5 and 2.5% respectively and are not considered significant .

***Table 4-9: Summary of the Bias of Stochastically Generated Rainfall***

| Catchment | Statistic | Historic rainfall | 100 Stochastic Rainfalls | Bias |
|---|---|---|---|---|
| Bella Vista | **Mean (mm/month)** | 58.357 | 58.516 | 0.3% |
| | **St. Dev. (mm/month)** | 59.912 | 60.866 | 1.6% |
| | **Skewness** | 1.608 | 1.640 | 2.0% |
| Bonjanala | **Mean (mm/month)** | 50.295 | 50.387 | 0.2% |
| | **St. Dev. (mm/month)** | 54.792 | 55.480 | 1.3% |
| | **Skewness** | 1.413 | 1.449 | 2.6% |
| Ficksburg | **Mean (mm/month)** | 60.327 | 60.321 | 0.0% |
| | **St. Dev. (mm/month)** | 52.738 | 53.315 | 1.1% |
| | **Skewness** | 0.851 | 0.888 | 4.4% |
| Howick | **Mean (mm/month)** | 91.250 | 91.404 | 0.2% |
| | **St. Dev. (mm/month)** | 78.021 | 79.372 | 1.7% |
| | **Skewness** | 1.292 | 1.299 | 0.6% |
| Potchefstroom | **Mean (mm/month)** | 52.496 | 52.514 | 0.0% |
| | **St. Dev. (mm/month)** | 50.785 | 51.575 | 1.6% |
| | **Skewness** | 0.972 | 1.031 | 6.1% |
| Sabie | **Mean (mm/month)** | 107.451 | 107.783 | 0.3% |
| | **St. Dev. (mm/month)** | 103.324 | 105.447 | 2.1% |
| | **Skewness** | 1.178 | 1.208 | 2.6% |
| Vanderkloof | **Mean (mm/month)** | 30.825 | 30.809 | -0.1% |
| | **St. Dev. (mm/month)** | 34.330 | 34.780 | 1.3% |
| | **Skewness** | 1.882 | 1.896 | 0.8% |

## 4.5 Analysis of Stochastic Areal Rainfalls for Individual Catchments

### 4.5.1 Overview

For each study catchment, the 5th, 15th, 25th, 50th, 75th, 85th and 95th percentile values of the historical rainfall during the study period were first identified. Percentile box plots were then produced for each of these percentiles using the stochastically generated rainfall values,

from each of the 100 generated stochastic sequences, that occurred at the same corresponding time step as the historical value. These percentile box plots were used to assess the impact of the data-based stochastic areal rainfall generator on individual monthly rainfalls. The extent of the whiskers on the box plots represent the minimum and maximum values; while the box represents the lower quartile, median and upper quartile values. A summary of the absolute mean deviation and coefficient of variation for the stochastically generated rainfall for each study catchment is shown in Figure 4-8 and Figure 4-9 respectively. It is important to note that (as for the coefficient of variation), the absolute mean deviation is interpreted here as a measure of variability of generation and not of bias. The actual bias values of various statistics are shown in Table 4-9 and are much lower than the absolute mean deviations.

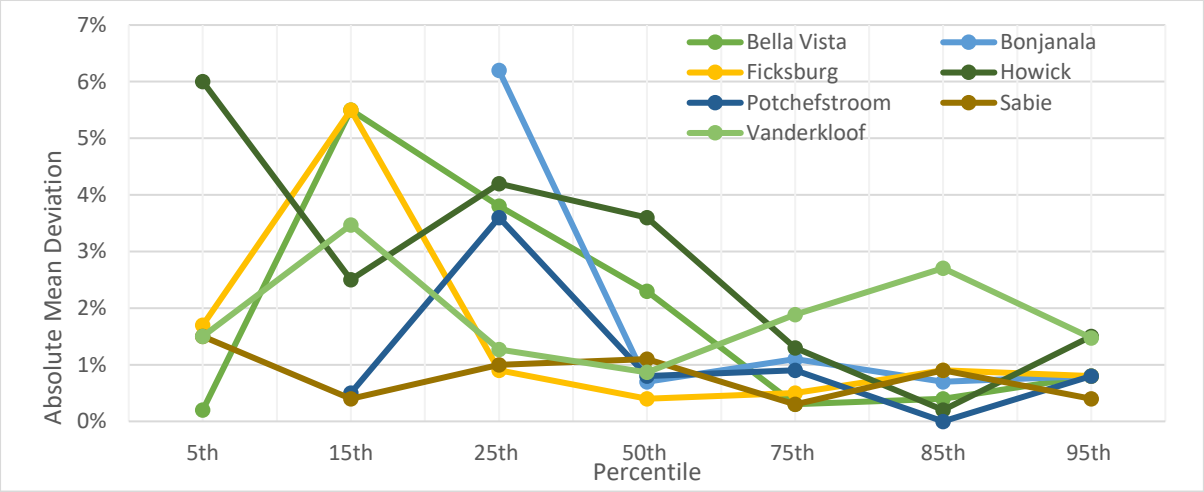



***Figure 4-8: Absolute Mean Deviation for Stochastically Generated Rainfall***

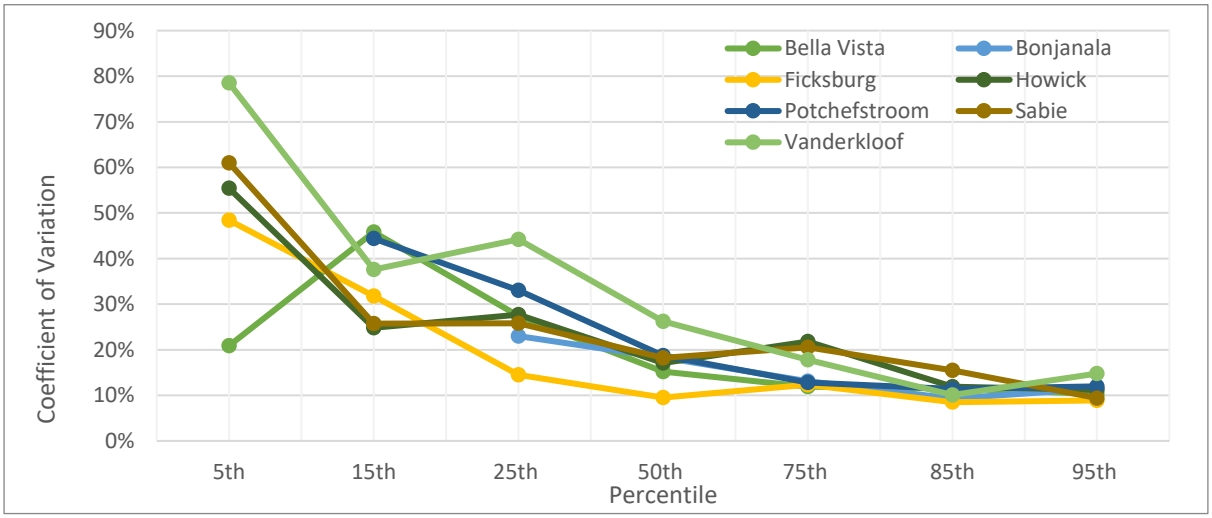



***Figure 4-9: Coefficient of Variation for Stochastically Generated Rainfall***

### 4.5.2 Bella Vista

Figure 4-8 and Figure 4-10 show that the 15th percentile of rainfall volumes experiences the highest degree of bias and bias reduces as the rainfall total increases while the lowest bias experienced by the 95th percentile rainfall totals. The historical areal rainfalls lie within the interquartile range for all stochastic areal rainfalls indicating negligible bias of central tendency. All rainfall totals are positively skewed. Figure 4-9 shows that the 15th percentile of rainfall volumes experiences the highest degree of variability and variability reduces as the rainfall volume increases, with the lowest variability experienced by the 95th percentile rainfall volumes.

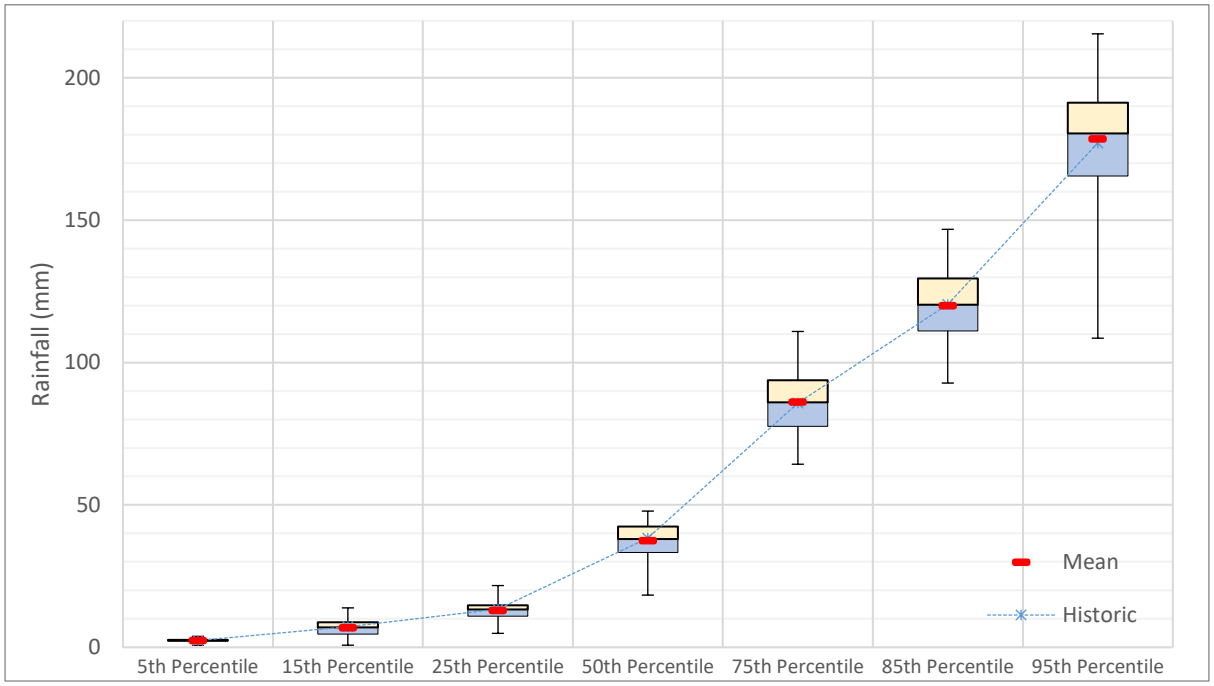



***Figure 4-10: Box plots of representative stochastic rainfalls for Bella Vista***

### 4.5.3 Bonjanala

Figure 4-8 and Figure 4-11 show that the 25th percentile of rainfall volumes experiences the highest degree of bias while the 50th and 85th percentiles experience lowest bias. The historical areal rainfalls lie within the interquartile range for all stochastic areal rainfalls indicating negligible bias of central tendency. All rainfall volumes are positively skewed. Figure 4-9 shows that the 25th percentile of rainfall volumes experiences the highest degree of variability while the lowest variability is experienced by the 85th percentile rainfall volumes.

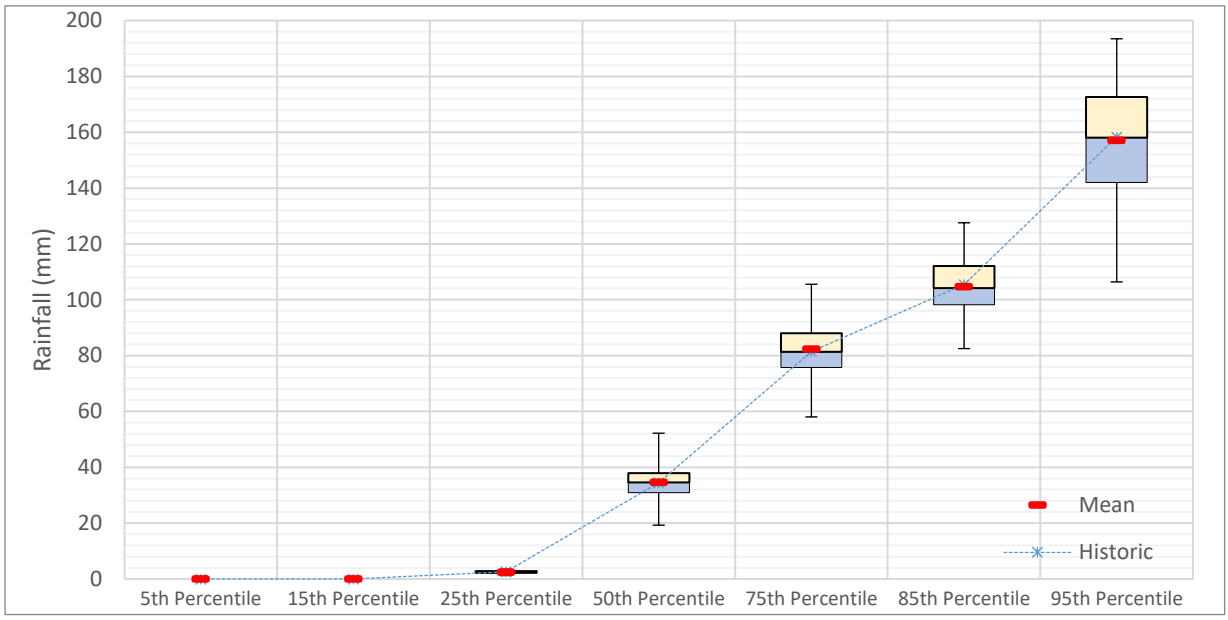



***Figure 4-11: Box plots of representative stochastic rainfalls for Bonjanala***

### 4.5.4 Ficksburg

Figure 4-8 and Figure 4-12 show that the 15th percentile of rainfall volumes experience the highest degree of bias while the 50th and 75th percentiles experiencing lowest bias. The historical areal rainfalls lie within the interquartile range for all stochastic areal rainfalls indicating negligible bias of central tendency. All rainfall volumes are positively skewed. Figure 4-9 shows that the 15th percentile of rainfall volumes experience the highest degree of variability and variability reduces as the rainfall volume increases, with the lowest variability experienced by the 85th percentile rainfall volumes.

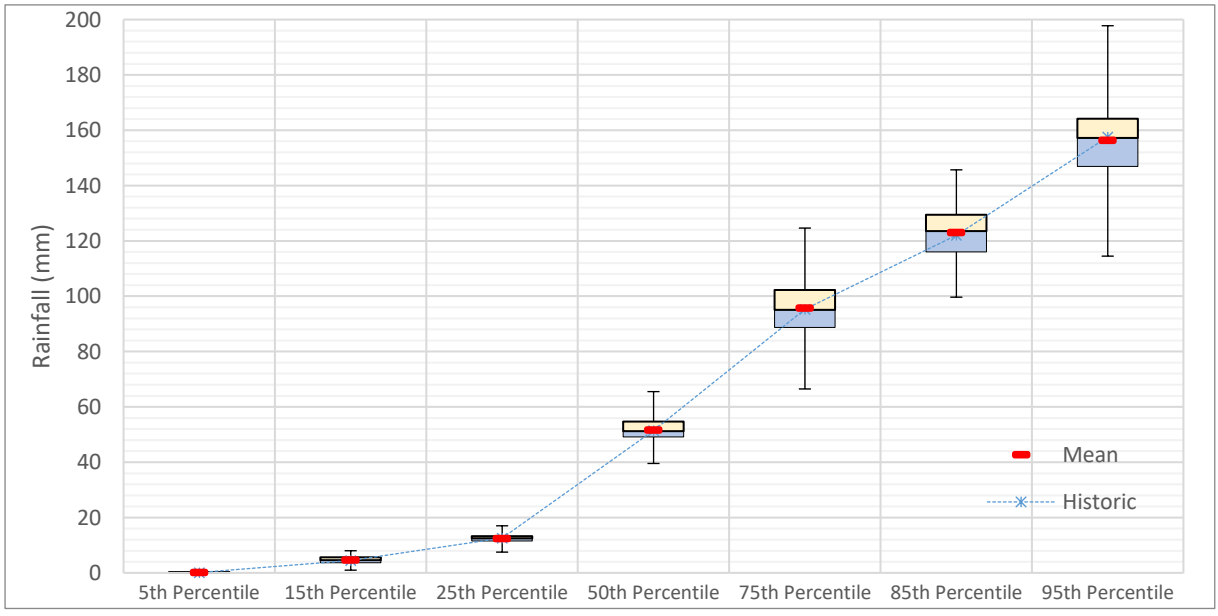



***Figure 4-12: Box plots of representative stochastic rainfalls for Ficksburg***

### 4.5.5 Howick

Figure 4-8 and Figure 4-13 show that the 5th percentile of rainfall volumes experiences the highest degree of bias while the 85th percentiles experience the lowest bias. The historical areal rainfalls lie within the interquartile range for all stochastic areal rainfalls indicating negligible bias of central tendency. All rainfall volumes are positively skewed. Figure 4-9 shows that the 5th percentile of rainfall volumes experiences the highest degree of variability and variability reduces as the rainfall volume increases, with the lowest variability experienced by the 95th percentile rainfall volumes.

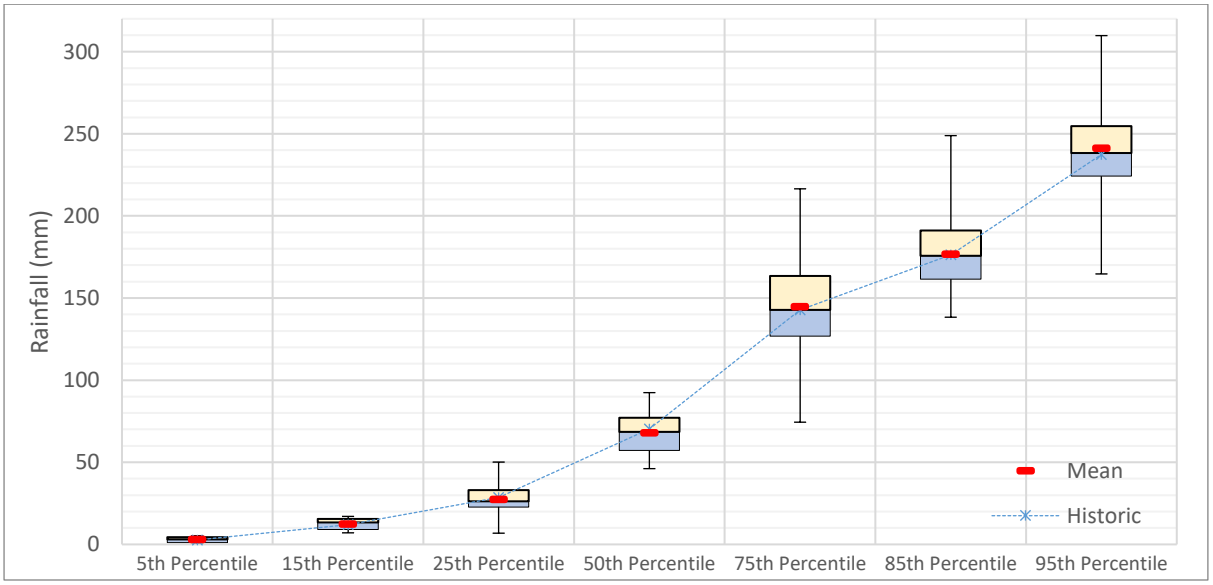



***Figure 4-13: Box plots of representative stochastic rainfalls for Howick***

### 4.5.6 Potchefstroom

Figure 4-8 and Figure 4-14 show that the 25th percentile of rainfall volumes experiences the highest degree of bias while the 85th percentiles experiences the lowest bias. The historical areal rainfalls lie within the interquartile range for all stochastic areal rainfalls indicating negligible bias of central tendency. All rainfall volumes are positively skewed. Figure 4-9 shows that the 15th percentile of rainfall volumes experiences the highest degree of variability and variability reduces as the rainfall volume increases, with the lowest variability experienced by the 85th percentile rainfall volumes.

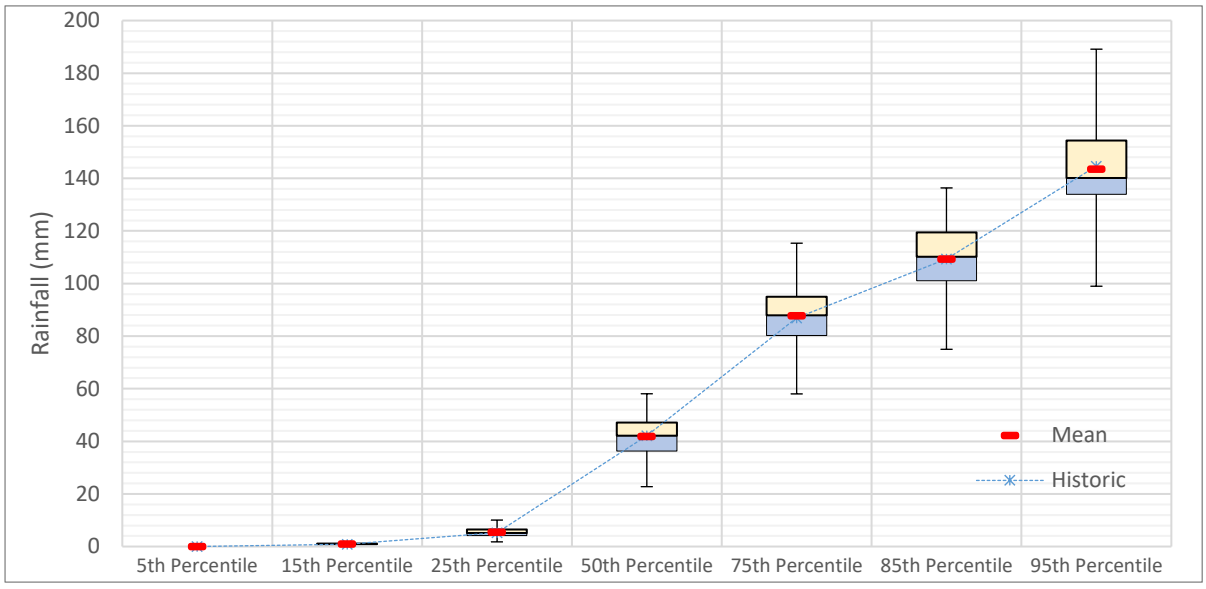



***Figure 4-14: Box plots of representative stochastic rainfalls for Potchefstroom***

### 4.5.7 Sabie

Figure 4-8 and Figure 4-15 show that the 5th percentile of rainfall volumes experiences the highest degree of bias while the 75th percentiles experience the lowest bias. The historical areal rainfalls lie within the interquartile range for all stochastic areal rainfalls indicating negligible bias of central tendency. All rainfall volumes are positively skewed. Figure 4-9 shows that the 5th percentile of rainfall volumes experiences the highest degree of variability and variability reduces as the rainfall volume increases, with the lowest variability experienced by the 95th percentile rainfall volumes.

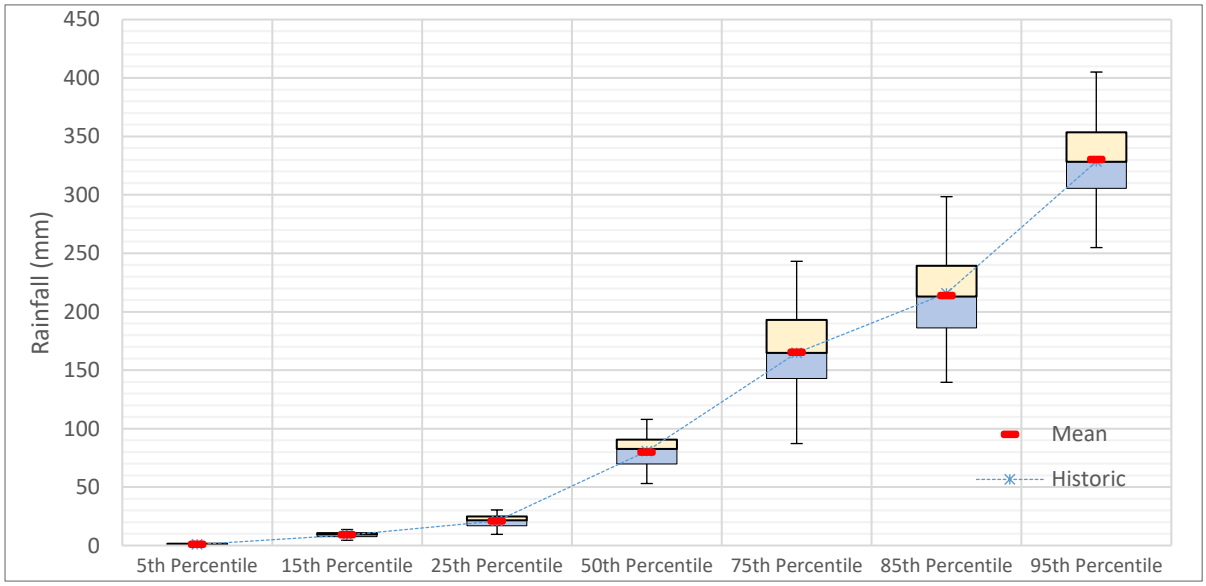



***Figure 4-15: Box plots of representative stochastic rainfalls for Sabie***

### 4.5.8 Vanderkloof

Figure 4-8 and Figure 4-16 show that the 85th percentile of rainfall volumes experiences the highest degree of bias while the 95th percentiles experiences the lowest bias. The historical areal rainfalls lie within the interquartile range for all stochastic areal rainfalls indicating negligible bias of central tendency. All rainfall volumes are positively skewed. Figure 4-9 shows that the 5th percentile of rainfall volumes experiences the highest degree of variability and variability reduces as the rainfall volume increases, with the lowest variability experienced by the 95th percentile rainfall volumes.

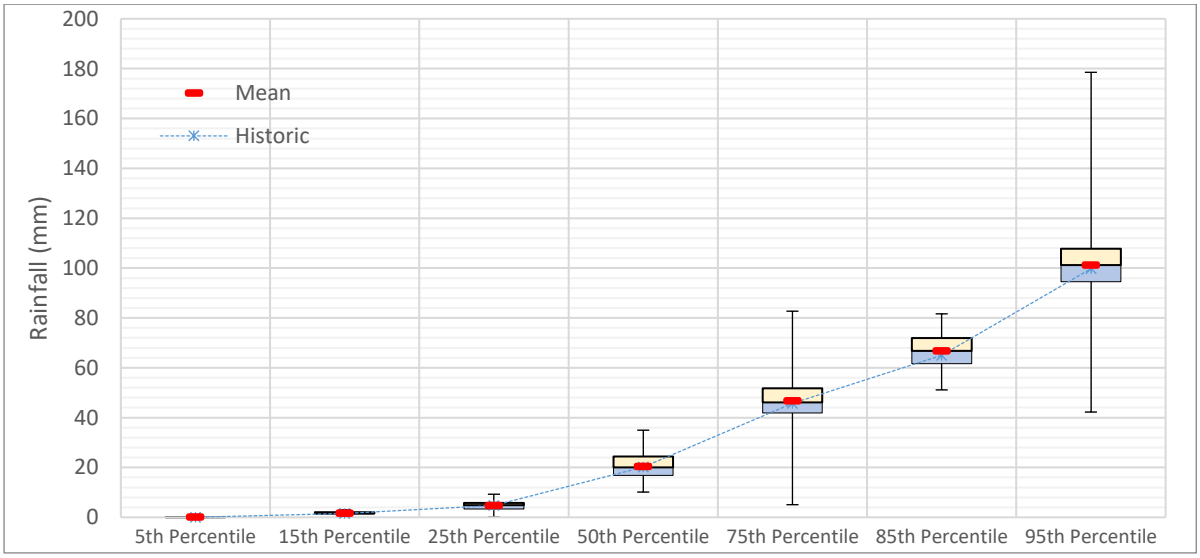



***Figure 4-16: Box plots of representative stochastic rainfalls for Vanderkloof***

## 4.5 Discussion of Stochastic Areal Rainfall Generation

The stochastic areal rainfall generation approach is based on the differences in areal rainfall that are obtained from rainfall groups with alternate omission of rainfall stations and an assessment of these rainfall differences was carried out.

The monthly areal rainfall differences were found to average 18.3% of the average monthly rainfalls for the seven study catchments and were considered significant. The generated stochastic areal rainfalls also exhibited large variabilities as illustrated in box plots and in the values of coefficients of variability and absolute mean deviation. The coefficients of variability and absolute mean deviation were found to increase as the rainfall magnitudes reduced. These observations are in agreement with findings from Ndiritu & Mkhize (2017).

The stochastically generated areal rainfalls, for all seven catchments, exhibited negligible degrees of bias of the mean, standard deviation and skewness when compared to the respective statistics of historic areal rainfalls. These observations concur with findings from Ndiritu (2013) and Ndiritu & Mkhize (2017).

# 5. Results, Analysis, and Discussion of Streamflow Simulation

## 5.1 Overview

Due to time constraints, the effect of areal rainfall uncertainty on streamflow generation was confined to two of the seven catchments; Bella Vista and Bonjanala.

The rainfall and streamflow data sets for each of the catchments were divided into a calibration and a validation set, to assess simulation performance and the impact of areal rainfall uncertainty on streamflow simulation.

The first part of the assessment involved carrying out 100 randomly-initialised calibration – validation runs using: i) the single observed monthly areal rainfalls and ii) 100 stochastic areal rainfall sequences obtained by the stochastic areal rainfall generator. This was followed by a comparison of the parameters, performance of simulation, and variability of simulated stream flows from the application of the single historic areal rainfalls and from 100 stochastic areal rainfalls.

## 5.2 Comparison of Pitman Model Parameters

### 5.2.1 Overview

The statistics of the parameter values from the 100 randomly-initialised calibration-validation runs, for the Bella Vista and Bonjanala, catchments using historic and stochastic rainfall are presented in Table 5-1 and Table 5-2. The boxplots showing the scaled ranges of values obtained for PI, Z1, Z3, SL1, SL2, ST, FT, GW, POW, GPOW and R during these runs are shown in Figure 5-1 and Figure 5-2. The extent of the whiskers on the box plots represents the minimum and maximum values; while the box represents the lower quartile, median and upper quartile values. The linear pots superimposed on the box plots show the initial (LL1 to UL1) and the limiting (LL2 to UL2) search ranges for the respective parameters in the hybrid manual-automatic calibration of the model.

### 5.2.2 Bella Vista

The time periods of calibration and validation data sets for the Bella Vista catchment were 1973 to 1988 and 1989 to 2004 respectively. Table 5-1 shows the statistics of the parameter values from the 100 randomly-initialised calibration-validation runs for the Bella Vista catchment using historic and stochastic rainfall. The mean interception storage (PI) obtained is higher than the recommended range by Bailey (2015) of 1-10mm, while the remaining parameters are within the recommended ranges.

***Table 5-1: Statistics of Pitman model parameters for Bella Vista obtained from 100 randomly-initialised runs (H: simulation using single historic rainfall series; S: simulation using 100 stochastic rainfall series)***

| Parameter | Mean | | Standard Deviation | | Skewness | | Coefficient of Variation | |
|---|---|---|---|---|---|---|---|---|
| | H | S | H | S | H | S | H | S |
| **PI** | 13.09 | 13.01 | 0.49 | 0.60 | -0.27 | -0.67 | 4% | 5% |
| **Z1** | 99.34 | 100.85 | 12.66 | 12.26 | -0.12 | 0.00 | 13% | 12% |
| **Z3** | 1392.37 | 1406.18 | 141.81 | 128.57 | 0.27 | 0.19 | 10% | 9% |
| **SL1** | 1.74 | 1.82 | 0.73 | 0.56 | 0.49 | -0.17 | 42% | 31% |
| **SL2** | 13.14 | 12.98 | 2.09 | 1.82 | 0.09 | -0.21 | 16% | 14% |
| **ST** | 439.71 | 470.30 | 86.31 | 97.87 | 0.14 | 0.26 | 20% | 21% |
| **FT** | 68.32 | 67.92 | 9.48 | 8.47 | 0.14 | 0.09 | 14% | 12% |
| **GW** | 33.56 | 33.09 | 7.77 | 7.32 | -0.06 | -0.51 | 23% | 22% |
| **POW** | 1.48 | 1.47 | 0.08 | 0.09 | 0.47 | -0.02 | 5% | 6% |
| **GPOW** | 1.64 | 1.65 | 0.14 | 0.14 | -0.41 | -0.13 | 9% | 9% |
| **R** | 0.53 | 0.55 | 0.16 | 0.16 | 0.13 | 0.29 | 30% | 29% |
| **Prop of Catchment with Lower Side GW Table** | 0.40 | 0.40 | 0.06 | 0.08 | -0.02 | 0.03 | 16% | 19% |
| **Riparian Strip** | 6.48 | 6.57 | 1.97 | 1.67 | 0.21 | -0.11 | 30% | 25% |
| **Transmissivity** | 3.69 | 3.76 | 1.20 | 1.22 | 0.67 | 0.54 | 32% | 33% |
| **Rest Water Level** | 2.48 | 2.50 | 0.33 | 0.29 | 0.03 | 0.21 | 13% | 12% |
| **Porosity** | 0.01 | 0.01 | 0.00 | 0.00 | 0.09 | -0.01 | 30% | 26% |
| **Initial Lower GW Slope** | 0.04 | 0.03 | 0.03 | 0.02 | 3.82 | 2.88 | 94% | 79% |
| **Initial Upper GW Slope** | 0.03 | 0.04 | 0.02 | 0.02 | 1.94 | 1.50 | 60% | 63% |
| **Objective Function** | 0.16 | 0.18 | 0.03 | 0.03 | -0.13 | 0.71 | 18% | 15% |

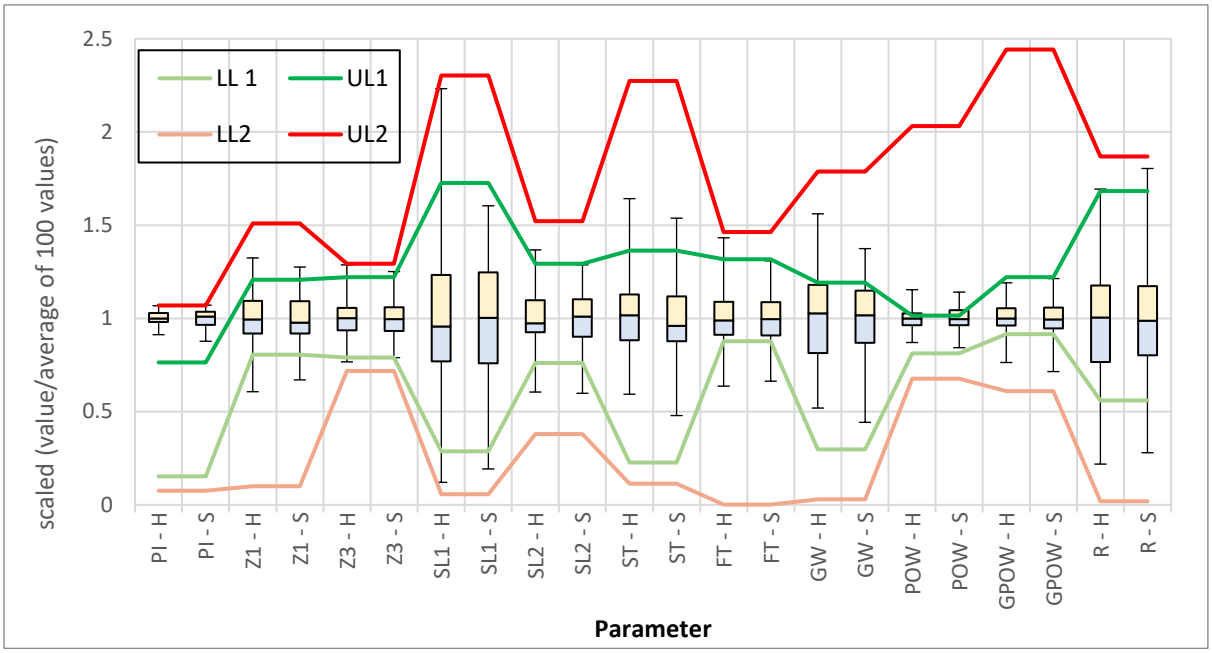



***Figure 5-1: Boxplots of scaled parameters for the 100 initialised calibration-validation runs for Bella Vista***

### 5.2.3 Bonjanala

The time periods of calibration and validation data sets for the Bonjanala catchment were 1963 to 1981 and 1982 to 2000 respectively. Table 5-2 shows the statistics of the parameter values from the 100 randomly-initialised calibration-validation runs for the Bonjanala catchment. As with Bella Vista, box plots for the parameter ranges are represented on Figure 5-2. The box plots are above the two lower limits and the error is therefore redundant.

The mean PI obtained is higher than the recommended range by Bailey (2015), while the remaining parameters are within the recommended ranges.

***Table 5-2: Statistics of Pitman model parameters for Bonjanala obtained from 100 randomly-initialised runs (H: simulation using single historic rainfall series; S: simulation using 100 stochastic rainfall series)***

| Parameter | Mean | | Standard Deviation | | Skewness | | Coefficient of Variation | |
|---|---|---|---|---|---|---|---|---|
| | H | S | H | S | H | S | H | S |
| **PI** | 12.55 | 12.69 | 0.57 | 0.60 | -0.11 | -0.33 | 5% | 5% |
| **Z1** | 99.25 | 99.76 | 10.08 | 10.62 | -0.10 | 0.02 | 10% | 11% |
| **Z3** | 1500.62 | 1490.95 | 99.70 | 92.20 | -0.18 | -0.37 | 7% | 6% |
| **SL1** | 1.99 | 1.98 | 0.55 | 0.58 | 0.25 | 0.17 | 28% | 29% |
| **SL2** | 13.12 | 12.79 | 1.61 | 1.92 | -0.53 | 0.13 | 12% | 15% |
| **ST** | 274.91 | 285.99 | 52.66 | 58.51 | 1.12 | 0.85 | 19% | 20% |
| **FT** | 72.91 | 72.27 | 8.14 | 7.79 | -0.59 | 0.28 | 11% | 11% |
| **GW** | 20.88 | 21.76 | 5.62 | 5.41 | 0.20 | 0.56 | 27% | 25% |
| **POW** | 1.96 | 1.97 | 0.14 | 0.14 | -0.13 | 0.33 | 7% | 7% |
| **GPOW** | 1.78 | 1.82 | 0.21 | 0.24 | -0.37 | 0.26 | 12% | 13% |
| **R** | 0.69 | 0.67 | 0.10 | 0.12 | -0.26 | -0.22 | 15% | 18% |

| Parameter | Mean | | Standard Deviation | | Skewness | | Coefficient of Variation | |
|---|---|---|---|---|---|---|---|---|
| | H | S | H | S | H | S | H | S |
| Prop of Catchment with Lower Side GW Table | 0.45 | 0.45 | 0.08 | 0.09 | 0.27 | 0.15 | 18% | 20% |
| Riparian Strip | 5.96 | 6.03 | 1.88 | 2.00 | 0.06 | 0.58 | 32% | 33% |
| Transmissivity | 4.97 | 5.02 | 1.47 | 1.62 | 0.08 | 0.04 | 30% | 32% |
| Rest Water Level | 2.50 | 2.53 | 0.23 | 0.31 | 0.12 | -0.06 | 9% | 12% |
| Porosity | 0.01 | 0.01 | 0.01 | 0.01 | 1.61 | 2.29 | 45% | 53% |
| Initial Lower GW Slope | 0.03 | 0.04 | 0.03 | 0.06 | 4.35 | 4.39 | 107% | 143% |
| Initial Upper GW Slope | 0.03 | 0.04 | 0.03 | 0.03 | 3.72 | 2.78 | 75% | 80% |
| Objective Function | 0.14 | 0.16 | 0.04 | 0.05 | 4.35 | 3.07 | 29% | 28% |

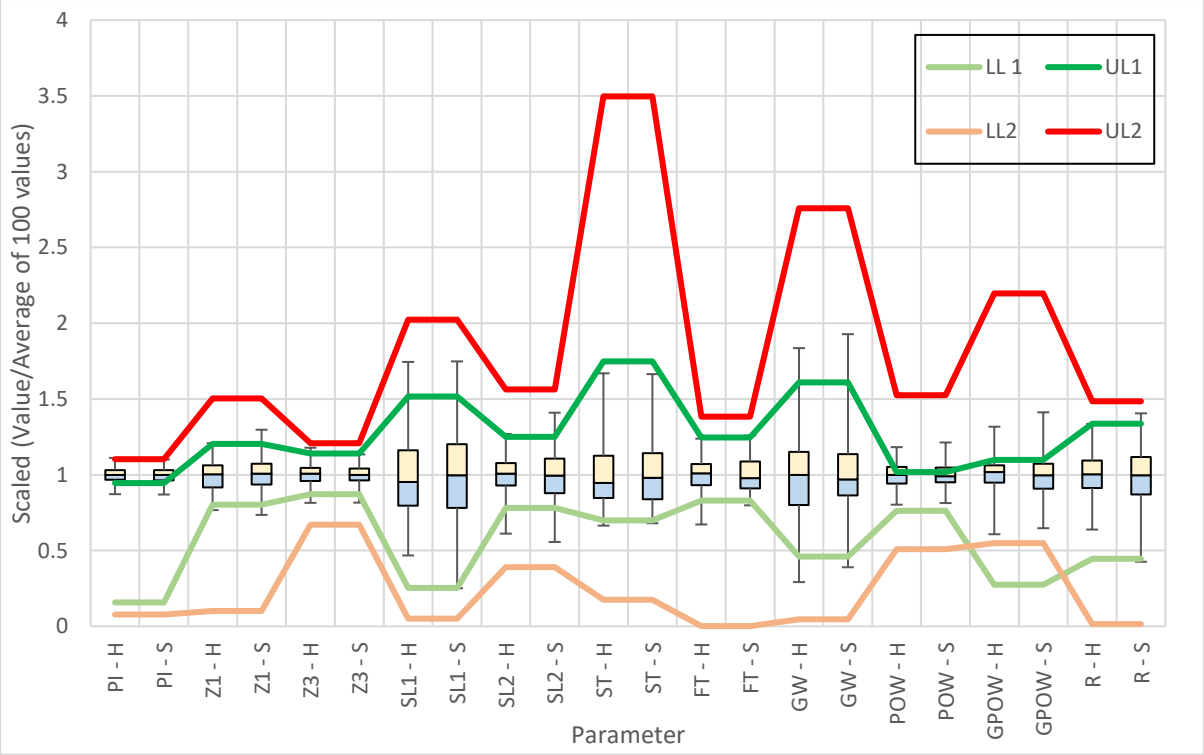



***Figure 5-2: Boxplots of scaled parameters for the 100 initialised calibration-validation runs for Bonjanala***

## 5.3 Comparison of Calibration Performance

### 5.3.1 Bella Vista

Figure 5-3 presents box plots of the Pitman model simulation performance for the Bella Vista catchment from the 100 randomly-initialised calibration-validation runs. These results reveal that the calibration obtained better CE values than the validation while the validation obtained

better RMCC values than calibration. Figure 5-3 also reveals that applying stochastic rainfalls does not lead to any significant loss in performance or significant change in variability in both calibration and validation.

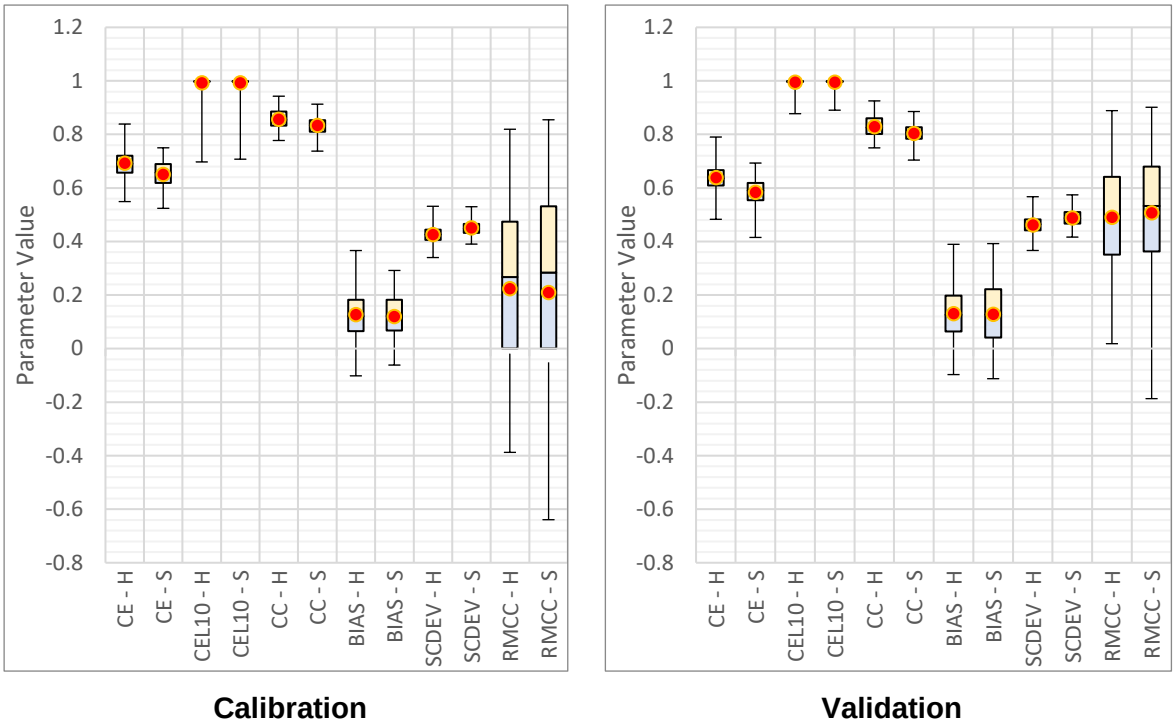



***Figure 5-3: Box plots of Pitman model simulation performance for Bella Vista (H: Historic Observed Rainfall; S: Monthly Stochastic Rainfalls)***

### 5.3.2 Bonjanala

Figure 5-4 presents box plots of the Pitman model simulation performance for the Bonjanala catchment from the 100 randomly-initialised calibration-validation runs. These results reveal that the bias and RMCC values were better in validation than calibration while the CE values in calibration were better than those in the validation. As for Bella Vista, applying stochastic rainfalls does not lead to any significant loss in performance or significant change in variability.

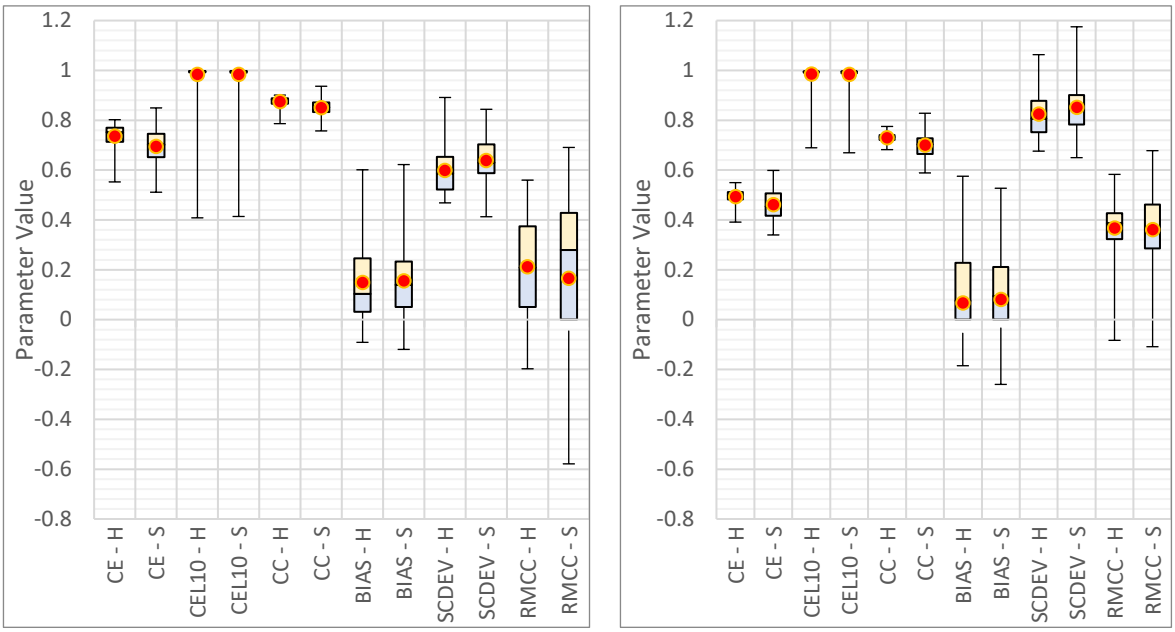



***Figure 5-4: Box plots of Pitman Model calibration simulation performance for Bonjanala (H: Historic Observed Rainfall; S: Monthly Stochastic Rainfalls)***

## 5.4 Comparison of Simulated Stream Flows

### 5.4.1 Overview

The percentile box plots of the stream flows obtained were used to assess the impact of the stochastically generated areal rainfall on the streamflow simulation. The box plots were represented graphically for 5th, 15th, 25th, 50$^{th}$, 75th, 85th and 95th percentiles from each of the 100 randomly-initialised calibration runs for each catchment as well as from calibration runs using the historic observed monthly rainfall. The extent of the whiskers on the box plots represents the minimum and maximum values; while the box represents the lower quartile, median and upper quartile values.

The absolute mean deviations and coefficients of variability of the simulated stream flows for the 7 percentiles were compared to assess the change in streamflow variability that resulted from using stochastic areal rainfalls rather than the single historic areal rainfalls.

### 5.4.2 Bella Vista

Figure 5-5 and Figure 5-6 present the box plots of the calibration and validation stream flows obtained for the Bella Vista catchment respectively; while Figure 5-7 presents the absolute mean deviations and coefficients of variability for each percentile. For the calibration runs, the naturalised stream flows fall within the ranges of 75th to 95th percentile of streamflow volumes.

For the validation runs, the naturalised stream flows fall within the ranges of the 5th, 25th, and 95th percentile of streamflow volumes. The interquartile (box) and whisker ranges (0% to 100%) of the box plot clearly reveal higher variability of the stochastic rainfall stream flows for the 75$^{th}$, 85$^{th}$, and 95$^{th}$ percentiles. For the lower percentiles, the box plots reveal similar variabilities for the historic and stochastic rainfall simulations.

The highest absolute mean deviations for the calibration and validation stream flows are the 15th and 25th percentiles respectively, while the 95th percentile of streamflow volumes gave the lowest deviations. The highest coefficients of variability obtained in both calibration and validation are for the 25th percentile while the 95th percentile stream flows have the lowest degree of variability. Figure 5-7 reveals that the absolute mean deviations for historic and stochastic rainfall simulations are almost similar while the coefficients of variation for the stochastic rainfall simulations are markedly higher than those from historic simulations for all the percentiles with the exception of the 25th.

The full range stream flows obtained for the calibration and validation runs for the Bella Vista catchment are shown in Figure 5-8 and Figure 5-9 respectively. The stream flows obtained from both the calibration and validation runs, for both the historic observed and stochastic rainfalls, are generally representative of the magnitudes of naturalised streamflow data. The ranges of stream flows obtained from using historic rainfalls are narrower than those obtained from the use of stochastic rainfalls.

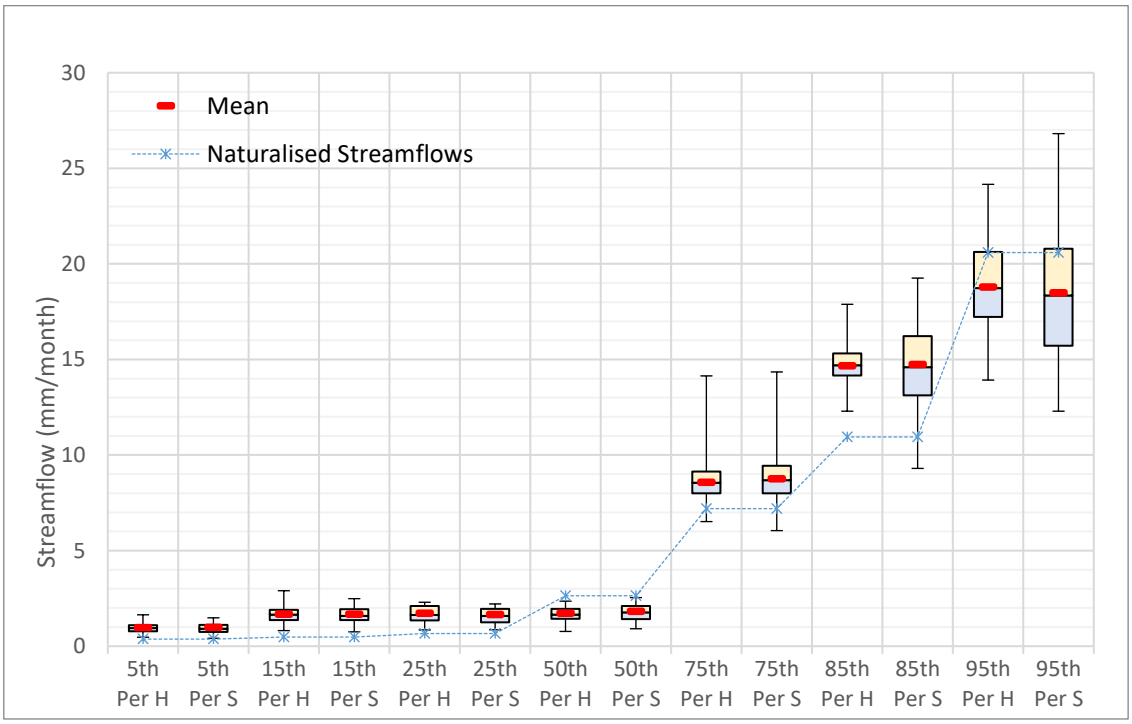



***Figure 5-5: Box plots of representative calibration stream flows for Bella Vista (H: Historic Observed Rainfall; S: Monthly Stochastic Rainfalls)***

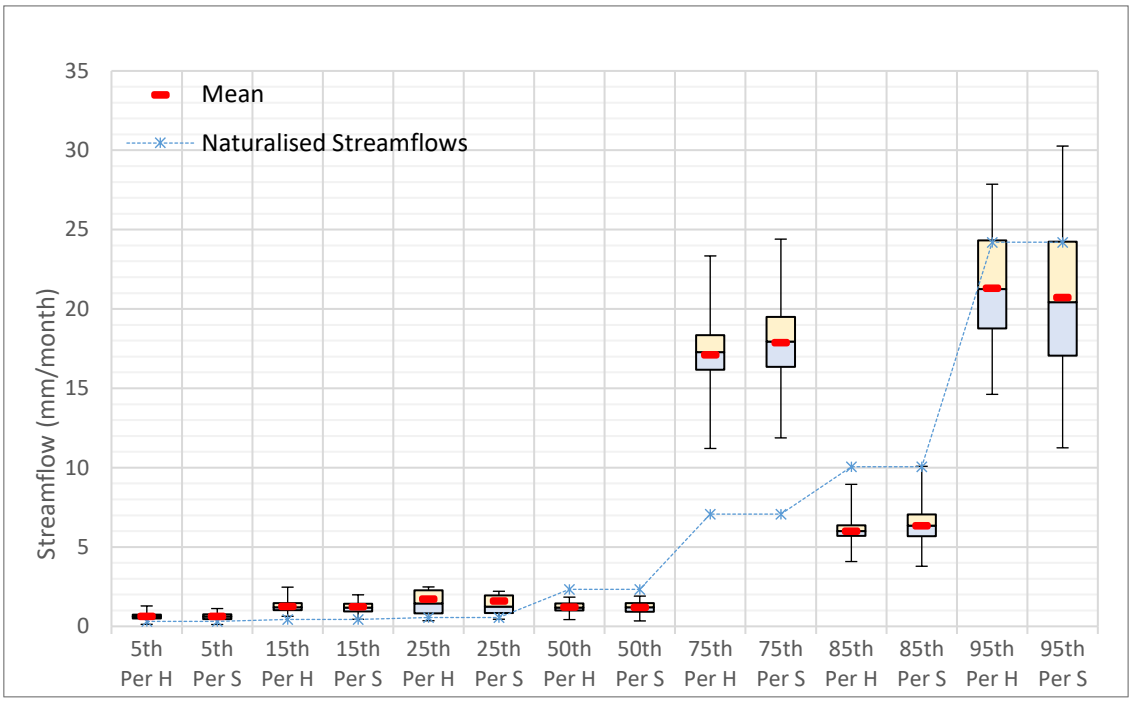



***Figure 5-6: Box plots of representative validation stream flows for Bella Vista (H: Historic Observed Rainfall; S: Monthly Stochastic Rainfalls)***

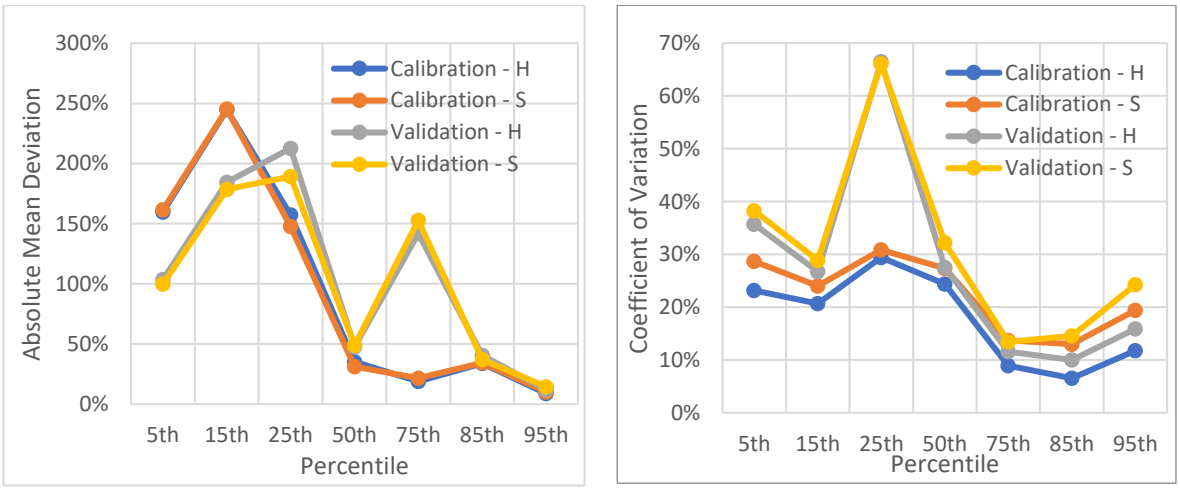



***Figure 5-7: Bias and Coefficients of Variation for Bella Vista (H: Historic Observed Rainfall; S: Monthly Stochastic Rainfalls)***

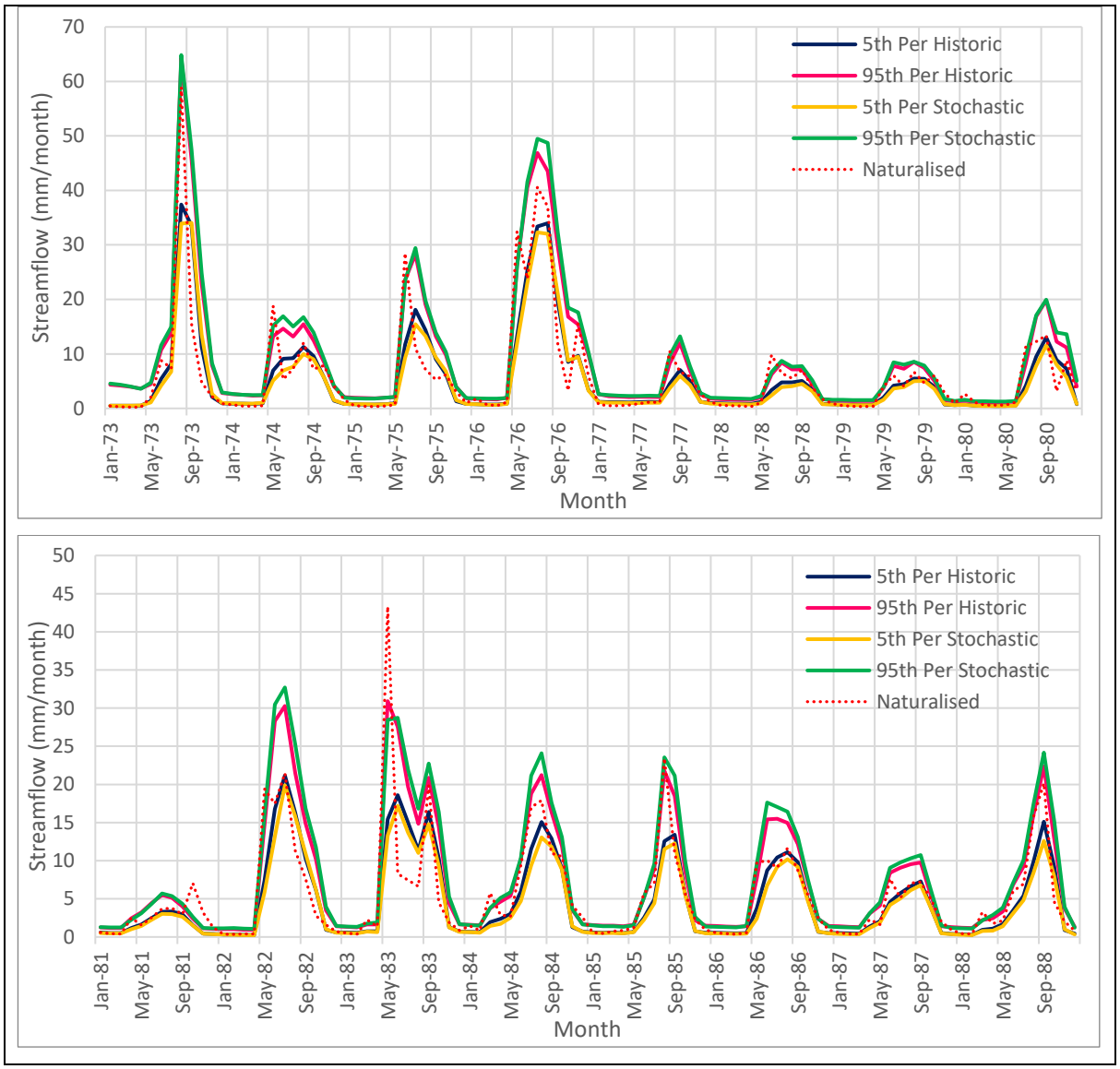



***Figure 5-8: Range of simulated stream flows from 100 calibration runs for Bella Vista***

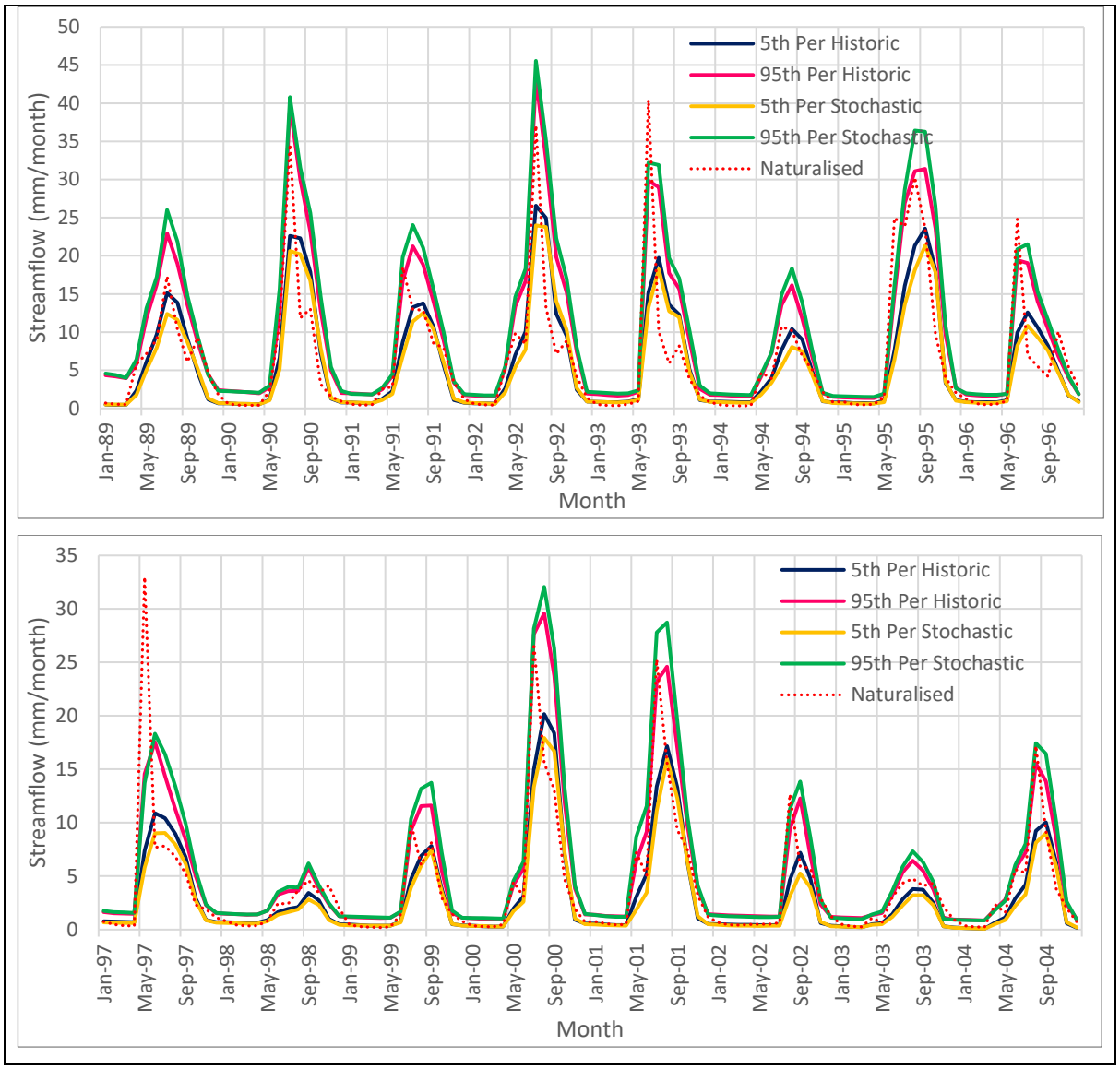



***Figure 5-9: Range of simulated stream flows from 100 validation runs for Bella Vista***

### 5.4.3 Bonjanala

Figure 5-10 and Figure 5-11 present the box plots of the calibration and validation stream flows obtained for the Bonjanala catchment respectively; while Figure 5-12 presents the absolute mean deviations and coefficients of variability for each percentile.

For the calibration runs, the naturalised stream flows fall within the boxplot whisker ranges of all percentiles of streamflow volumes. For the validation runs, the naturalised stream flows fall within the boxplot whisker ranges of all percentiles of streamflow volumes except the 95$^{th}$ percentile. The interquartile (box) and whisker ranges (0% to 100%) of the box plot clearly reveal higher variability of the stochastic rainfall stream flows for the 75$^{th}$, 85$^{th}$, and 95$^{th}$ percentiles. For the lower percentiles, the box plots reveal similar variabilities for the historic and stochastic rainfall simulations.

The lowest absolute mean deviation experienced by the calibration and validation stream volumes are the 75th and 50th percentiles respectively, while the 15th percentile of streamflow volumes experiences the highest degree of bias.

The highest degrees of variability experienced by the both calibration and validation stream volumes is the 15th percentile while the 95th percentile streamflow volumes experience the lowest degree of variability.

The full range stream flows obtained for the calibration and validation runs for the Bonjanala catchment are shown in Figure 5-13 and Figure 5-14 respectively. The stream flows obtained from both the calibration and validation runs, for both the historic observed and stochastic rainfalls, are generally representative of the magnitudes of the naturalised streamflow data. The ranges of stream flows obtained from the historic data sets are prominently narrower than those obtained from the stochastic data sets.

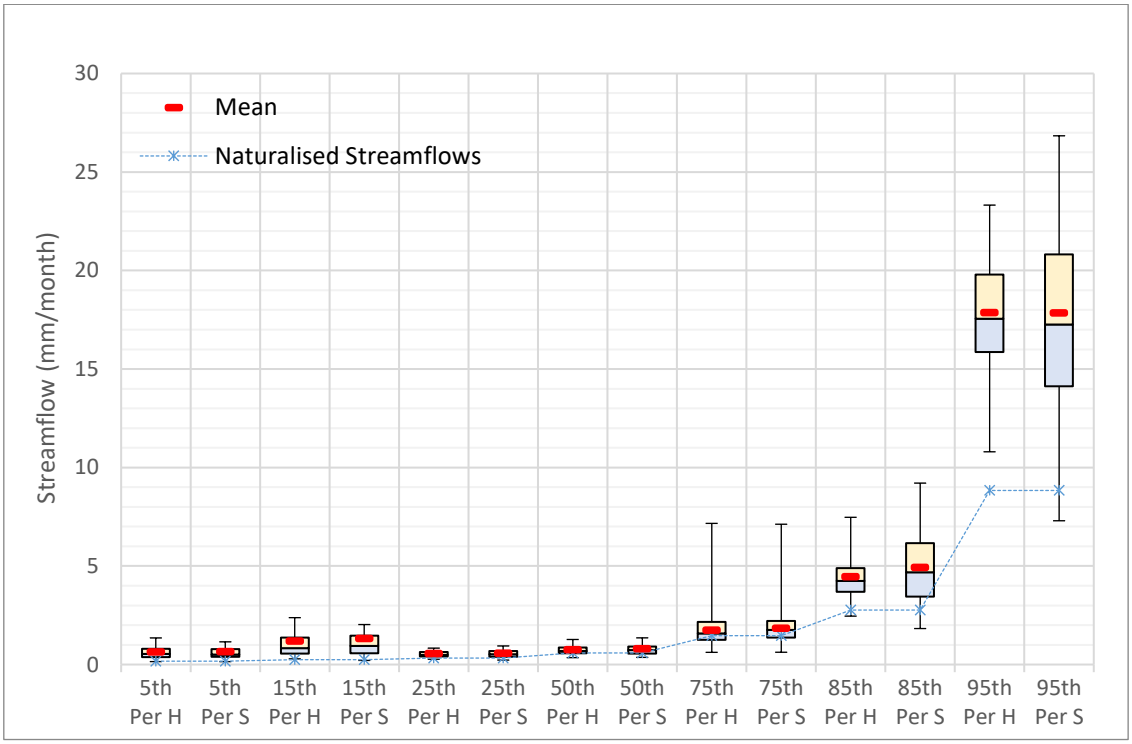



***Figure 5-10: Box plots of representative calibration stream flows for Bonjanala (H: Historic Observed Rainfall; S: Monthly Stochastic Rainfalls)***

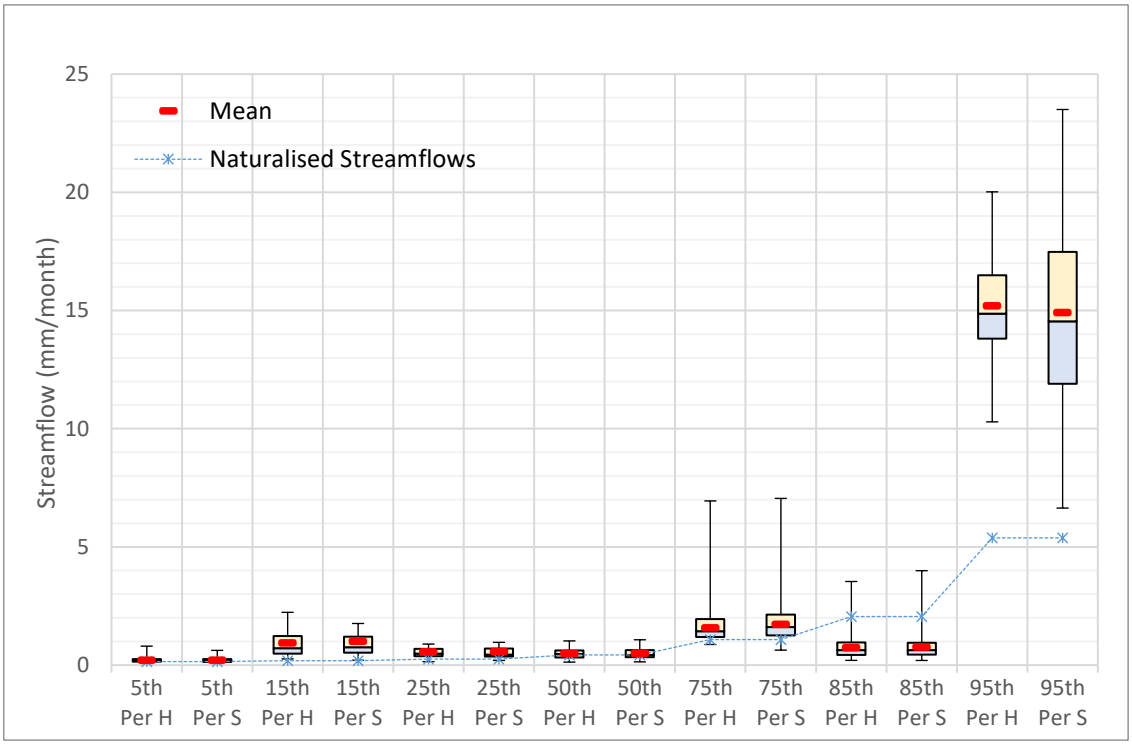



***Figure 5-11: Box plots of representative validation stream flows for Bonjanala (H: Historic Observed Rainfall; S: Monthly Stochastic Rainfalls)***

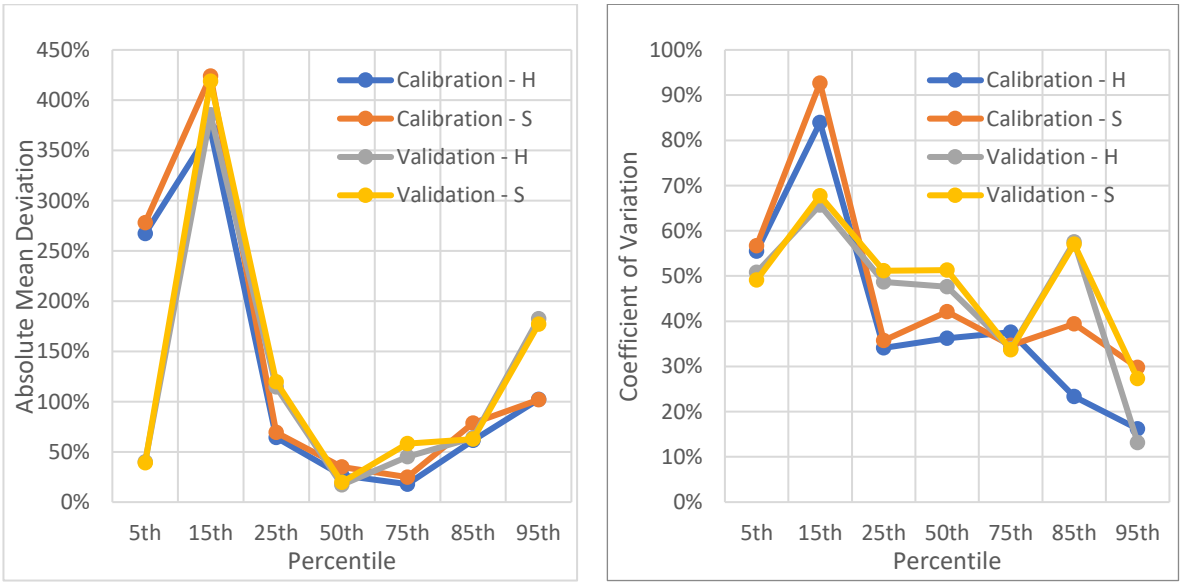



***Figure 5-12: Bias and Coefficients of Variation for Bonjanala (H: Historic Observed Rainfall; S: Monthly Stochastic Rainfalls)***

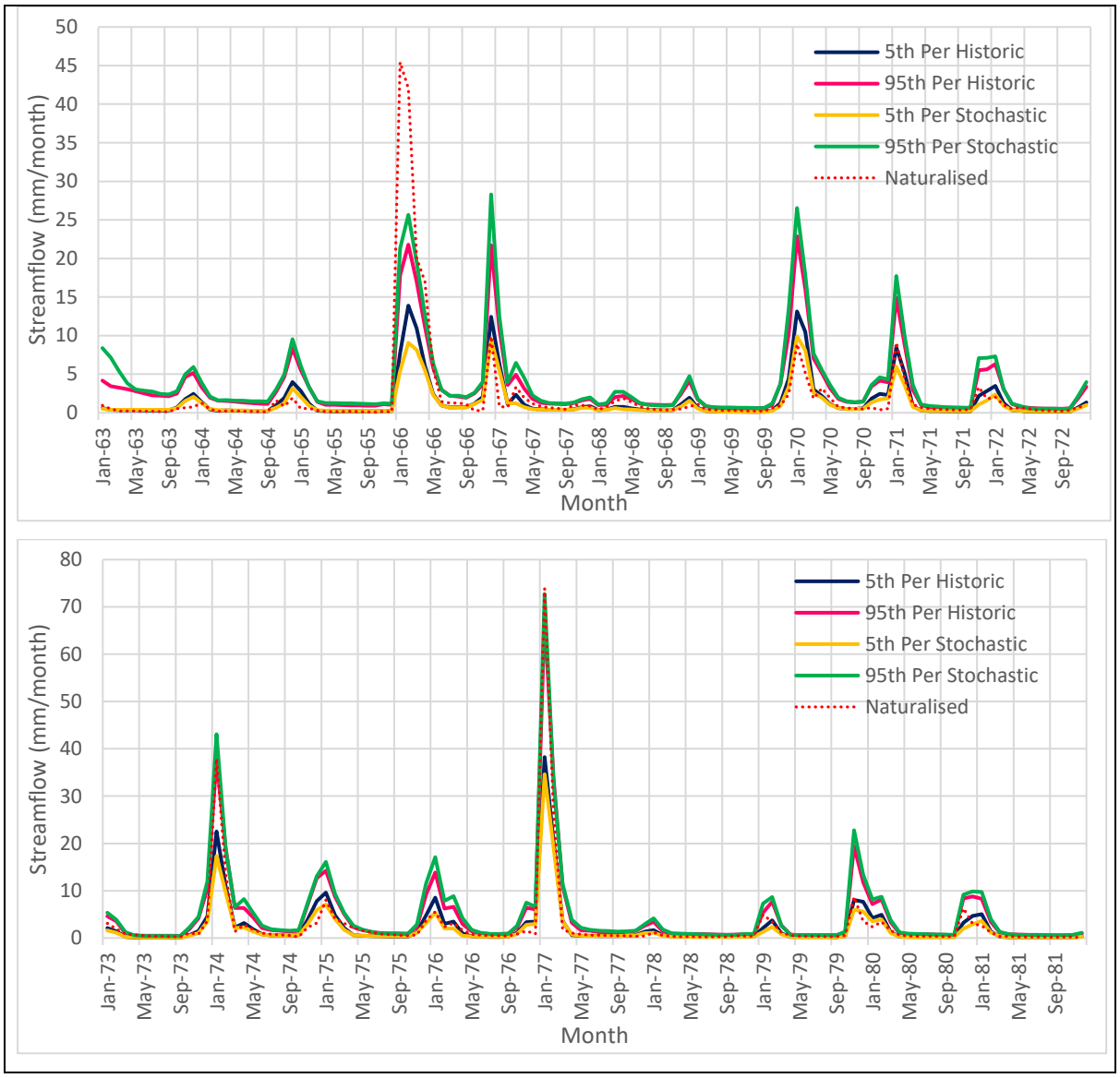



***Figure 5-13: Range of simulated stream flows from 100 calibration runs for Bonjanala***

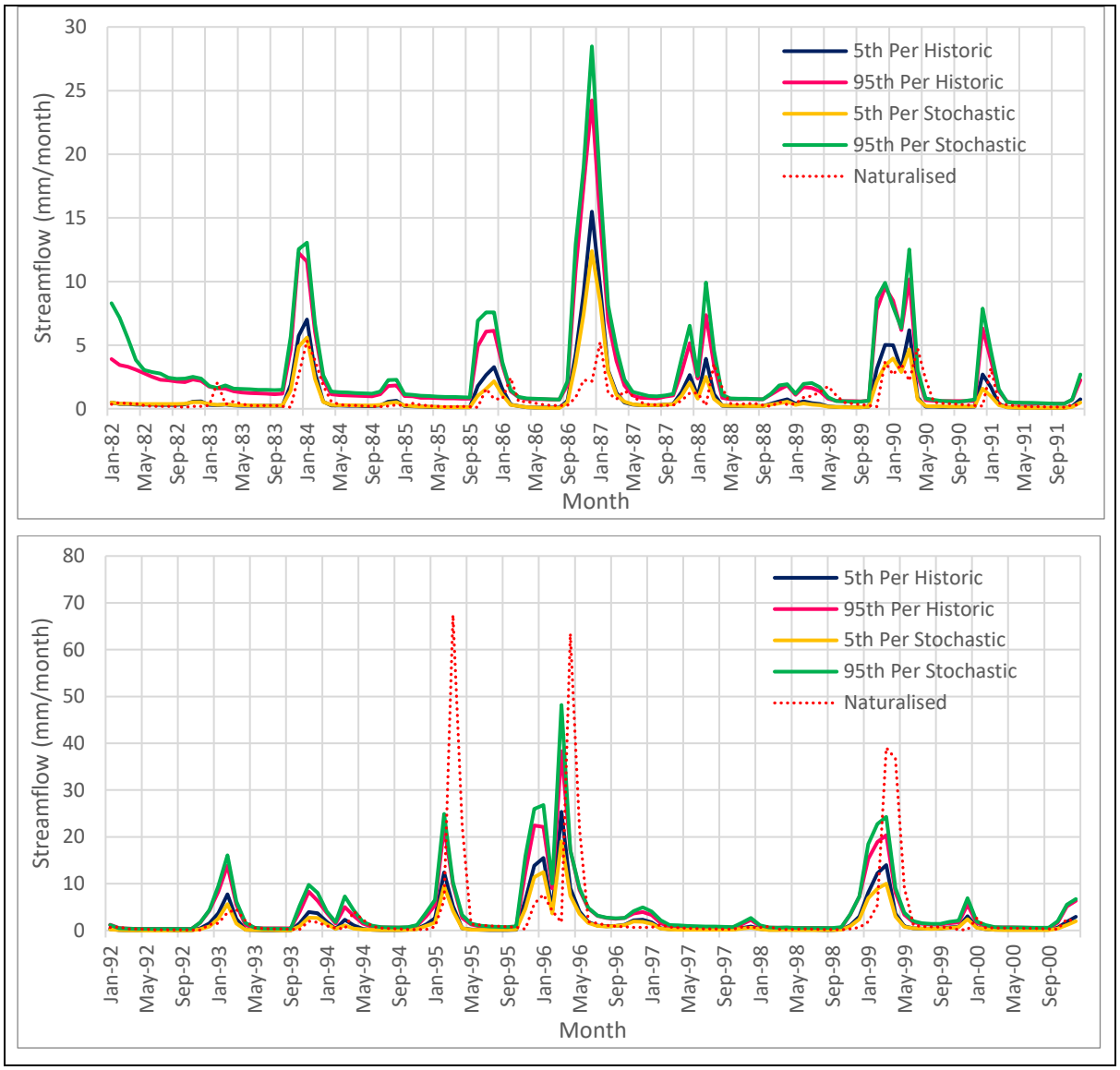



***Figure 5-14: Range of simulated stream flows from 100 verification runs for Bonjanala***

## 5.5 Discussion

This chapter presented the streamflow simulation analysis aimed at informing whether incorporating areal rainfall uncertainty affects simulation performance and variability of generated simulated stream flows. Streamflow simulation was carried out in the Pitman model at a monthly time step for two of the seven catchments using observed monthly rainfalls and 100 stochastically generated rainfall sequences. The calibration of the Pitman model parameters for the catchments was carried out by applying a manual-automatic calibration approach. The rainfall and streamflow data sets for each of the catchments were divided into a calibration set and a validation set.

The Pitman model parameters obtained for both catchments were allocated initial ranges based on the parameter ranges widely applied for Pitman model simulations in South Africa (Bailey and Pitman, 2016) and these were manually adjusted as required to achieve satisfactory calibration. The mean parameters obtained for both of the catchments analysed were within reasonable ranges, although the mean interception storage (PI) obtained was higher than the recommended range by Bailey (2015) of 1-10mm by about 3 mm. This observation has previously been encountered (Ndiritu, 2009) and probably indicates the presence of additional interception (either natural or human) that is not explicitly incorporated in the GW Pitman model applied.

Both test catchments exhibited slightly better coefficients of efficiencies (CE) in calibrations than validations while the validations obtained slightly better residual mass curve coefficiencts (RMCC). For both catchments, applying stochastic areal rainfalls (instead of historic ones) did not introduce any significant loss in model performance or the variability of this performance. The 18 parameters of the model obtained from the calibrations applying historic and those applying stochastic areal rainfalls also exhibited matching statistical characterstics (means, standard deviations and skewness).

Percentile bands of the streamflows generated from the simulations were assessed using box plots. This revealed that naturalised streamflows for the Bella Vista catchment was between the simulated streamflow ranges for the 75th to 95th percentiles for the calibration runs; while the naturalised streamflows was within all ranges except the 50th and 75th percentiles for the validation runs. The naturalised streamflows for the Bonjanala catchment was within the simulated streamflow ranges for almost all percentiles for both the calibration and validation runs. The box plots revealed that for the higher streamflows ($75^{th}$, $85^{th}$ and $95^{th}$ percentiles), using stochastic areal rainfalls lead to considerable increase in streamflow variability. For lower streamflow, the range of variabilities were similar.

Further assessment of the effect of incorporating areal rainfall uncertainty on streamflows was done by a comparison of the absolute mean deviations and coefficients of variation of the streamflows. For both calibration and validation runs, lower streamflows generally exhibited higher absolute mean deviations and coefficients of variation than higher streamflows. The absolute mean deviations applying stochastically generated rianfalls were similar to those obtained from applying historic rainfalls. However, for the higher ($\geq 50^{th}$ percentile), streamflows, most of the coefficients of variability from the simulations applying stochastic areal rianfalls were however notably higher than those based on historic rainfalls. This was in agreement with the observed larger interquartile and whisker ranges (0% - 100%) observed from the boxplots for the large streamflows.

Plots of the full range of stream flows obtained for the calibration and validation runs for both catchments also revealed narrower ranges for historic rainfall simulations than the simulations based on stochastic areal rainfalls.

These results reveal that incorporating areal rainfall uncertainty using the approach applied in this study leads to a significant increase in the range of simulated stream flows without significant loss of simulation performance. These results are in agreement to the findings by Ndiritu and Mkhize (2017) and are considered a verification of the concepts of areal rainfall uncertainty quantification applied by the stochastic areal rainfall generator.

# 6. Conclusion and Recommendations

Rainfall uncertainty is one of the major challenges encountered in streamflow modelling for water resources assessment. The objective of this research was therefore to assess the performance of an approach for quantifying rainfall uncertainty and to further assess the effects of this uncertainty on streamflow simulation. The stochastic areal rainfall generator developed by Ndiritu (2013) was selected as an appropriate rainfall uncertainty quantifier. The Pitman model was selected for streamflow simulation as it is a widely applied catchment modelling method for regional scale water resources planning in South Africa. Areal rainfall uncertainty was studied using seven catchments located in South Africa; while the impacts of this uncertainty on streamflow simulation used two of the seven catchments.

The seven catchments had datasets of rainfalls from 8 rainfall stations within or close to the catchments. By determining areal rainfalls by alternately omitting 4 of the rainfall stations while maintaining uniform areal coverage, the differences in areal rainfalls were found to average 18.3% of the average monthly rainfalls for the seven study catchments. These were considered significant and was in agreement with previous studies. Box plots of various percentiles of the stochastically generated rainfalls revealed that the mean monthly stochastic rainfalls were unbiased. In addition, the average standard deviations and skewness values of the stochastic areal rainfalls matched closely to the historic areal rainfalls.

Streamflow simulation carried out on two catchments using the historic and stochastically generated areal rainfalls; and calibration for the Pitman modelling was carried out using a manual-automatic approach that included the use of the SCE-UA optimizer.

Similar model simulation performances were obtained by both historic and stochastic data sets. The stochastic areal rainfalls however produced prominently wider streamflow ranges for both catchments. Because this impact led to wider bands of simulated stream flows without degrading streamflow performance, stochastic areal rainfall generator and the principles underlying the approach are considered realistic.

Further research on the stochastic rainfall generator and applications on streamflow simulations could include the following:

1. The influence of temporal inter-dependence of rainfall on the stochastic areal rainfall generation could be studied.
2. The stochastic areal rainfall generator could be tested on catchments with higher range gauge densities or reliable radar rainfall datasets.

3. Catchments with natural rather than naturalized stream flows could be applied to study the effect of areal rainfall uncertainty on streamflow simulation to provide higher confidence in the results.
4. The analysis could be carried out at shorter time steps (daily, hourly, 15 minutes, 5 minute) to assess the applicability of the approach to other hydrological analysis such as flood design.
5. Other methods of streamflow simulation (other than the Pitman model) and areal rainfall determination (other than inverse distance weighting) could be applied in the analysis.
6. How the stochastic rainfall generator outputs vary with different dominant types of rainfall, as might be experienced in different parts of the country, which may have different spatial variability characteristics.

# 7. References

Bailey, A., 2015. *WRSM2000/Pitmam Water Resources Simulation Model for Windows,* Pretoria: Water Research Commission.

Bailey, A. K. & Pitman, W. V., 2016. *Water Resources of South Africa, 2012 Study (WR2012),* Johannesburg: Water Resource Comission.

Barbalho, F. D., da Silva, G. F. N. & Formiga, K. T. M., 2014. Average Rainfall Estimation: Methods Performance Comparison in the Brazilian Semi-Arid. *Journal of Water Resource and Protection,* Volume 6, pp. 97-103.

Barth, T., 2005. *A Brief Overview of Uncertainty Quantification and Error Estimation in Numerical Simulation.* [Online] Available at: https://web.stanford.edu/group/cits/pdf/lectures/barth.pdf [Accessed 30 August 2021].

Cristiano, E., ten Veldhuis, M. & van de Giesen, N., 2017. Spatial and temporal variability of rainfall and their effects on hydrological response in urban areas - a review. *Hydrological Earth System Sciences,* Volume 21, pp. 3859-3878.

Duan, Q. Y., Sorooshian, S. & Gupta, V., 1992. Effective and efficient global optimisation for conceptual rainfall-runoff models. *Water Resources Research,* 28(4), pp. 1015-1031.

Duan, Q. Y., Sorooshian, S. & Gupta, V., 1994. Optimal use of the SCE-UA global optimisation method for calibrating watershed models. *Journal of Hydrology,* Volume 158, pp. 265-284.

Ghanem, R., Higdon, D. & Owhadi, H., 2017. *Handbook of Uncertainty Quantification.* 1st ed. Cham: Springer International Publishing.

Hughes, D. A., 2004. Incorporating groundwater recharge and discharge functions into an existing monthly rainfall-runoff model. *Hydrological Sciences,* 49(2), pp. 297-311.

Hughes, D. A., 2013. Review of 40 years of hydrological science in practice in Southern Africa using the Pitman rainfall-runoff model. *Journal of Hydrology,* Volume 501, pp. 111-124.

Hughes, D. A., Sawunyama, T. & Kapangaziwiri, E., 2008. *Incorporating estimation uncertainty into water resource development planning in ungauged basins in Southern Africa,* s.l.: BHS 10th National Hydrology Symposium, Exeter.

Kapangaziwiri, E. & Hughes, D. A., 2008. *Revised physically-based parameter estimation methods for the Pitman monthly rainfall model,* In Press: Water SA.

Leonhardt, G., Sun, S., Rauch, W. & Bertrand-Krajewski, J., 2014. Comparison of two model based approaches for areal rainfall estimation in urban hydrology. *Journal of Hydrology,* Volume 511, pp. 880-890.

Merker, C., Geppert, G., Clemens, M. & Ament, F., 2019. *Estimating the uncertainty of areal precipitation using data assimilation,* s.l.: Tellus A: Dynamic Meterology and Oceanography.

Miller, D. C. et al., 2014. *Advanced Computational Tools for Optimization and Uncertainty Quanitifcation of Carbon Capture Processes.* Washington, Computer Aided Chemical Engineering.

Mkhize, N., 2014. *Quantifying Monthly Areal Rainfal Uncertainty Using Data-base Stochastic Rainfall Generator,* s.l.: University of the Witwatersrand, South Africa (unpublished MSc thesis).

Moulin, L., Gaume, E. & Obled, C., 2009. Uncertainties on Mean Areal Precipitation: Assessment and Impact on Streamflow Simulations. *Hydrological Earth System Sciences,* Volume 13, pp. 99-114.

Mwelwa, E. M., 2004. *The Application of the Monthly Time Step Pitman Rainfall-Runoff Model to the Kafue River Basin of Zambia,* MSc Thesis: Rhodes University.

Ndiritu, J., 2013. Using data-derived perturbations to incorporate uncertainty in generating stochastic areal rainfall from point rainfall. *Hydrological Sciences Journal,* 8(58), pp. 1704-1717.

Ndiritu, J. G., 2009. Automatic Calibration of the Pitman Model using the Shuffled Complex Evolution Method. *Physics and Chemistry of the Earth,* Volume 34, pp. 729-740.

Ndiritu, J. G. & Mkhize, N., 2017. Effectly of monthly areal rainfall uncertainty on streamflow simulation. *Physics and Chemistry of the Earth,* Volume 100, pp. 51-61.

Pitman, W. V., 1973. *A mathematical model for generating daily river flows from meteorological data in South Africa, Report 2/73.,* University of the Witwatersrand: Hydrological Research Unit.

Robinson, M. & Ward, R., 2017. *Hydrology: Principles and Processes.* 1st ed. London: IWA Publishing.

Sawunyama, T., 2008. *Evaluating Uncertainty in Water Resources Estimation in South Africa: A Case Study in South Africa,* Rhodes University: PhD Thesis.

Sawunyama, T. & Hughes, D. A., 2007. Assessment of rainfall and evaporation input data uncertainties on simulated runoff in southern Africa. *Quantification and Reduction of Predictive Uncertainty for Sustainable Water Resource Management (Proceedings of Symposium HS2004 at IUGG2007, Perugia, July 2007),* pp. IAHS Publ. 313, 98-106.

Schulze, R., 1989. *ACRU: Background, Concepts and Theory,* s.l.: Report 35, Agricultural Catchments Research Unit, Department of Agricultural Engineering, University of Natal, Pietermaritzburg, South Africa.

Schulze, R. E. & Tarboton, K. C., 1991. The "ACRU" Modelling System for Large Catchment Water Resources Management. *Hydrology for the Water Management of Large River Basins (Proceedings of the Vienna Symposium, August 1991). IAHS Publ. no. 201, 1991.*

Selase, A. E., Agyimpomaa, D. E., Selasi, D. D. & Hakii, D. M., 2015. Precipitation and Rainfall Types with their Characteristic Features. *Journal of Natural Sciences Research,* 5(20), pp. 89-92.

Selase, A. E., Agyimpomaa, D. E., Selasi, D. D. & Hakii, D. M., 2015. Precipitation and Rainfall Types with their Characteristic Features. *Journal of Natural Sciences Research,* 5(20).

Steiner, M., 1996. Uncertainty of estimates of monthly areal rainfall for temporally sparse remote observations. *Water Resources Research,* 32(2), pp. 373-388.

Volodina, V. & Challenor, P., 2021. *The Importance of Uncertainty Quantification in Model Reproducibility,* London: The Royal Society Publishing.

Ward, R. C. & Robinson, M., 2000. *Principles of Hydrology.* 4th ed. Crydon: McGraw-Hill Publishing Company.

Yoo, C., Kim, J. & Yoon, J., 2012. Uncertainty of areal average rainfall and its effect on runoff simulation: A case study for the Chungju Dam Basin, Korea. *KSCE Journal of Civil Engineering,* 16(6), pp. 1085-1092.